

**Use of Comparative Proteomics to Study a Novel Osteogenic
Nanotopography**

Fahsai Kantawong

MSc



**University
of Glasgow**

**Centre for
Cell Engineering**

**This thesis is submitted for the degree of Doctor of
Philosophy**

**Centre for Cell Engineering
Biochemistry & Cell Biology Research Group
Division of Molecular and Cell Biology
Faculty of Biomedical and Life Science
University of Glasgow, G12 8QQ**

July 2009

Abstract.

The principal aim of this thesis was to investigate the ability of surface topography in inducing bone cell differentiation for biomedical purposes. In orthopedic research, regeneration of bone defects can be performed *in vitro* using biomaterials. Third generation biomaterials aim not only to support tissue (first generation) and not only to be 'bioactive' (second generation), but to stimulate specific, known and desirable responses at the molecular level. Nanoscale topography offers a possible route to the development of third generation biomaterials.

Two-dimensional fluorescence difference gel electrophoresis (2D DIGE) is a new method for assessing protein expression strategies and here, a micro-grooved topography was used as a model for protocol optimization. The protocol was successfully developed and proved that 2D DIGE can be used as a powerful tool in the evaluation of biomaterial can direct cell behavior and cell fate.

Next, the refined protocol was applied to the evaluation of the novel nanotopographic features; near-square nanopits (120 nm diameter, 100 nm depth with the pitch between the pits was set to an average of 300 nm with a ± 50 nm error). Protein expression profiles indicated that ERK1/2 might play part in cell proliferation and cell differentiation. However, to make a clear conclusion about molecular signalling, the study of sub-cellular proteome is needed in the future work.

Additionally, the use of another comparative proteomic technique; dimethyl labelling, implicated the possibility of sub-population differentiation, i.e. the formation of multiple cell types that could be advantageous in tissue engineering of complex organs. Furthermore, the application of fluid-flow bioreactors was shown to enhance the growth rate and possibly increased differentiation of cells cultured on nanotopographical features.

Table of Contents

Abstract	ii
Table of Contents	iii
List of Tables	xi
List of Figures	xii
List of Abbreviations	xiv
Presentations	xviii
Publications	xix
Acknowledgements	xx
Author's declaration	xxi
Dedication	xxii
Chapter I General Introduction	
1.1 Introduction	1
1.2 Bone structure	1
1.2.1 Compact bone	2

1.2.2 Spongy bone	3
1.2.3 Bone cells	3
1.2.3.1 Osteoblasts	3
1.2.3.2 Osteocytes	3
1.2.3.3 Osteoclasts	3
1.3 Bone modeling and remodeling	5
1.4 Stem cells and Osteoblast differentiation	6
1.5 Bone mineralization	8
1.6 Mechanotransduction	10
1.6.1 Mechanical forces control cells	10
1.6.2 Focal adhesions	11
1.6.3 Cytoskeleton	13
1.6.3.1 Microfilaments (MFs) or actin filaments	14
1.6.3.2 Intermediate filament (IFs)	14
1.6.3.3 Microtubule (MTs)	15
1.6.4 Tensegrity model and signal transduction of surface topography	15
1.7 Scaffolds and surface topography	18
1.8 Bioreactors for bone tissue engineering	22
1.9 Proteomics	23

1.9.1 Differential In Gel Electrophoresis (DIGE)	23
1.9.1.1 Saturation labelling	24
1.9.1.2 Basic methodology in 2D gel electrophoresis	25
1.9.2 Dimethyl labelling	27
1.9.3 Mass Spectrometry	28
1.9.3.1 MALDI-Tof-MS	30
1.9.3.2 The advantages of MALDI	30
1.9.3.3 Matrix and soft ionization technique	30
1.9.3.4 MALDI/TOF/TOF	31
1.9.4 Database search	32
 Chapter II Protocol optimizations and the application of micro-grooved topography	
2.1 General introduction	35
2.1.1 Part I. Optimisation of DIGE for osteoprogenitor cells	35
2.1.2 Part II. Application of DIGE for topographical matrices	37
2.1.3 Part III The reference gel and protein identification by mass spectrometry	38
2.2 Materials and methods	39
2.2.1 Part I: Optimisation of DIGE for osteoprogenitor cells	39
2.2.1.1 Cell Culture, Protein Extraction and Protein	

Precipitation (from flask)	39
2.2.1.2 Protein quantification	39
2.2.1.3 2D-Gel Electrophoresis	40
2.2.1.4 Differential In Gel Electrophoresis (DIGE)	40
2.2.2 Part II: Application of DIGE for topographical matrices	42
2.2.2.1 Photolithographical Material Fabrication	42
2.2.2.2 Cell Culture	42
2.2.2.3 Histology	43
2.2.2.4 Alizarin staining	44
2.2.2.5 Protein Extraction and Protein Precipitation from cells cultured on microtopography	44
2.2.2.6 The Saturation labelling of protein extract from cells cultured on microtopography	44
2.2.3 Part III The reference gel and protein identification by mass spectrometry	45
2.2.3.1 Preparative 2D gel (reference gel)	45
2.2.3.2 Mass spectrometry and Data Analysis	46
2. 3 Results	47
2.3.1 Part I: Optimisation of DIGE for osteoprogenitor cells	47
2.3.1.1 Protein assay	47
2.3.1.2 Protein extraction and protein separation by 2D gel electrophoresis	47
2.3.1.3 Optimisation of saturation labelling	49

2.3.2 Part II: Optimisation of DIGE for topographical matrices	51
2.3.2.1 Materials	51
2.3.2.2 Histology	51
2.3.2.3 Cell culture in the flow condition	53
2.3.2.4 DIGE	55
2.3.3 Part III The reference gel and protein identification by mass spectrometry	55
2.3.3.1 Reference gel and protein identification	55
2.3.3.2 This allowed the identification of modulated proteins thus	57
2.4 Discussion	63
CHAPTER III The optimisation of the DIGE protocol for disordered nanopits	
3.1 Introduction	66
3.2 Disordered nanoscale topography (NSQ50)	66
3.3 Materials and methods	68
3.3.1 Nanotopographical Fabrication	68
3.3.2 Cell Culture	70
3.3.3 Histology	70

3.3.4 Scanning Electron Microscopy (SEM)	70
3.3.5 Alizarin staining	71
3.3.6 Protein Extraction and Protein Precipitation	71
3.3.7 DIGE – analytical gels	72
3.3.8 Preparative 2D gels	72
3.4 Results	73
3.4.1 Fabrication	73
3.4.2 Cell morphology and histology	74
3.4.3 DIGE	78
3.4.4 Preparative gel and protein identification	78
3.4.4.1 Proteins with Increased Expression	79
3.4.4.2 Proteins with Decreased Expression	82
3.5 Discussion	86
 Chapter IV Temporal proteomic analysis of novel disordered nanopit topography	
4.1 Introduction	89
4.2 Materials & Method	91

4.2.1 Cell Culture	91
4.2.2 Histology	92
4.2.2.1 Coomassie Blue	92
4.2.2.2 Alizarin Red	92
4.2.3 Protein Extraction and Protein Precipitation	92
4.2.4 Dimethyl labelling	93
4.2.4.1 Protein extraction	93
4.2.4.2 Protein labelling	93
4.2.4.3 SDS-PAGE & In-gel digestion	94
4.2.4.4 LC-MS/MS	94
4.2.4.5 Dimethyl Labelling Data Processing	95
4.3 Results	95
4.3.1 Histology	95
4.3.1.1 Cell morphology	95
4.3.1.2 Tissue mineralization	95
4.3.2 DIGE	98
4.3.3 Dimethyl labelling	107
4.3.4 The effects of fluid flow bioreactor compared with static culture	110
4.3.4.1 The Histology of cells cultured in fluid-flow bioreactor	110
4.3.4.2 DIGE analysis of cells cultured in the bioreactor	111
4.3.4.3 Protein expression for cells cultured in the bioreactor	113
4.4 Discussion	114

Chapter V General Discussion	
5.1 Introduction	120
5.2 Technical development	120
5.2.1 DIGE	120
5.2.2 Dimethyl labelling	120
5.2.3 Bioreactor	121
5.3 Nanotopography and biological observations	121
5.4 Future work	127
5.4.1 Cell compartment proteome	127
5.4.2 Phosphoproteomeomics	129
5.4.3 Adding bioactive composites to the polymers being embossed with the osteogenic nanotopographies	130
5.5 Conclusion	131
VI Appendices	132
References	137

List of Tables

Chapter I Introduction

Table 1.1 The advantages and disadvantages of dimethyl labelling	29
--	----

Chapter II Protocol optimizations and the application of micro-grooved topography

Table 2.1 DIGE condition	41
--------------------------	----

Table 2.2 Protein expression profiles	61
---------------------------------------	----

CHAPTER III The optimisation of the DIGE protocol to study the effect of disordered nanopits on osteoprogenitor cell differentiation

Table 3.1 Names and functions of proteins modulated by the NSQ50 topography	85
---	----

Chapter IV Temporal proteomic analysis of novel disordered nanopit topography

Table 4.1 Protein expression profile from dimethyl labelling	108
--	-----

Table.4.2 A comparison between protein expression profiles from the fluid-flow bioreactor and static culture	112
--	-----

List of Figures

Chapter I General Introduction

Figure 1.1 Cross section of long bone	2
Figure 1.2 Bone cells	4
Figure 1.3 Bone remodeling	6
Figure 1.4 Association between integrins and ECM	13
Figure 1.5 The three major IF assembly	15
Figure 1.6 Schematic of labelling reaction of protein	27
Figure 1.7 The dimethyl labelling reaction	28
Figure 1.8 Principle of matrix-assisted laser desorption/ionization	32
Figure 1.9 Differential In Gel Electrophoresis	34

Chapter II Protocol optimizations and the application of micro-grooved topography

Figure 2.1 Work plan	35
Figure 2.2 The bioreactor	43
Figure 2.3 Standard curve of protein assay	48
Figure 2.4 The 2D SDS-PAGE of protein extract from flask	49
Figure 2.5 Saturation labelling optimisation	50
Figure 2.6 Atomic Force Microscopy	51
Figure 2.7 Osteoprogenitor cells (OPGs) cultured	52
Figure 2.8 Alizarin red staining for calcium accumulation	53
Figure 2.9 Quantification of protein extracts from static	54
Figure 2.10 Typical DIGE images	56
Figure 2.11 BVA images and gel matching	57

CHAPTER III The optimisation of the DIGE protocol to study the effect of disordered nanopits on osteoprogenitor cell differentiation

Figure 3.1 Electron Beam lithography	69
Figure 3.2 SEM image of NSQ50 nanopitted substrates	73
Figure 3.3 AFM image of planar control and NSQ50 nanopit substrates	74
Figure 3.4 Osteoprogenitor cells (OPGs) cultured on PCL	75
Figure 3.5 Higher magnification of Osteoprogenitor cell morphology	76
Figure 3.6 Scanning electron micrographs of osteoprogenitor	77
Figure 3.7 Alizarin red staining for calcium accumulation	78
Figure 3.8 Typical DIGE images	80
Figure 3.9 Spot matching and protein identification	81

Chapter IV Temporal proteomic analysis of novel disordered nanopit topography

Figure 4.1 Cell culture diagram	91
Figure 4.2 Coomassie blue staining of osteoprogenitor cells (OPGs) cultured on PCL substrates in static culture	96
Figure 4.3 Alizarin red staining for calcium accumulation	97
Figure 4.4 Typical DIGE images as were analyze by DeCyder	98
Figure 4.5 Temporal monitoring of protein expression	104
Figure 4.6 Differences in isomeric expression	105
Figure 4.7 Different in isomeric expression of Trx	106
Figure 4.8 SDS-PAGE of proteins tagged by dimethy labelling	107
Figure 4.9 Cell morphology in fluid flow bioreactor	111

Chapter V General Discussion

Figure 5.1 Cell cycle and ERK1/2	123
----------------------------------	-----

List of Abbreviations

µg	Microgram
µl	Microlitre
2D	Two dimensions
2X	Two times
AFM	Atomic Force Microscopy
AGT	Alanine : glyoxylate aminotransferase
Akt	v-akt murine thymoma viral oncogene homolog
ANX	Annexin
APS	Ammonium persulfate
ATF	Activating transcription factor
ATP	Adenosine triphosphate
BiP	Binding immunoglobulin protein
BMPs	Bone Morphogenetic Proteins
BSA	Bovine Serum Albumin
BVA	Biological Variation Analysis
CBR	Cytochrome b5 reductase
CD	Compacts disk
Cdk	Cyclin-dependent kinases
CHAPS	3-((3-Chloromidopropyl)dimethylammonio)-1-propanesulfonate
CHCA	alpha-cyano-4-hydroxycinnamic acid
CLIC	Chloride intracellular channel
Da	Dalton
DIA	Differential Analysis
DIGE	Difference Gel Electrophoresis
DMSO	Dimethyl Sulfoxide
DNA	Deoxyribonucleic acid
DTT	Dithiothreitol
DVD	Digital video disc

EBL	Electron Beam Lithography
ECM	Extracellular matrix
eIF4G	Eukaryotic initiation factors 4G
ERK	Extracellular signal-regulated kinases
ESI	Electrospray ionization
FAK	Focal adhesion kinase
FBS	Fetal bovine serum
FCS	Fetal calf serum
FDA	Food and Drug Administration
GAL	Galectin
Glr1	Glutathione reductase
GRASP55	Golgi reassembly stacking protein of 55 kDa
GRP78	Glucose Regulated 78kDa Protein
GSH	Reduced Glutathione
GSSG	Oxidized glutathione
GST	Glutathione <i>S</i> -transferase
GTP	Guanine Triphosphate
HCl	Hydrochloric acid
HEPES	4-(2-hydroxyethyl)-1-piperazineethanesulfonic acid
HFOB	Human foetal osteoblast
HPLC	High performance liquid chromatography
Hsp	Heat shock protein
IEF	Isoelectric focusing
IFs	Intermediate filaments
IGF	Insulin-like growth factor
IPG	Immobilized pH gradient
JNK	Jun N-terminal Kinase
kDa	Kilodalton
LC	Liquid chromatography
LPA	Lysophosphatidic acid
M	Molar

MALDI	Matrix-assisted laser desorption/ionization
MAP	Mitogen-activated protein
MAPK	Mitogen-Activated Protein Kinase
MEK	MAP kinase or ERK kinase
MEM	Minimum essential medium
MFs	Microfilaments
ml	Mililitre
MLCK	Myosin Light Chain Kinases
mM	Milimolar
mRNA	Messenger Ribonucleic acid
MSCs	Mesenchymal stem cells
mTOR	Mammalian Target of Rapamycin
MTs	Microtubules
MW	Molecular weight
MYL	Myosin light chain
NCBI	National Center for Biotechnology Information
Ni	Nickle
nM	Nanomolar
NPM	Nucleophosmin
NSQ	Nanosquare
OPG	Osteoprogenitor
OSX	Osterix
PBS	Phosphate buffer saline
PCL	Polycaprolactone
PCR	Polymerase Chain Reaction
pFAK	Phosphorylated Focal Adhesion Kinase
PGE ₂	Prostaglandin E2
PI3K	Phosphoinositide 3-kinase
pI	Isoelectric point
PKA	Protein Kinase A
PKC	Protein Kinase C

Ra	Roughness average in microns
RACK1	Receptor of activated C kinase 1
RANBP1	RAN binding protein 1
RANKL	Receptor activator of nuclear factor kappa B ligand
RNA	Ribonucleic acid
RNH1	Ribonuclease/angiogenin inhibitor 1
RUNX2	Runt-related transcription factor 2
SD	Standard deviation
SDS-PAGE	Sodium dodecyl sulfate polyacrylamide gel electrophoresis
SEM	Scanning Electron Microscopy
SPARC	Secreted Protein Acidic and Rich in Cystein
SPT	Serine : pyruvate aminotransferase
SUMO	Small ubiquitin-like modifier
TCEP	Tris(2-carboxyethyl)phosphine
TCR	T cell receptor
TFA	Trifluoroacetic acid
TGF	Transforming growth factor
TGN	Trans-Golgi network
TPA =	12-O-tetradecanoylphorbol-13-acetate
TRX	Thioredoxin
Tyr	Tyrosine
UV	Ultraviolet
v/v	Volume by volume
VSMC	Vascular smooth muscle cell
Wnt	Wingless-type MMTV integration site family member
W/GEL	Watt per gel
w/v	Weight by volume
YWHAZ	Tyrosine 3-monooxygenase/tryptophan 5-monooxygenase activation protein, zeta

Presentations

Some of the work in this thesis has been the subject of the following presentations:

Conference proceedings

- 2006 **Society for Experimental Biology**
‘Comparative Cell Engineering Using Differential In Gel Electrophoresis (DIGE) Technique’. *Glasgow, UK* (oral presentation).
- 2007 **TERMIS-EU 2007 Conference**
‘Differential In Gel Electrophoresis (DIGE) Analysis of Osteoprogenitor Cell Contact Guidance’. *London, UK* (oral presentation).
- 2008 **8th World Biomaterials Congress**
‘Proteomic Analysis of Human Osteoprogenitor Cells Responding to Disordered Nanotopography’. *Amsterdam, Netherlands* (poster presentation).

Publications

Original research publications authored by the candidate on work relating to this thesis.

1. KANTAWONG, F. (2009a) Effects of Surface Topography Composite *Puerariae radix* on Human STRO-1 Positive. *Submitted*.
2. KANTAWONG, F. (2009b) Temporal proteomic analysis of novel disordered nanopit topography. *Submitted*.
3. KANTAWONG, F., BURCHMORE, R., GADEGAARD, N., OREFFO, R. O. & DALBY, M. J. (2008a) Proteomic analysis of human osteoprogenitor response to disordered nanotopography. *J R Soc Interface*.
4. KANTAWONG, F., BURCHMORE, R., WILKINSON, C. D., OREFFO, R. O. & DALBY, M. J. (2008b) Differential in-gel electrophoresis (DIGE) analysis of human bone marrow osteoprogenitor cell contact guidance. *Acta Biomater*.

Acknowledgements

I would like to acknowledge the support and encouragement from many people during the time I spent on my study. First of all, I would like to express my best regards to Dr. Matthew Dalby and Dr. Richard Burchmore who always supervised with patience and care throughout this work. This work could not have been completed without their instruction and guidance.

Thank you to The Royal Thai Government and BBSRC for the financial support in this thesis.

My thanks to Prof. Chris Wilkinson my assessor who gave advice during my laboratory work. Thanks Prof. Adam Curtis for his advice and comments in all these years.

Thank you to Dr. Mathis Riehle the head of CCE who facilitated many experimental devices in this work. Many thanks to Dr. Andrew Pitt for the convenient and friendly atmosphere in SHWFGF.

Thank you to Dr. Nikolaj Gadegaard for providing the nanotopography mould used in this study.

Thank the technicians: Andrew Hart, Jay Jayawardena, Ann McIntosh, Margaret Mullin, Mary Robertson for all technical help and their kindness.

Thank you to all friends in CCE: Laura Elizabeth McNamara, Rebecca McMurray, Abhay Andar, Manus Biggs, Tobias Lammel, Panwong Kuntanawat, Lewis Ross and etc. who shared my moment of joy and stress during my PhD.

Many thanks to Dr. Karl Burgess for his technical support and my final thank you to Dr. Richard Goodwin for the friendly and happy atmosphere in SHWFGF.

Author's Declaration

The work presented in this thesis was performed solely by the author except where the assistance of others has been acknowledged.

Fahsai Kantawong, April 2009

Dedication

I dedicate this thesis to Monta & Yongyut Kantawong

CHAPTER I General Introduction

1.1 Introduction

Bone tissue engineers aim to produce new bone in the laboratory that can then be used to repair or replace damaged bone in the body. Because of bone's important structural role, bone tissue engineering is a field with major research drive. In January 2000, the Bone and Joint Decade was launched in Geneva by the World Health Organisation to underpin this effort on bone regeneration (Weinstein, 2000). Due to the rapidly increasing life span of the world population, musculoskeletal disease such as injury, osteoporosis, and arthritis will have increasing social and economic impact. To achieve success in bone tissue engineering, a basic knowledge about the nature of bone and bone growth must be developed.

This study uses nanotechnology and a cell-based approach combining osteogenic cells *in vitro* and nanotopographic features fabricated on biomaterial scaffolds to allow the development of a bone tissue. A flow perfusion bioreactor was also used to aid the culture process and improve nutrient supply.

1.2 Bone structure

There are two major types of bone structure (figure 1.1); the outer bone layer is known as compact bone and the inner bone layer is spongy or trabecular bone. Bones develop from cells of both ectodermal and mesodermal tissues during embryonic development. Craniofacial structures are formed from the prechordal mesoderm and the craniofacial ectoderm (Elsen and Carels, 2008). Three main cell types are located in mature bones including osteoblasts, osteocytes and osteoclasts. These cell types have different origins and different roles in bones.

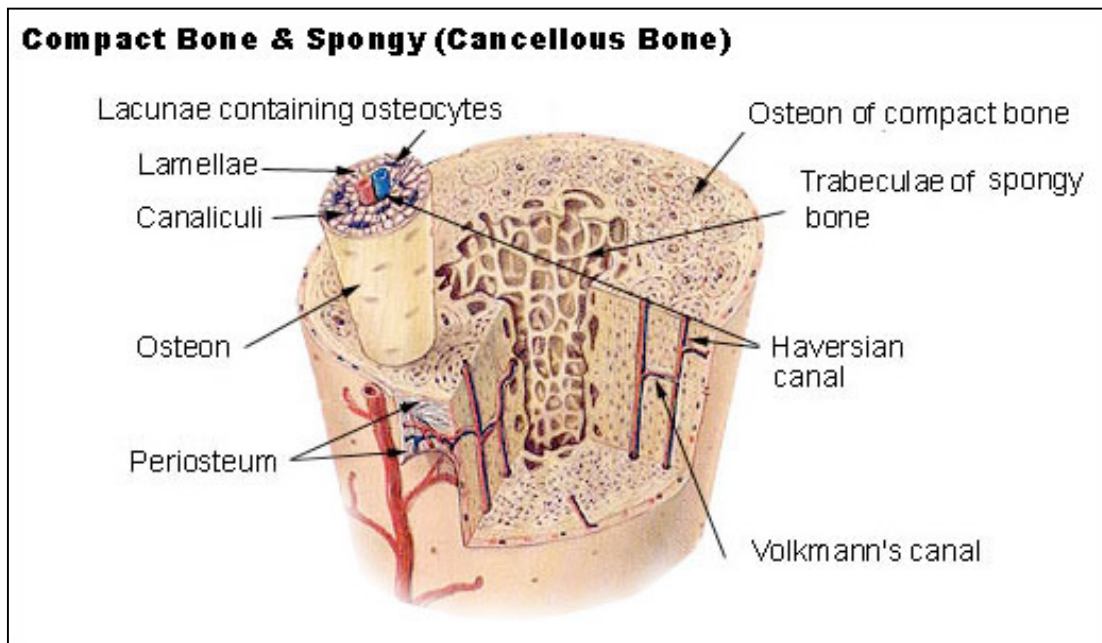


Figure 1.1 Gross section of long bone. The infrastructure of compact and spongy bone can be seen in this picture. The Haversian systems and blood supply system are noted in the compact bone while the trabeculae meshwork can be seen in spongy bone (<http://www.daviddarling.info/encyclopedia/B/bone.html>).

1.2.1 Compact bone

Compact bone consists of closely packed osteons or Haversian systems. The osteon contains a central osteonic (Haversian) canal, which is surrounded by concentric rings (lamellae) of matrix. Between the rings of matrix, the bone cells (osteocytes) are located in spaces called lacunae. Small channels (canaliculi) radiate from the lacunae to the osteonic (Haversian) canal to provide passageways through the hard matrix. In compact bone, the Haversian systems are packed tightly together to form what appears to be a solid mass. The osteonic canals contain blood vessels that are parallel to the long axis of the bone. These blood vessels interconnect, by way of perforating canals, with vessels on the surface of the bone (Datta et al., 2008).

1.2.2 Spongy bone

Spongy (cancellous) bone is lighter and less dense than compact bone. Spongy bone consists of plates (trabeculae) and bars of bone adjacent to small, irregular cavities that contain red bone marrow. The canaliculi connect to the adjacent cavities, instead of a central Haversian canal, to receive their blood supply. It may appear that the trabeculae are arranged in a haphazard manner, but they are organized to provide maximum strength, similar to braces that are used to support a building. The trabeculae of spongy bone follow the lines of stress and can realign if the direction of stress changes (<http://www.daviddarling.info/encyclopedia/B/bone.html>).

1.2.3 Bone cells

There are three main types of bone cells: osteoclasts, responsible for bone resorption; osteoblasts, responsible for bone formation; and osteocytes, fully differentiated osteoblasts that have become embedded in matrix, whose function is to maintain the bone (Hillsley and Frangos, 1994):

1.2.3.1 Osteoblasts: Bone-forming cells that synthesize and secrete unmineralised ground substance, generally abundant in areas of high bone metabolism such as under the periosteum and next to the medullary cavity. They are also responsible for the production of bone mineral as will be discussed.

1.2.3.2 Osteocytes: Osteocytes lie encased within the bone matrix (Nefussi et al., 1991, Palumbo et al., 1990). They have long slender cell processes connected by gap junctions that connect to each other and also to connect to bone lining cells (Doty, 1981).

1.2.3.3 Osteoclasts: Large, multinuclear cells that enzymatically break down bone tissue, influencing bone growth, remodeling, and healing.

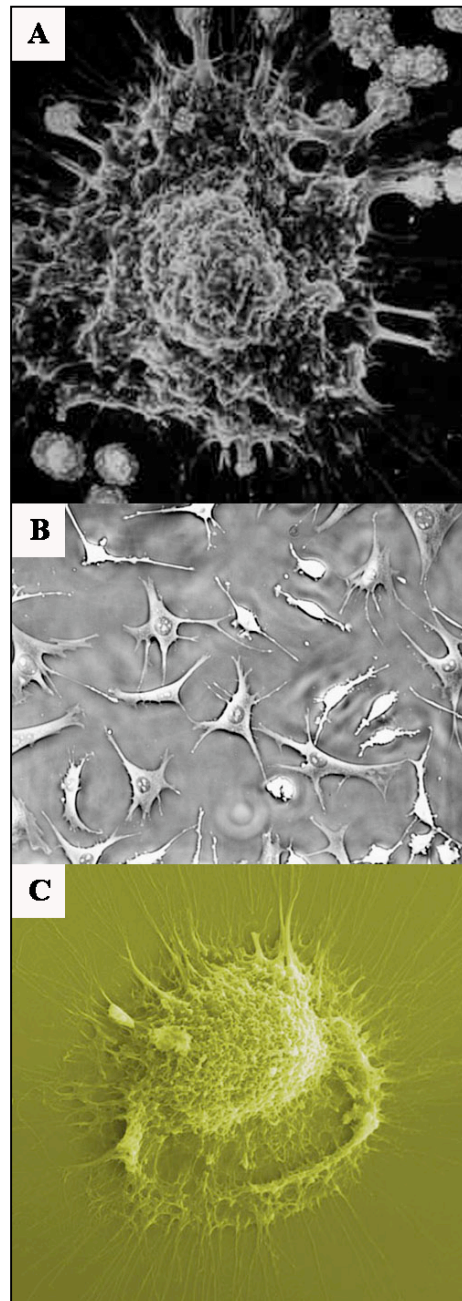


Figure 1.2 Bone cells: (A) Osteoblasts are responsible for synthesis, deposition and mineralization of the bone matrix (<http://www.mypondsoftware.com/bone.jpg>).

(B) Osteocytes are mature bone cells involved in bone response to mechanical loading (https://vault.swri.org/cms/upload/cells_500pixels.jpg).

(C) Osteoclasts are large multinucleated cell responsible for the dissolution and absorption of bone (http://www.weizmann.ac.il/sb/faculty_pages/Addadi/osteoclast.html).

1.3 Bone modeling and remodeling

As has been described, the basic multicellular unit of bone comprises the osteocytes, osteoclasts and osteoblasts. Activities of this unit are regulated by mechanical forces, bone cell turnover, hormones (e.g. parathyroid hormone, growth hormone), cytokines and local factors. The activation process is at least partly regulated by the osteocytes, which detect mechanical stress and respond to biochemical stimuli. Direct communication via gap junctions (or hemichannels) between osteocytes and osteoblasts is critical for osteoblast response to physical stimuli (Civitelli, 2008). Activation results in the lining cells of the endosteal surface being retracted, and digestion by matrix metalloproteinases of the endosteal collagenous membrane. Osteoclasts are then recruited and mediate resorption of the underlying bone. Subsequently, osteoblasts are recruited to the resorption cavity and lay down new osteoid, which eventually becomes calcified; this process is completed in approximately 3–6 months. The rate of bone turnover varies according to the type of bone; being highest in sites where trabecular bone predominates such as vertebrae and lowest at sites high in cortical bone such as the hip (Chen et al., 1997, Datta et al., 2008, Modder and Khosla, 2008). Bone remodeling can, in fact, be separated into three phases: initiation phase, transition phase and termination phase as shown in figure 1.3 (Matsuo and Irie, 2008, Hadjidakis and Androulakis, 2006, Fernandez-Tresguerres-Hernandez-Gil et al., 2006).

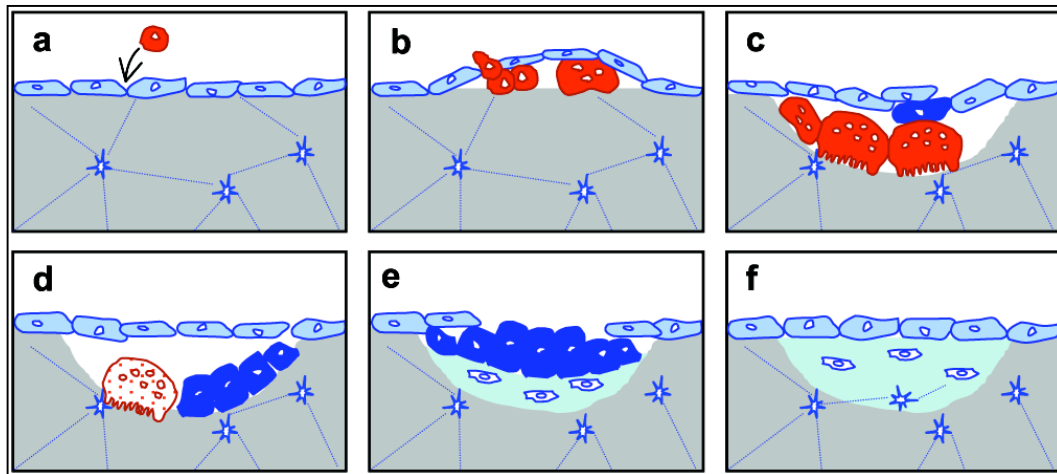


Figure 1.3 Bone remodeling and possible osteoclast–osteoblast interactions (Matsuo and Irie, 2008). Cells from osteoclast (red) and osteoblast (light and dark blue) lineages are shown. (a) Recruitment of osteoclast precursors in the early initiation phase. (b) Differentiation of osteoclasts on the bone surface beneath lining cells (light blue) in the initiation phase. (c) Bone resorption by multinucleated osteoclasts, which induce osteoblast differentiation (dark blue) in the transition phase. (d) Osteoclast apoptosis in resorption lacunae in the transition phase. (e) Bone formation by osteoblasts and osteocyte generation in osteoid in the termination phase. (f) Entry into quiescence in the termination phase.

1.4 Stem cells and Osteoblast differentiation

Bone marrow contains the hematopoietic stem cells and mesenchymal stem cells (MSCs). The MSCs are multipotent stem cells that give rise to progenitors for several mesenchymal tissues, including bone, cartilage, tendon, adipose, and muscle (Caplan, 1994, Majumdar et al., 1998). This characteristic is known as multipotency. Bone marrow stromal or mesenchymal stem cells are fibroblastic in appearance (they were originally termed fibroblastic colony forming units) and have osteogenic differentiation potential (Friedenstein et al., 1992). These cells are located at the perivascular spaces surrounding the vascular sinusoids in the bone marrow (Sacchetti

et al., 2007) and can roughly be isolated from hematopoietic cells of bone marrow by selective adherence to plastic surfaces (Rickard et al., 1996). That said, the adherent population is, in fact, heterogeneous and contains primitive MSCs, cells that have started to commit and mature, terminally differentiated, cells (e.g. committed osteoprogenitor, pre-osteoblast and osteoblast), and is better described as the osteoprogenitor population (Triffitt JT, 1998). The use of the monoclonal antibody STRO-1 to bind specifically to an MSC surface marker is helpful in separating the most primitive MSCs as a homogeneous fraction from the total adherent cells – i.e. the true stem cells rather than e.g. committed osteoprogenitors etc. These cells are multipotent stem cells that may give rise to different tissues. Bone marrow is not the only source of osteoprogenitor cells, however, it is still by far the best characterized source (Vaananen, 2005).

For MSCs to differentiate along the osteoblastic lineage requires activation of key transcription factors and coordinated interaction among diverse endocrine, paracrine and autocrine factors (Datta et al., 2008). Examples of known signalling pathways of bone differentiation are reported below:

(1) Wnt: Wnt/ β -catenin signaling regulates osteogenesis through multiple mechanisms. Wnts repress alternative mesenchymal differentiation pathways such as adipocyte and chondrocyte differentiation and promotes osteoblast differentiation, proliferation, and mineralization activity while blocking osteoblast apoptosis. By increasing the ratio of osteoprotegerin (OPG) to RANKL, β -catenin represses osteoclastogenesis. (Krishnan et al., 2006).

(2) Bone morphogenic protein (BMP): Activation of BMP receptors initiates phosphorylation of the downstream effector proteins, known as receptor-regulated Smads (SMADs are molecules of relative molecular mass 42K–60K with two regions of homology at the amino and carboxy terminals, termed Mad-homology domains MH1 and MH2, respectively, which are connected with a proline-rich linker sequence (Heldin et al., 1997)), leading to signal transduction. Receptor-regulated Smads form

a hetero-oligomeric complex with a common mediator Smad, which translocates into the nucleus and regulates target gene transcription (ten Dijke, 2006).

(3) Runx2: Runx2 enhanced PI3K-Akt signaling by up-regulating the protein levels of PI3K subunits and Akt, whereas PI3K-Akt signaling greatly enhanced DNA binding of Runx2 and Runx2-dependent transcription (Fujita et al., 2004). Osterix, beta-Catenin and ATF which act downstream of Runx2 contribute to the control of osteoblastogenesis (Marie, 2008). Osterix (Osx) is a zinc finger transcription factor specifically expressed by osteoblasts which is important for osteoblast differentiation (Caetano-Lopes et al., 2007).

Better understanding of the molecular signaling involved in osteogenic differentiation of osteoprogenitor cells and how materials can influence these processes is a key to the development of next-generation biomaterials. Specifically, 3rd generation biomaterials have been described as materials that will not only support tissue (1st generation), not only be bioactive / biodegradable (2nd generation) but will also allow known control of individual cells at the molecular level (Hench and Polak, 2002).

In this thesis, the adherant cells of the marrow; the osteoprogenitor cells were used. This is because they are the most representative of the cell type an implant would have to influence *in vivo*, they contain MSCs and also, for bone tissue engineering purposes, they allow rapid expansion of cells that can form bone. If pure MSCs were to be use, the very low numbers in the marrow would necessitate very long isolation, purification and culture times until usable numbers were available. In the meantime, the patient would be waiting for therapy and the cells would stand a greater chance of e.g. infection.

1.5 Bone mineralisation

The bone mineral substance has two main functions:

(1) Biomechanical control for maintaining the stability of the skeleton.

(2) Metabolic control as a reservoir of many ions and control of mineral homeostasis. Mature bone tissue is composed of 60–70% mineral substance and 30–40% organic substance (mainly consists of type I collagen fibrils). Bone mineral is metabolically active and interactions between ions from the extracellular fluid and ions constituting apatite crystals are possible. This can happen in every step of bone formation from initial formation to growth, maturation and dissolution. Crystal growth depends on diffusion of ions and the degree of mineralization slows if the water content becomes too low. Consequently, in young bone tissue, the water content is high and ions are constantly exchanged with apatite. Conversely, in old bone tissue, these exchanges decrease considerably (Boivin and Meunier, 2003).

Matrix vesicles are extracellular vesicles with a diameter of 100 nm thought to be important in new mineral growth, i.e. they protect the nucleation of mineral. The biogenesis of these vesicles occurs by polarized budding and pinching from specific regions of the outer plasma membrane of chondrocytes, osteoblasts, and odontoblasts and selectively located within the matrix of bone (or cartilage during endochondral ossification). The mineralization process has two stages:

Phase 1 mineralization: production of initial apatite mineral crystals occurs within the matrix vesicle membrane and is controlled by phosphatases such as alkaline phosphatase and Ca-binding molecules such as annexin1 and phosphatidyl serine.

Phase 2 mineralization: begins with breakdown of matrix vesicle membranes, exposing preformed apatite to the extracellular fluid. After that mineral crystal proliferation is governed by extracellular conditions. The extracellular fluid normally contains sufficient Ca^{2+} and PO_4^{3-} to support continuous crystal proliferation. (Anderson, 1995, Anderson, 2003).

1.6 Mechanotransduction

Bones are designed to cope with and respond to mechanical force during their lifetime, thus mechanotransduction is likely to impact upon bone formation. Physical forces, including gravity, tension, compression and shear force influence growth and remodeling in all living tissues at the cellular level (Ingber, 1997a, Ingber, 1997b). Mechanotransduction is the process by which mechanical changes in the extracellular environment are converted in genomic and ultimately proteomic (e.g. phenotypical) changes (Lele et al., 2006).

1.6.1 Mechanical forces control cells

In mature bone tissue, mechanical response is largely controlled by osteocytes, which respond to a loading-induced flow of interstitial fluid through the lacuno-canalicular network by producing biochemical molecules such as prostaglandins E₂ (PGE₂) and insulin-like growth factor I (IGF) (Burger and Klein-Nulend, 1999). These signalling molecules can induce bone modeling and remodeling. Other than via biochemical molecules, osteoclasts and osteoblasts can communicate with each other through cell–cell contact and cell–bone matrix interaction (Matsuo and Irie, 2008).

Interactions between cells and their environment can induce cell deformation (changes in cellular morphology) and in-turn, induce cytoskeleton rearrangements. In tissues, there are many nanoscale cues for cells to interact with and that will alter cell morphology. For example, the fibers of the ECM and basement membrane (10 to 300 nm in diameter), their interconnecting nanopores, and hydroxyapatite crystals (4 nm) found in natural bone, typically have nanoscaled dimensions (Stevens and George, 2005). As cells respond to their nanoenvironment they can develop (or indeed depolymerise) contractile stress fibres through adhesion remodeling, producing forces that act on themselves (change of morphology) and upon their adhesions which then, in-turn, will organize the ECM and neighbouring cells (Curtis and Riehle, 2001). The cytoskeleton and cell adhesions interact with a large number of signalling

molecules, as will be discussed. In this context, mechanotransduction is the conversion of physical force, such as contractile forces, occurring at cell–extracellular matrix contacts (focal contact and focal adhesion), into biochemical signaling (Bershadsky et al., 2003).

Cellular adhesion molecules that play an important role in focal adhesion formation and subsequent signalling are the α and β subunits of the integrin family. Integrins link the extracellular matrix with the actin cytoskeletons via the cytoplasmic domains of β -integrin subunits. At this site, adaptor molecules such as talin, actinin, filamin and tensin connect directly to actin cytoskeletons (Bershadsky et al., 2003, Geiger et al., 2001, Liu et al., 2000). Some of these adaptor proteins (talin and tensin) belong to a phosphotyrosine-binding module that links the integrin receptors to the actin cytoskeleton (Calderwood et al., 2003). The role of talin is not only to link the cytoplasmic tail of β -integrins to the actin cytoskeleton but also to increase the affinity of the extracellular domain of integrin for the extracellular matrix while tensin negatively regulates actin assembly by capping the barbed end of filaments through its central domain (Le Clainche and Carlier, 2008). As previously discussed, osteocytes respond to mechanical stimuli with the production of signaling molecules which modulate the activities of osteoblasts and osteoclasts, thus converting mechanical stimuli into cellular signals (Klein-Nulend et al., 2005).

1.6.2 Focal adhesions

Cells start by forming small dot-like adhesion sites with diameters less than 1 μm called focal contacts (or focal complexes). Adhesion takes place when lamellipodia are formed. Protruding lamellipodia contain a polymerizing network of actin filaments (Bershadsky et al., 2003, Geiger and Bershadsky, 2001). The maturation of focal contacts to focal adhesions happens by conversion of actin filament networks to contractile stress fibers (Heath and Dunn, 1978). These stress fibers apply tensile force to the contacts, resulting in integrin gathering into larger focal adhesions; these focal adhesions are essential for subsequent cell signaling (Bershadsky et al., 2003,

Mogilner and Oster, 2003). Association between integrins and the extracellular matrix proteins, the starting point of focal contact formation is shown in figure 1.4.

The cell cytoskeleton which is tethered to the adhesions plays a central role in cellular mechanotransduction in all vertebrate cells (Ingber, 1997b). The cytoskeleton is thought to provide the cytoplasm with the inhomogeneity required for long-distance force propagation (Wang and Suo, 2005). Furthermore, it is considered to act as an interconnected percolation network made of the microfilaments, microtubules and intermediate filaments (as will be described) that relay mechanical signals from adhesion to nucleus. The percolation theory is analogous to a spider in a web whereby the web is the extracellular matrix that relays mechanical signals (from changes in flow, stiffness, chemistry or topography) to the spiders legs (the cytoskeleton) which in-turn replay the signal to the spiders body (the nucleus) allowing the spider to act (change genomic / proteomic output). A specialization on this theory is cellular tensegrity.

The cytoskeletal networks are thought to maintain a constant, basal level of tension, so that small, local deformations affect overall cytoskeletal tension, initiating cellular deformation. For this to be achieved, the cytoskeleton would have to be stabilized both through compression and tension with applied pre-stress from the focal adhesions. This is, in fact, an old architectural principle that describes tensile structure stabilization and when applied to a cell, the balance of tension between cytoskeleton is called cellular tensegrity (Ingber, 2003a, Ingber, 2003b). Tensegrity theory will be expanded on further in the introduction.

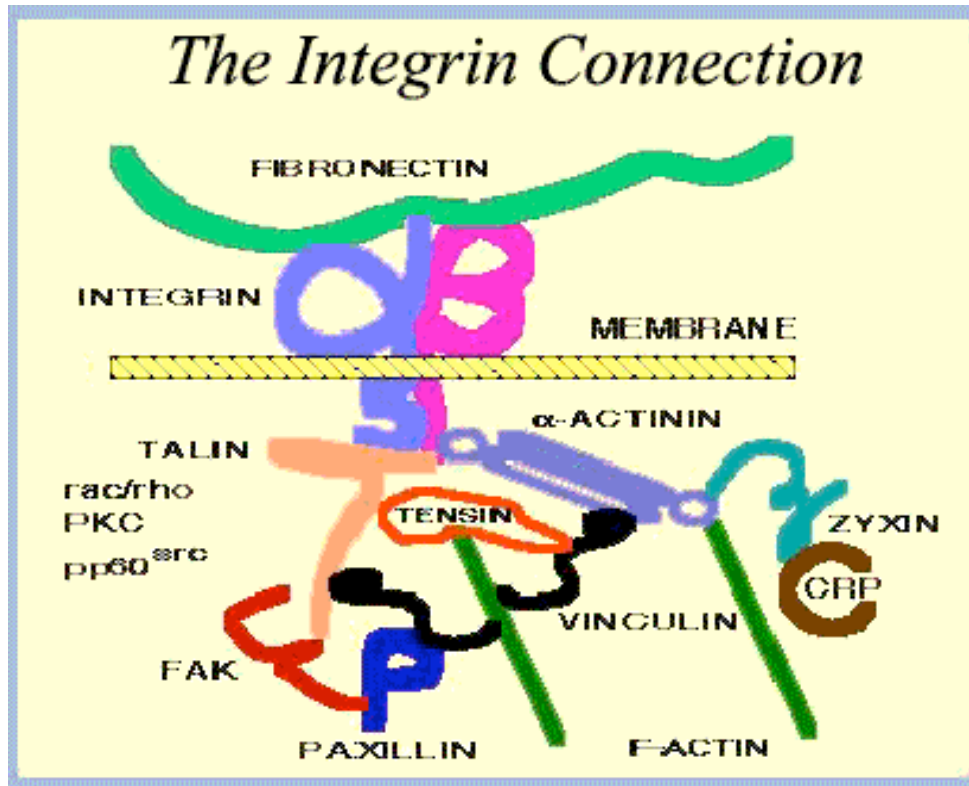


Figure 1.4 Association between integrins and extracellular matrix proteins such as fibronectin is a key event in cell adhesion. This phenomenon will recruit many adaptor proteins which may affect cytoskeletal rearrangement. Adapted from (<http://www.palaeos.com/Eukarya/Eukarya.Origins.2.html>).

1.6.3 Cytoskeleton: The cytoskeleton is composed of three distinct elements: actin microfilaments, tubulin microtubules and intermediate filaments (intermediate filaments vary in composition but, in mesenchymal cells, they are made of vimentin). The actin cytoskeleton allows formation of cell protrusions (filopodia, lamellipodia) and contractile forces through stress fibre polymerization. Microtubules form a polarized network allowing organelle and protein movement throughout the cell and are thus important in metabolism and e.g. guidance of new proteins through the golgi body. Intermediate filaments are generally considered the most rigid component, responsible for the maintenance of the overall cell shape and are thought to be involved in cushioning the nucleus from sudden shock.

1.6.3.1 Microfilaments (MFs) or actin filaments: Actin filaments (F-actin) are formed by two polymers of globular subunits (G-actin) that bind and hydrolyse ATP. These filaments have a 6 nanometer diameter. Actin filaments have inherent polarity, a plus ('barbed') end and a minus ('pointed') end. These filaments can form stress fibres which are composed of bundles of approximately 10-30 actin filaments. These bundles are held together by the actin-crosslinking protein α -actinin and alternate with bands containing non-muscle myosin and tropomyosin (Pellegrin and Mellor, 2007). Actin filaments are also dynamic polymers, of which each end can either polymerize or depolymerize and net growth depends on free subunit concentrations (Li and Gundersen, 2008).

1.6.3.2 Intermediate filament (IFs): The IFs have a 10-nanometer diameter. In contrast with MFs and MTs, the molecular building blocks of IFs are not globular proteins but fibrous proteins (Herrmann and Aebi, 2004). They are dimers composed of two α -helical chains oriented in parallel and intertwined in a coiled-coil rod (Herrmann and Aebi, 2000, Herrmann and Aebi, 2004). The association of dimers results in linear arrays, four of which associate in an anti-parallel, half-staggered manner to produce protofibrils; and three to four protofibrils intertwine to produce an apolar intermediate filament. There are a number of IF proteins including: desmin in muscle, cytokeratin in hair and epithelia, lamins (these are nucleoskeletal proteins which line the inner surface of the nuclear membrane) and vimentin IFs of fibroblasts and other cells from the mesenchymal route (Fuchs and Cleveland, 1998). Dimer association of these IFs are slightly different as shown in figure 1.5.

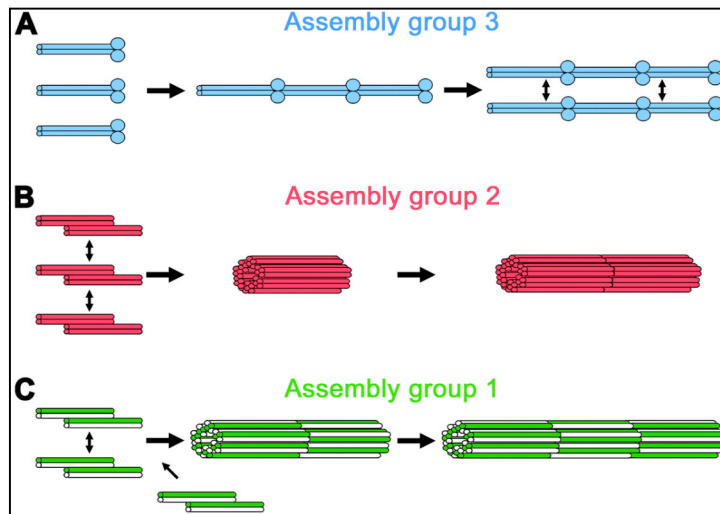


Figure 1.5 The three major IF assembly groups (Herrmann and Aebi, 2004). (A) Lamin dimers associate first into head-to-tail filaments that later laterally associate. The orientation of the two associating filaments is arbitrary. (B) Vimentin assembly starts from antiparallel, half-staggered double dimers (or tetramers) to form full-width, unit-length filaments. (C) Keratins assemble from heterodimeric tetramers by lateral and nearly concomitant longitudinal assembly into heterogenous full-width filaments.

1.6.3.3 Microtubule (MTs): MT functions are varied and include chromosome movement and vesicular trafficking. MTs are cylindrical organelles of varying lengths and an overall diameter of 25 nm. The central hollow core is 15 nm in diameter and the MTs wall is approximately 5 nm thick. MTs are composed of α - and β -tubulin heterodimers of which each monomer is a 55-kDa globular protein, arranged head-to-tail to form a polar protofilament. Thirteen protofilaments assemble by lateral interactions to form the MTs wall lattice (Brinkley, 1997).

1.6.4 Tensegrity model and signal transduction of surface topography

It is now widely considered that cells act as percolation structures in order to relay mechanical signals to the nucleus. This is both biochemical and biomechanical, with alterations in cytoskeletal tension resulting in changes to linked biochemical signaling

and also to the shape of the nucleus. However, simple percolation does not fully explain how the cytoskeleton distorts the nucleus. One elegant theory, where tension is central does start to address cell behaviours in a biomechanical manner, has been proposed.

The cellular tensegrity model proposes that the whole cell is a prestressed tensegrity structure. In the model, tensional forces are borne by cytoskeletal microfilaments and intermediate filaments, and these forces are balanced by interconnected structural elements under compression, most notably, internal microtubule struts and extracellular matrix (ECM) adhesions. A key observation in support of this is morphology of cytoskeletal fibres within a cell. In a Petri dish: microfilaments are wavy - in a cell they are straight suggesting they are under tension, intermediate filaments are curly – in a cell they are merely wavy, again suggesting tension, microtubules are straight – in a cell they are wavy suggesting compression (Ingber, 2003a, Ingber, 2003b).

The topography of a surface engineered with nanoscale structural features can be used to control cell behavior (Biggs et al., 2008a, Curtis and Wilkinson, 1997). Cell growth, differentiation, secretion, movement, signal transduction, and gene expression all can be altered by applying mechanical stresses directly to cultured cells (Ingber, 1997a). Changes in the topographical features of a surface affect the structural organization and interconnection of the cytoskeleton, akin to application of mechanical forces, and provides a physical basis for translating mechanical forces into a biochemical response (Curtis et al., 2006, Ingber, 1997a).

The tensegrity models predict that living cells and nuclei may be hard-wired to respond immediately to mechanical stresses transmitted over cell surface receptors that physically couple the cytoskeleton to extracellular matrix or to other cells. Tensegrity also offers a mechanism to explain how the cytoskeleton remodels in response to stress and, hence, how signaling molecules that are immobilized on this insoluble scaffold might change their distribution and function when force is applied

to the cell surface. For example, changes in cellular deformity can affect stretch-activated ion channels and contribute to Ca^{2+} (Iribe and Kohl, 2008) or chloride (Han et al., 2008) release that can then influence signal transduction. Changes in topography will cause the cells to remodel their adhesions and this has been shown to change integrin, paxillin and phosphorylated focal adhesion kinase (pFAK) arrangements on nanostructured silicon surfaces (Heydarkhan-Hagvall et al., 2007). Furthermore, topography will regulate stabilization of adhesions through changes in scaffolding proteins such as RACK 1. RACK 1 is recruited to large focal adhesions to stabilize the cell. If the cell needs to contact guide to e.g. grooves, this protein is then downregulated to allow the formation of smaller focal contacts, in turn allowing increased cell motility (Dalby et al., 2008b). Changes in proteins such as FAK, an important adhesion regulated kinase, will impact greatly on biochemical signalling within the cell. FAK is involved in regulation of G-proteins, for example Rho (involved in cell lamellipodial formation), Rac (involved in stress fibre formation) and Cdc42 (involved in filopodia formation). It also forms part of the extracellular receptor kinase pathway (ERK) which influences many transcription factors responsible for cell differentiation, e.g. Runx2 / Cbfa1, the osteogenic mastergene) (Franceschi et al., 2007).

It is thus likely that there are two modalities of adhesion and cytoskeletal signaling, indirect and direct. Indirect describes biochemical pathways effecting transcription factors while direct refers to changes in the extracellular environment, e.g. topography that result in deformation of the nucleus via the cytoskeleton. This is likely to be by tensile ‘pulling’ of the nucleus as it is unlikely that the cytoskeleton has the necessary stiffness to compress the nucleus (perhaps when compressed, the nucleus experiences tension at 90° to the direction of force). It is postulated that this will alter the arrangement of chromosomes within the interphase nucleus and that this will in turn affect diffusion of transcription factors, location of genes and transcription factors, alter the efficiency of polymerase motors etc; the net result being changes in genome and proteome regulation (Dalby et al., 2007a, Dalby et al., 2007c, Bryant et al., 2003, Osborne et al., 2004). This said, it is very hard to dissect

out the distinct effects of either mechanotransductive mechanism.

1.7 Scaffolds and surface topography

The cellular scaffold can be the extracellular matrix (ECM) *in vivo* and e.g. a synthetic substratum *in vitro* and provides signaling cues based upon the architecture and chemistry presented to the cells (Takezawa, 2003). Cell-substratum and cell-cell interactions play crucial roles in tissue engineering in terms of adhesion, proliferation, migration, differentiation and gene expression. *In vivo*, interaction of cells with the extracellular matrix (ECM) via cell adhesion molecules is key to subsequent changes and this is also true *in vitro*. Thus, the use of synthetic surfaces/scaffolds is one of the underpinning strategies in biomaterials and tissue engineering. Cells respond to the topography of substrates in the micro/nano range in terms of adhesion, proliferation, migration, and gene expression (Jager et al., 2007). However, cells in their natural environment also interact with extracellular matrix components in the nanometer scale, as has been described (Yim and Leong, 2005).

In this present study, both micro- and nanoscale topographies have been used to direct cell behavior. Primarily, the focus for this thesis is the use of nanoscale topography for bone tissue engineering purposes. The topographies were prepared using a three-step process. Firstly, either photolithography or electron beam lithography was used to define patterns in silicon (as is traditionally used in the microelectronics industry; photolithography has been the workhorse of microchip fabrication for many years and EBL has developed from this and is the most high-resolution top-down fabrication tool available) (Vieu C, 2000, Wilkinson CDW, 2002) . Secondly, the silicon masters were sputter-coated and electroplated with nickel (Ni) to create a negative ‘shim’. This is similar to the process currently employed to fabricate DVDs and CDs, whereby polycarbonate is injection moulded against Ni shims. These methodologies will be expanded on in the Materials and Methods.

The topography can then be transferred into a thermo-sensitive biopolymer such as polycaprolactone (PCL) by embossing. PCL is one of the most popular biopolymers used in tissue engineering and it is a FDA (Food and Drug Administration) approved biocompatible and biodegradable polymer (Sinha et al., 2004). PCL is a synthetic polyester that can easily be degraded by microorganisms. PCL is degraded by lipases, esterases and PCL depolymerases (Shimao, 2001). It can be prepared by ring-opening polymerization of ϵ -caprolactone and has melting point ranging between 59 and 64 °C (Sinha et al., 2004).

Surface topography is desirable as it can regulate cell behavior in a reproducible manner. Depending on individual topographic features, the desired cell function may vary e.g., adhesion preference to specific substrates, patterning ability on predetermined substrate regions, variable migration, improved proliferation, controlled cell-to-cell communication, modulated phenotypic differentiation, altered responsiveness to chemical and physical extracellular signals, and programmable apoptosis (Spatz and Geiger, 2007, Tung et al., 1988). The development of purpose-specific regulators of cellular systems would enable the regeneration of neo-tissue in tissue engineering (Lim and Donahue, 2007). Cellular developments such as proliferation, differentiation, migration or apoptosis are guided by multiple surface cues that are potentially remodeled during cell culture assays. The cell responses are controlled by intracellular signaling pathways that are originally triggered by transmembrane proteins interacting with the engineered surface (Falconnet et al., 2006, Hynes, 2002).

The use of surface topography to direct stem cell differentiation has been proposed as a new and innovative strategy in bone tissue engineering. Cells require an adhesive surface to exert forces and consequently spread. The ability to constrain the spreading to a specific cell-surface contact area has been shown to dramatically affect cellular development (McBeath et al., 2004). In this study, it was shown that microcontact printing of fibronectin squares of either 1000 μm^2 or 10000 μm^2 could alter MSC

fate. The squares were printed on a low-adhesion background and the small squares caused adipogenic differentiation (with rounded cells) and the large squares caused osteogenic differentiation (with large, well-spread cells).

Mechanical compliance of cell-adhering substrates can also substantially affect the cellular response and development. For example, MSCs cultured on a low stiffness substrate (Young's modulus of 0.1-1 kPa) will form neuronal cells, on a medium stiffness (Young's modulus of 8-17 kPa) they will form smooth muscle cells and on a stiffer materials (Young's modulus of 25-40 kPa – similar to unmineralised osteoid) they will form osteoblasts (Engler et al., 2006).

Microtopography has been shown to initiate preosteoblast cell differentiation associated with Runx2 and osteocalcin gene expression (Schneider et al., 2004). Furthermore, highly controlled microstructures on PMMA could induce rat MSC differentiation into an osteogenic lineage (Engel et al., 2009).

At the nanoscale, different features of nanoscale topography can influence a number of cell types in various ways. Well-defined nanopillar arrays of polyethylene glycol were used to modulate the adhesion and growth of cardiomyocytes (Kim et al., 2005a). Ridges/grooves fabricated in polystyrene can induce contact guidance and produce oriented growth of glioma cells along defined axes (Zhu et al., 2004). The morphology and proliferation of smooth muscle cells was altered when cultured on nanogrooved surfaces (Yim et al., 2005). Microneedle-like posts have been used as mechanical sensors to control cell adhesion and it was found that RhoA had a vital role in this mechanism (Tan et al., 2003). Nano-porous alumina membranes with different sizes can alter molecular responses of smooth muscle cells (Nguyen et al., 2007). These, and similar, studies indicate a role for nanotopography in modulation of tissue formation.

The definition of 'nano' depends on which genre/field it is applied to. The nanno prefix used to classify very small organisms whose dimensions are now measured to

be as small as 200 nm in diameter (Joachim, 2005). Generally nanotechnology deals with structures of the size 100 nanometers or smaller, and involves developing materials or devices within that size.

More recently, it has been shown that nanotopography is critical for MSC differentiation. Ordered materials, typically generated by e.g. electron beam lithography, produce surfaces with low cell adhesion. Random roughening, on the other hand, has yielded interesting results and has shown that changes in skeletal stem cell differentiation can be influenced that are different from planar controls (Leven et al., 2004). However it is impossible for the researcher to identify which features of a random surface are influencing stem cells. A novel, third way with controlled-disorder patterns defined using electron beam lithography has recently been reported. Employing pits with 120 nm diameter (100 nm deep) with either fixed 300 nm centre-centre spacing in a square pattern or through random placement both the highly-ordered and random cell environments were mimicked. Cell growth substrates were also fabricated with deliberately disordered pits in a square arrangement. This gave an average of 300 nm centre-centre spacing but with either ± 20 nm or ± 50 nm error in X and Y from a true square placement. Whilst planar control, true square and random substrates produced negligible differentiation, bone differentiation with similar efficiency as with chemical (dexamethasone and ascorbate) treatment was observed on the disordered patterns (Dalby et al., 2007b).

These three key observations (chemistry, stiffness and topography) are described as biomimetic. Cell bodies have different shapes and sizes and confinement to these sizes through mechanics or adhesion modulation may instruct the stem cells take on the roles of differentiated cells naturally found in those size ranges. Different organs have different Young's moduli and it would appear that growth substrates of moduli typical to specific organs can in turn induce tissue-specific differentiation. In addition, cells are surrounded by the nanoscale shapes of fibrillar protein assemblies (Stevens and George, 2005). However, these features will have a greater variation in size and position than can be achieved with electron beam lithography and it may be

that the degrees of order that are biologically achievable are important whereas either strict order or randomness is not as biomimetic. Moreover, cells in the body experience these cues not as static parameters but as stimuli which vary in space and time. Therefore cells are highly responsive to signalling gradients including:

- chemotaxis (Kay et al., 2008) and haptotaxis (Thiery, 1984) for chemical gradients (free from and attached to a surface respectively).
- galvanotaxis (Mycielska and Djamgoz, 2004) for electrical gradients.
- durotaxis (Lo et al., 2000) for elasticity gradients.
- contact guidance for topography (Curtis and Varde, 1964).

Thus, it would appear logical that for a cell type that is actively seeking their fate, i.e. stem cells, these will be critical environmental cues and their display in a tissue engineered application must mimic their natural *in vivo* presentation (Boonen et al., 2009, Heidi Au et al., 2009, Sanchez-Fernandez et al., 2008).

1.8 Bioreactors for bone tissue engineering

To achieve the biomass production for potential clinical applications of tissue engineering, a system or compartment that can accelerate tissue growth is required. This compartment will serve to contain the engineered construct under sterile conditions and provide the appropriate stimuli that would result in a neotissue with biochemical and biomechanical properties comparable to *in situ* tissue (Abousleiman and Sikavitsas, 2006). In the tissue engineering field such a system is described as a “bioreactor” and it is required to provide appropriate *ex vivo* conditions for cultured tissues. The bioreactor can be used as an optimum medium delivery system (e.g. flow, stirred or rotary) and can further be used to provide e.g. shear force to stimulate the cells via mechanosensitive signal transduction. Here, however, the bioreactor has simply been used to deliver a constant supply of fresh media to the cells to enhance growth. Due to the size of the flow chambers and the slow flow rate, the flow would be negligibly turbulent and the forces tiny.

The conventional method of using bioreactors in tissue engineering is to seed the appropriate cells onto biodegradable, biocompatible scaffolds which contain, for example, the desired topographic feature and cultivate the cell-scaffold constructs in the bioreactor, delivering a constant supply of fresh media.

1.9 Proteomics

Once cells were stimulated by e.g. topography, signal transduction cascades will be initiated. Conventionally, using biochemical or molecular analysis, researchers will investigate the regulation of the genome using PCR for a few specific genes or protein analysis (e.g. Western blot) for a limited number of selected proteins. However, it is possible that many other pathways could also be stimulated alongside the pathways traditionally considered of importance. Thus, the monitoring of global changes induced by the stimulator is of potential value, since all signaling pathways function as a co-network with many interactions and feedback loops. The global observation of changes is even more important with the description of third-generation biomaterials that will not only provide mechanical support, but will have known molecular control over cells (Hench and Polak, 2002).

There is presently limited understanding of how surface topography directs stem cell differentiation - really all that is known is that it does. The comparison of global changes in protein expression in cells cultured on different topographies may provide novel data. The goal of comparative proteomics is to analyse proteome changes in response to different development or environment and is thus suitable for the observation of global protein changes to topographically structured surfaces compared to flat control surfaces (Minden, 2007). Due to the small sample size of tissue cultured material, sensitive analytical methods need to be employed.

1.9.1 Differential In Gel Electrophoresis (DIGE)

Recently, a fluorescent labelling based on traditional 2D gel electrophoresis but allowing direct comparison between control and test conditions has been developed.

In traditional 2D gel electrophoresis, two separate gels are run and compared by eye. However, dimorphism between two electrophoretic gels can cause difficulties such as coordinated spot mismatch. In DIGE, the control and test samples are labeled by different fluorescent dyes and then co-electrophoresed in the same gel. The differential intensity of the same 'spot' can then simply be considered. To achieve the highest volume of data while using the smallest amount of sample, for this thesis a highly sensitive saturation labelling technique was employed.

1.9.1.1 Saturation labelling: In minimal labelling (the standard, cheaper, alternative), lysine residues are covalently labeled at the ϵ -amino group with very low ratio of dye to protein, thus only 3–5% of the total protein present in the sample are labeled and at least 50 μg protein is needed (Marouga et al., 2005). Recently, Amersham developed a saturation Cy3 and Cy5 based system to enable co-electrophoresis of up to two samples on the same gel suitable for detecting differences in protein after only 5 μg total protein loading.

In all proteins, cysteines are low in prevalence and less abundant than lysine. Moreover, cysteine contains a thiol group which is needed for the labelling reaction (figure 1.6). This allows the saturation dyes to label all available cysteine groups on each protein (Westermeier and Scheibe, 2008). In contrast with minimal labelling, to achieve optimum labelling of cysteine residues, a high ratio of dye to protein is required. This set of dyes has a maleimide reactive group which is designed to form a covalent bond with the thiol group of cysteine via a thioether linkage. The saturation dyes have a neutral charge and they are matched in molecular weight (adding approximately 677 Da to the labeled protein). Consequently, as the CyDye DIGE fluor saturation (also referred to as scarce sample labelling) dyes are matched for charge and molecular weight, the same protein labeled with any of these dyes will migrate to the same position on a 2D gel. The Cy3, and Cy5 dye images are scanned sequentially with 532, and 633 nm lasers, respectively, and emission filters of 580 (band pass 30), and 670 nm (band pass 30), respectively. The CyDye DIGE filter and

laser combinations are selected to give the optimum results with minimal cross-talk between fluorescent channels.

1.9.1.2 Basic methodology in 2D gel electrophoresis:

First dimension: isoelectric focusing (IEF): Proteins are amphoteric molecules containing acidic and basic groups. They become protonated or deprotonated, depending on the pH environment. In a basic environment, the acidic groups become negatively charged; in acidic environments the basic groups become positively charged; the net charge of a protein is the sum of all negative or positive charges of the amino acid side chains. When an electric field is applied, the protein will start to migrate towards the electrode of the opposite sign of its net charge. At the isoelectric point (pI), the protein has no net charge and stops migrating (Lopez, 2007).

Immobilised pH gradient (IPGs) are prepared by co-polymerising acrylamide monomers with acrylamide derivatives containing carboxylic groups. In this case, the gradient cannot drift and it is not influenced by the sample composition. Several wide gradients of IPG strip have been used for the work presented in this study (e.g. 3–10, 4–7). The complete voltage load during IEF is defined in volt–hour integrals (Vh). If the applied Vh are insufficient, spots are not round and horizontal streaks are produced. Thus higher Vh loads are needed for samples containing high molecular weight proteins, more hydrophobic proteins and preparative runs. On the other hand, when the proteins are focused for too long, cysteines become oxidised and the pI of the proteins changes. This results in some proteins becoming unstable at their isoelectric point. The modified proteins have different pI values and start to migrate again with the horizontal streaks radiating from the spots. The best results are obtained with the shortest possible focusing phase at the highest possible voltage (Lopez, 2007).

The sample application is also important to obtain good 2D results. There are different modes of sample application to the first dimension IPG strip. In-gel rehydration loading is currently the preferred method, since it facilitates higher loads

and reduces focusing times. With this technique, the dehydrated IPG strip is directly reswollen with the protein sample dissolved in the rehydration solution. After a suitable rehydration time, the IPG strip is ready for the first dimension, with the proteins already uniformly distributed within the gel matrix. The advantage of in-gel rehydration is the large volume of sample that can be applied with the minimization of sample aggregation and precipitation since the sample is diluted through the entire gel strip (Lopez, 2007).

The strips containing the focused proteins are equilibrated in SDS buffer to transform the focused proteins into SDS-protein complexes, which are completely unfolded and carry negative charges only. They are then ready to be run on the second dimension, or they can be stored at - 60 to - 80 °C in a deep-freezer. In this study equilibration is performed once on a shaker. SDS at 2% is also sufficient for preparative protein loads. Recently, it has been demonstrated that by increasing the SDS concentration (from 2% to 10%), the solubilisation of hydrophobic proteins is improved. DTT is included in the equilibration buffer, to ensure that proteins are reduced prior to SDS-PAGE; when very high protein loads are analysed, the concentration of DTT needs to be increased.

Second dimension: SDS-PAGE: The second dimension of 2D separates proteins on the basis of their apparent molecular weights in polyacrylamide gels in the presence of SDS. In this step, large amounts of SDS is incorporated into the SDS-protein complex in a ratio of approximately 1.4 g SDS/ 1 g protein. Thus, SDS masks the charge of the proteins themselves and the anionic complexes formed have a more or less constant net negative charge per unit mass. Therefore, the electrophoretic mobility of proteins treated with SDS depends on the molecular weight of the protein alone.

The size of the gel clearly influences protein resolution. Typically, high-resolution 2D systems use 1–1.5 mm thick slab gels measuring 20 cm × 20 cm and are capable of resolving over 1500 proteins. Large gels provide a three- to four-fold increase in

the number of proteins detected. An appropriate acrylamide concentration is 12.5%. Lower percentages worsen the resolution of two-dimensional maps, and higher percentages (e.g. 15%) make the extraction of proteins from the gel more difficult for later studies. When the optimal conditions have been found, replicate gels should be run, to check whether the pattern differences observed are caused by the noise of the system or by variations between different samples (Lopez, 2007).

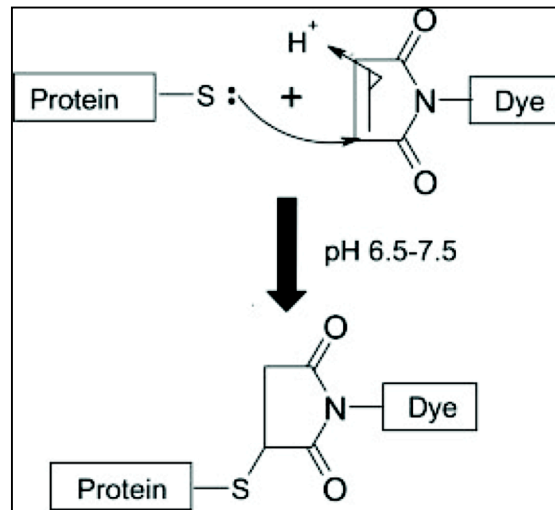


Figure 1.6 Saturation labelling: Schematic of labelling reaction of protein thiols with maleimide cyanine dyes (Shaw et al., 2003).

1.9.2 Dimethyl labelling

DIGE does have a number of limitations (e.g. the recovery of hydrophobic proteins) and thus some important data can be misinterpreted. Thus, another labelling method was applied to confirm the effect of nanotopography on osteoprogenitor cell differentiation. This method uses non-isotopic and isotopic formaldehyde to globally label the N-terminus and ϵ -amino group of lysine through reductive amination (figure 1.7). This labelling reaction is fast (less than 5 min) and complete without any detectable byproducts based on the analysis of matrix-assisted laser desorption/ionization tandem time-of-flight (MALDI/TOF) and electrospray mass spectrometry (ESI-Q-TOF). (Hsu et al., 2003). Since proteins from control and test

samples were differentially labeled by non-isotopic and isotopic formaldehyde, determined by comparison between the two labeled products can be performed by using LC/MS for quantification and LC/MS/MS for peptide sequencing. By modification of the protocols described by (Hsu et al., 2005, Hsu et al., 2006), this method has been applied in this thesis to detect the differential regulation of osteoprogenitor cell proteomes cultured on topography.

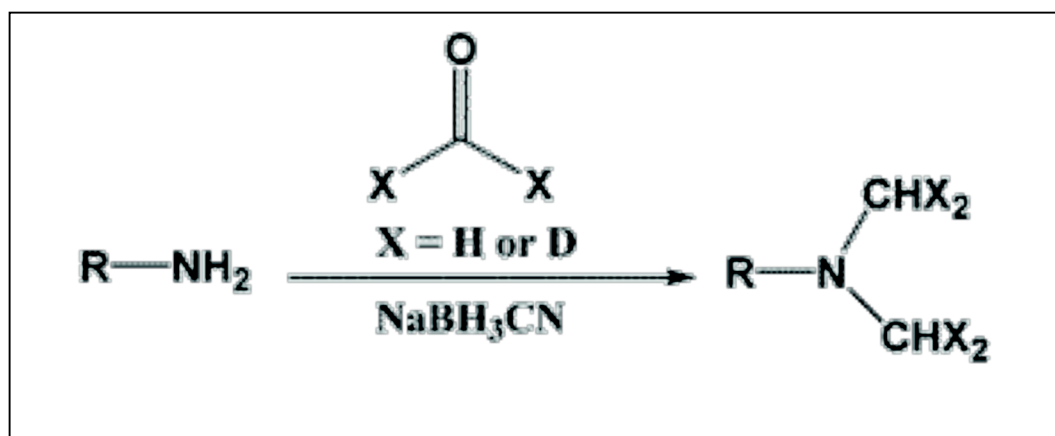


Figure 1.7 The dimethyl labelling reaction adapted from (Hsu et al., 2003). Formaldehyde reacts with the N-terminus, or an ϵ -amino group of a lysine residue, of a peptide to form a Schiff base that is reduced by sodium cyanoborohydride to form a secondary amine, which is relatively more reactive than the primary amine.

There are several advantages and disadvantages when compared to the other methods. The table 1 conclusively compares the advantages against the disadvantages of dimethyl labelling (Hsu et al., 2005, Krusemark et al., 2008).

1.9.3 Mass Spectrometry

Mass spectrometric analysis followed by database searching has become a well-established tool for the identification of biomolecules including proteins, nucleic acids, and carbohydrates. This thesis only focuses on peptide and protein identification. Traditionally, proteins are separated by 2D gel electrophoresis,

followed by staining, excision, in-gel digestion and the resulting peptides are analyzed by mass spectrometry

Table 1.1 The advantages and disadvantages of dimethyl labelling.

Advantage	Disadvantage
<ul style="list-style-type: none">• The isotopic formaldehyde used as the dimethyl labelling reagent is inexpensive and commercially available• The derivatization procedure for dimethyl labelling is relatively fast and simple• The ionic state is not changed significantly by dimethyl modification• The dimethyl modification is a global labelling that labels not only lysine residues but also the N-terminus of the peptide, without significant isotopic effects	<ul style="list-style-type: none">• It produces a large number of peaks, which requires a relatively pure sample or a greater separation power to resolve these peaks.

1.9.3.1 Matrix-assisted laser desorption/ionization time-of-flight mass spectrometry (MALDI-Tof-MS)

MALDI is a technique of transferring biomolecules into the gas phase as ions, by adding one charge to these molecules or analytes. The principle of this method is the embedding of such molecules into a crystal-like structure of weak organic acids called “matrix”. The matrix is responsible for ionization, facilitates desorption and protects the analytes from decomposition. Thus, the chosen matrix should be a substance that strongly absorbs the energy of the laser beam at a wavelength where analytes exhibit only weak absorption. After ionization and desorption, the charged molecules are accelerated in an electric field and gain a fixed kinetic energy. Subsequently, the mass/charge ratio is measured by the time of flight. The minimal amount of analyte needed in MALDI depends on sample purity and usually is in the low picomole range (Bonk and Humeny, 2001). Tandem MS (MS/MS) is an advanced MS technique utilizing two coupled mass spectrometric analyses.

1.9.3.2 The advantages of MALDI

- (1) A wide mass range can be analysed: Biomolecules of molecular weight from 1-300 kDa can be identified.
- (2) High accuracy. Mass accuracy is in the range of 0.01% so peptides up to 2 kDa can be measured with isotope resolution. Molecules up to 300 kDa can be analyzed within a few seconds.
- (3) High sensitivity: Analyte of picomolar concentration can be identified.

1.9.3.3 Matrix and soft ionization technique: As previously mentioned, the selection of the used matrix is important as well as sample–matrix preparation. The high excess of matrix : sample (from 100:1 to 10,000:1) is important, since the matrix serves as the absorber of the UV laser radiation and breaks down rapidly expanding into the gas phase. Additionally, the high matrix : sample ratio reduces associations

between analyte molecules and provides protonated and free-radical products that ionize the molecules of interest. As the analyte itself does not absorb the laser energy directly, the method is considered a soft ionization technique, allowing the analysis of complex biomolecules up to several hundred kilodaltons (Marvin et al., 2003).

1.9.3.4 MALDI/TOF/TOF

MALDI is traditionally coupled to TOF analysers. After the analyte molecules are ionized, they are drawn from the evaporation chamber into the MS by the voltage applied across the chamber. The principle of the TOF mass analysis is to measure the flight time of ions accelerated out of an ion source into a field-free drift tube to a detector. Mass-to-charge ratios are determined by measuring the time that ions take to move through a field-free region between the source and the detector as shown in figure 1.8 (Lane, 2005). The flight time is related to the mass-to-charge ratio (m/z) values of the gas-phase ions. Light ions arrive at the detector faster than heavy ions if they carry the same number of charges (Jonsson, 2001). Mass resolution is affected by slight variations in flight time, ions with the same m/z value but with different distances to the detector (different energetic ion) will consequently be detected at different time points and result in poor mass resolution. This problem was solved by the use of ion mirrors, or reflectrons (Mamyurin, 1973). The reflectron creates a retarding field that deflects the ions, sending them back through the flight tube. The more energetic the ion, the deeper it penetrates the retarding field of the reflectron before being reflected. Thus a more energetic ion will travel a longer flight path and arrive at the detector at the same time as less energetic ions of the same mass. For better sensitivity, coupling ion sources to mass analysers such as TOF-TOF analysers, in which two TOF sections are separated by a collision cell can be used. The Applied BioSystems (Framingham, MA, USA) model 4700 TOF/TOF mass spectrometers decelerate the precursor ions from 20 keV to 1–2 keV using a series of retarding lenses. The precursor ions are mass selected by a timed ion selector, composed of a dual deflector gating system and then dissociated in a collision chamber floating at 18

kV. The product ions enter a second source where they are reaccelerated (toward ground) and refocused by pulsed extraction. The product ions thus have a relatively narrow energy spread (1 or 2 keV) relative to the precursor energy, and are therefore easily focused by the reflectron (Cotter et al., 2007). The 10 most intense precursor ions from each spot were selected for MS/MS.

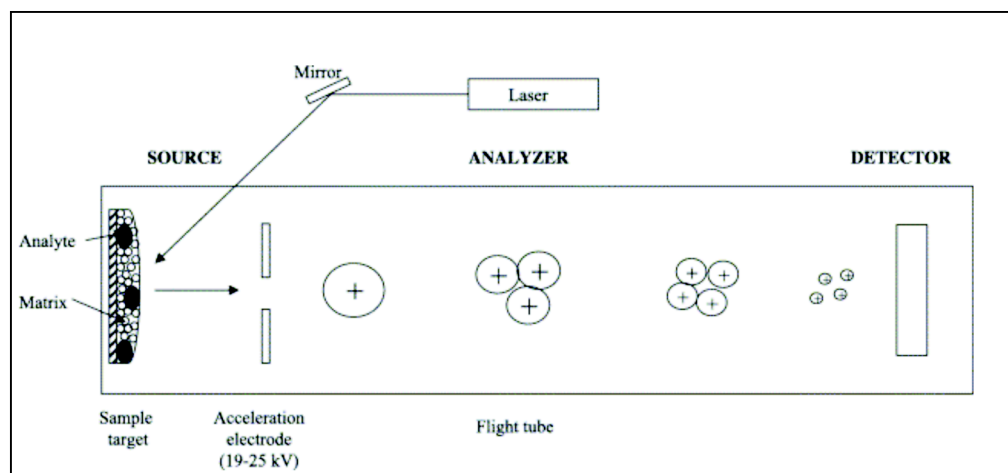


Figure 1.8 Principle of matrix-assisted laser desorption/ionization mass spectrometry. The analyte mixed with a saturated matrix solution forms crystals. The irradiation of this mixture by the laser induces the ionization of the matrix, desorption, transfer of protons from photo-excited matrix to analyte to form a protonated molecule (Marvin et al., 2003).

1.9.4 Database search

Database searching in proteomics represents the alignment of experimental mass fingerprints (mass analysis of proteolytic digests) against theoretical digests of whole databases. There are two main steps involved in this. The first is to assign to each of thousands of spectra a single putative sequence and an associated score related to the accuracy of the assignment. The second step is that of assigning an interpretable measure of confidence to one or a group of those identifications (Fitzgibbon et al., 2008). Mascot search engine was used to identify proteins in each spot. After the peptide mass fingerprint was recorded by a mass spectrometer (MALDI or ESI/MS), Mascot matches the fingerprints to a list of given masses held in the NCBItr

database.

These techniques have been developed in this thesis, as will be described, for use in biomaterials research and in the following chapters, the influence on proteins of mesenchymal stem cells cultured on topographical surface features will be analysed using a proteomic approach. Histology techniques and scanning electron microscopy were also used to determine the effects of surface topography upon cell morphology. This work aimed to improve the knowledge of biomaterials related to tissue engineering.

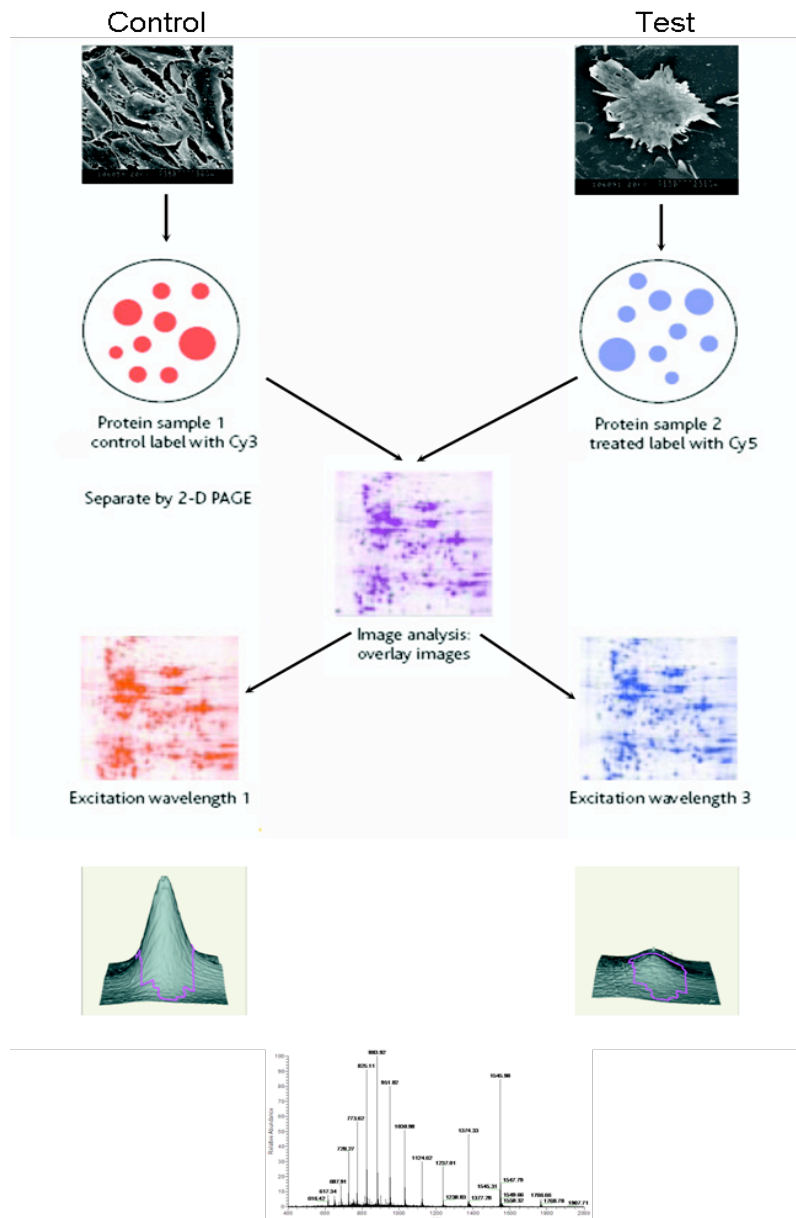


Figure 1.9 Differential In Gel Electrophoresis. The diagram presents the complete steps of using DIGE technique to analyse protein expressions in cells cultured on two different conditions, biomaterials compared to control. Adapted from (<http://www.medicalproteomics.com/images/DIGE.jpg>)

Chapter II Protocol optimizations and the application of micro-grooved topography

2.1 General Introduction

2.1.1 Part I. Introduction to the optimisation of DIGE for osteoprogenitor cells

The aim of this chapter is finding the optimal conditions for protein extraction and DIGE then to use those conditions to analyse the differential protein expression in cell culture on a micro-grooved model topography versus a flat surface. The following diagram (figure 2.1) presents the workflow of this protocol development chapter.

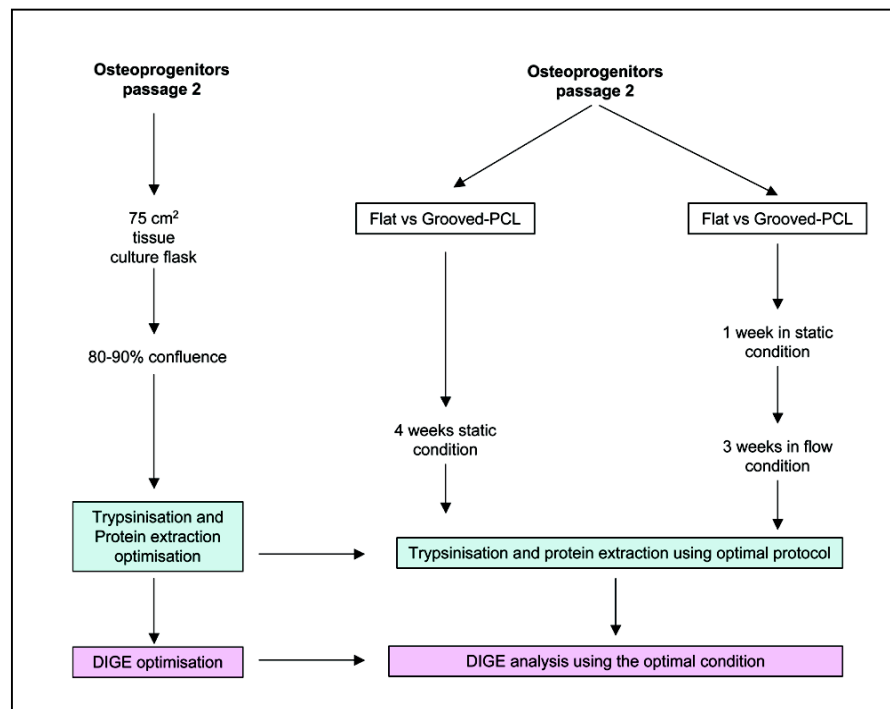


Figure 2.1 Work plan. The diagram presents working plan and the purpose of this chapter. On the left, the initial optimisation (part I) was performed from cells cultured in a standard tissue culture flask before moving onto (on the right) cells cultured on topographical substrates (part II).

The chapter starts by firstly developing the DIGE protocol for osteoprogenitor cells cultured in tissue culture flasks. Then, secondly, photolithographically fabricated grooves were used to optimise protocols for topographical matrices.

There are three main steps to DIGE to optimise as will be discussed in the materials and methods:

2.1.1.1 Protein extraction. Protein extraction using lysis buffer is one of the critical steps, since it involves sample solubilisation, denaturation and reduction to completely break up the interactions between the proteins prior to the first dimension 'isoelectric focusing (IEF)'. The lysis buffer in this study was composed of 7M Urea, 2M Thiourea, 4% CHAPS and 30 mM Tris-base pH 8.0.

(1) Urea has the ability of denaturing and disrupting monofunctional hydrogen bonds in aqueous solution. Secondly, it forms a complex with nonpolar amino acid residues in aqueous solutions. Urea also denatures proteins by weakening the forces between nonpolar amino acid residues (Gordon and Warren, 1968).

(2) Thiourea improves solubilization of membrane proteins. Thiourea was recommended for use with IPGs, which are prone to adsorptive losses of hydrophobic and isoelectrically neutral proteins. Typically, thiourea is added at concentrations of 2 M in conjunction with 5–7 M urea. The high concentration of urea is essential for solvating thiourea, which is poorly water-soluble. However, the use of thiourea should not exceed 2 M concentrations because this chaotrope inhibits binding of SDS in the equilibration step between the first and second dimension, thus leading to poor transfer of proteins into the 2D gel (Galvani et al., 2001).

(3) 3-((3-Cholamidopropyl)dimethylammonio)-1-propanesulfonate (CHAPS). The zwitterionic detergent CHAPS offers greater solubilizing characteristics and has no net charge. Thus it is ideal, when used in conjunction with urea, for solubilizing

membranes, gaining increased resolution and achieving decreased protein streaking (Perdew et al., 1983).

2.1.1.2 Two-dimensional gel electrophoresis. Basic knowledge of 2D gel electrophoresis is described in chapter 1 section 1.9.1.2. A slight modification used in this study is the active sample loading, termed in-gel rehydration loading under low voltage. This technique is distinguished from the previous one (termed passive) as a small voltage (typically 50 V) is applied during IPG strip rehydration. It is considered that this procedure would further facilitate gel entry of high molecular weight proteins.

2.1.1.3 Protein labelling. Basic knowledge of protein labelling is described in chapter 1 section 1.9.1.1.

2.1.2 Part II. Introduction to the application of DIGE for topographical matrices

In part II, osteoprogenitor cells were cultured on micrometric grooves. These micro-grooves were used to influence progenitor cell differentiation. Additionally, a fluid-flow bioreactor was used to improve the medium supply according to tissue engineering principles – i.e. the production of bone *in vitro*. The micro-grooved topography was chosen as it is well characterised biologically (Walboomers and Jansen, 2001).

The aim of tissue engineering is to form complex tissues *in vitro* using bioactive materials to guide cell growth. Ideally the cell choice should be multipotent and available from an autologous source and the scaffold materials should be bioactive and biodegradable. Here, human bone marrow osteoprogenitor cells have been used which have been isolated from trabecular bone marrow and contain a mixture of cells from primitive mesenchymal stem cells to mature osteoblasts with precursor cells in between different stages of commitment (Triffitt et al., 1998, Oreffo et al., 2005). This heterogenous cell mix has the potential to differentiate into bone-forming

cells/osteoblasts under appropriate conditions using selected hormones/growth factors (Rickard et al., 1994, Pei et al., 2003, Bellows et al., 2006), vitamins/chemical reagents (Inui et al., 1997, D'Ippolito et al., 2002) and/or defined surface topographical guidance (Dalby et al., 2006b, Dalby et al., 2006a, Dalby et al., 2007d, Dalby et al., 2008a). As mentioned in chapter 1, the rationale behind using this cell type rather than a homogeneous, e.g. Stro-1 selected, MSC population was that for practical tissue engineering the yield of progenitors is far higher than that of stem cells and thus the time-in-lab could be significantly reduced for tissue engineered products.

As a bioactive cue, grooves have been used here as they have previously been shown to alter osteoprogenitor differentiation and allow the formation of bone nodules *in vitro* without media supplements (Dalby et al., 2007d, Dalby et al., 2006b, Hamilton and Brunette, 2007). The grooves were embossed into the biodegradable polymer polycaprolactone (PCL, an FDA approved biomaterial with good biocompatibility and excellent micro and nano replication characteristics) (Mas Estelles et al., 2008, Gadegaard, 2006). In order to facilitate improved cell growth to obtain higher protein yields, a flow system bioreactor was used to perfuse basal media (Abousleiman and Sikavitsas, 2006). It is important to use basal media so that we can access directly the bone inducing potential of the material rather than using stimulants such as dexamethasone or ascorbate.

2.1.3 Part III The reference gel and protein identification by mass spectrometry

Reference gels are used to facilitate mass spectroscopy and protein identification because the analytical DIGE gels are loaded with too small volumes of protein for successful identification. Dedicated software is used in reference gel analysis to allow the generation of a pick-list of spots to be digested for mass spectroscopy. These spots are excised and trypsinised. Trypsin cleaves on specific site of peptide (C-terminal to arginine and lysine) (Olsen et al., 2004) and this allows the generation of peptide mass fingerprint that can be searched against protein sequence databases.

2.2 Materials and methods

2.2.1 Part I: Optimisation of DIGE for osteoprogenitor cells.

2.2.1.1 Cell Culture, Protein Extraction and Protein Precipitation (from flask)

Human bone marrow osteoprogenitors were obtained from hematologically normal patients undergoing routine surgery. Only tissue that would have been discarded was used with the approval of the Southampton & South West Hants Local Research Ethics Committee. Primary cultures of bone marrow cells were established as previously described (Oreffo et al., 1999a).

Osteoprogenitor cells (passage 2) were grown in 75 cm² tissue culture flasks until 80-90% confluent. Cells sheets were rinsed with HEPES saline before trypsinization from the flask by adding 5 ml of trypsin solution (700 µl in 20 ml versine) and incubating at 37 °C for 5 minutes. Cell suspensions were collected by centrifugation at 1,400 rpm for 5 minutes. The resulting cell pellet was washed by 5 ml of HEPES saline before centrifugation. Cells were re-suspended in 1 ml of DIGE lysis buffer (7M Urea, 2M Thiourea, 4% CHAPS and 30 mM Tris-base pH 8.0) with 1X final concentration of protease inhibitor cocktail (Sigma-Aldrich). The cell suspension was left at room temperature for 1 hour with vigorous mixing every 20 minutes. The suspension was then centrifuged at 2,100 rpm for 10 minutes to remove insoluble material. Proteins were then precipitated from the supernatant by addition of 4 volumes of 100% cold acetone (-20 °C). After centrifugation, the protein pellets were washed in 80% acetone and re-suspended in DIGE lysis buffer.

2.2.1.2 Protein quantification

The Bradford protein assay (Bio-Rad) was used to determine the amount of protein extracted from each material. Briefly, varying concentrations of BSA (50, 25, 12.5,

6.25 and 3.125 $\mu\text{g/ml}$) were prepared and used as a standard curve. 10 μl of each standard and sample was mixed with 200 μl of protein assay reagent. The reaction was left to progress at room temperature for 5 minutes. Absorbance was measured using a microplate reader, TECAN (GENios), at 595 nm. Protein concentration of the extract was determined from the standard curve.

2.2.1.3 2D Gel Electrophoresis

First dimension isoelectric focusing (IEF) was performed on IPG strips (24 cm; linear gradient pH 3–10) using an Ettan IPGphor system (GE-Healthcare). IEF was performed using the following voltage programme: 30 V constant for 12 h, 300 V constant for 1 h, linear up to 600 V over 1 h, linear up to 1,000 V over 1 h, linear up to 8,000 V over 3 h, then 8,000 V constant for 8.30 h. The current was limited to 50 μA *per* strip and the temperature maintained at 20 $^{\circ}\text{C}$. After focusing, strips were equilibrated for 15 min in 5 ml of reducing solution (6 M urea, 100 mM Tris-HCl pH 8, 30% v/v glycerol, 2% w/v SDS, 5 mg/mL DTT). For the second dimension SDS-PAGE, IPG strips were placed on the top of 12% acrylamide gels cast in low fluorescence glass plates and then sealed by 0.5% (w/v) agarose overlay solution. Gels were run at constant power 50 W/gel until the bromophenol blue tracking front had reached the base of the gel. The gel was stained with colloidal coomassie blue-R and rinsed with tap water.

2.2.1.4 DIGE

Optimization: Labelling optimisation was performed according to the protocol provided in CyDye DIGE Fluor labelling kit for scarce samples (Amersham Biosciences). The total amount of protein loaded into the gel was fixed at 5 μg due to cell growth limitations. The appropriate amount of Tris(2-carboxyethyl)phosphine hydrochloride (TCEP) and CyDye DIGE fluor were varied as suggested in the instruction manual for scarce sample. Two conditions were tested as shown in table

2.1. Thus, 5 μg of the extracted protein (from 2.2.1) were added into 4 sterile microcentrifuge tubes. Proteins in tubes A1&A2 were reduced with 1 μl of 2 mM TCEP and tubes B1&B2 were reduced with 2 μl TCEP. The reactions were incubated at 37⁰C in the dark for 1 hour. Protein in tubes A1&A2 were labelled with 2 μl of Cy3 and Cy5 while tubes B1&B2 were labelled with 4 μl of Cy3 and Cy5. The reactions were set in the dark at 37⁰C for 30 minutes. Equal volumes of 2X sample buffer (7M Urea, 2M Thiourea, 4% w/v CHAPS, 2% w/v PharmalyteTM broad range pH 4-7 and 2% w/v DTT) were added to stop the reactions. Proteins labelled with Cy3 and Cy5 in tube A1&A2 were mixed together as same as tube B1&B2. 2D Gel electrophoresis was performed using the same condition 2.2.3. except the pH 4-7 IPG strips were used instead of pH 3-10 strips. Fluorescence images of the gels were obtained by scanning on a Typhoon 9400 scanner (GE Healthcare). Cy3 and Cy5 images were scanned at 532 nm/580 nm and 633 nm/670 nm excitation/emission wavelengths respectively at a 100 μm resolution. Image analysis was performed using DeCyderTM 6.1 software (GE Healthcare).

Table 2.1 Two conditions were determined in the optimisation of DIGE protocol.

Conditions		Protein extract (μg)	2 mM TCEP (μl)	2 mM Cy3 (μl)	2 mM Cy5 (μl)
A	A1	5	1	2	-
	A2	5	1	-	2
B	B1	5	2	4	-
	B2	5	2	-	4

2.2.2 Part II: Application of DIGE for topographical matrices.

2.2.2.1 Photolithographical Material Fabrication

Quartz slides were cleaned in 7 parts sulphuric acid and 1 part hydrogen peroxide for 5 mins. The slides were then spincoated with AZ primer at 4,000 rpm for 30 secs. Shipley S1818 photoresist was next added, and the slides were spun for a further 30 secs. After spinning, the slides were soft baked at 90°C for 30 mins. The samples were then exposed to UV light through a chrome mask (Hoya) with a 12.5µm wide line pattern. The exposed resist was developed using 1:1 (v/v) Shipley AZ developer: water. The slides were next etched to produce 2 µm deep grooves in a Plasma Technology RIE80 unit (Tri-chloromethane environment, pressure of 15 mTorr (1 Torr = 133.322 Pa), R.F. power of 100W, giving an etch rate of 25 nm/min). The mastering resist was then removed and the whole slide was etched for a further minute to produce a uniform chemistry (by Mary Robertson).

For embossing, a polycaprolactone (PCL; Sigma-aldrich) sheet was cut into 2 cm² squares before being cleaned with 75% ethanol then deionized water and finally blown dry with cool air. The PCL substrates were heated until they started to melt. Either the grooved or flat slides were embossed onto the PCL substrates. PCL substrates were cooled down and the glass slides were removed. Flat controls and test grooves were checked by atomic force microscopy (Nanoscope IIIA, please note that controls had a mean Ra of 28.406 nm).

2.2.2.2 Cell Culture

Osteoprogenitor cells (the same batch as used in the experiment in Part I) were cultured in 75 cm² tissue culture flasks at passage 2 as previously described in 2.2.1. Passage 2 was used to allow for expansion of the cells to experimental numbers, but to ensure progenitor status. Confluent cell sheets were trypsinized and 1x10⁵ cells were seeded onto grooved and control flat PCL sheets. The experiment was separated

into two groups. The first group was maintained in a static culture for 4 weeks, the second group was maintained in static culture for 1 week prior to culture in the flow bioreactor system (Minucell, Germany) for 3 weeks. Media was changed twice per week for static culture conditions and continually in the bioreactor.

The bioreactor consisted of a media reservoir connected to three ‘tissue container’ cassettes with continuous media flow controlled by a peristaltic pump. Basal media was supplied to osteoprogenitor cells at a flow-rate of 0.5 ml/min. 500 ml of basal medium was reused for one week (figure 2.2).



Figure 2.2 The bioreactor. The flow system bioreactor used in this study contained medium reservoirs (one fresh media, one used media) at both ends of the system, three cassettes of tissue containers and a peristaltic pump which generated 0.5 ml/min medium flow-rate.

2.2.2.3 Histology

Cell morphology was monitored at two time points (5 days and 4 weeks). PCL sheets with cultured cells were fixed in 4% formaldehyde in PBS for 5 minutes. Cell staining was performed using 5% Coomassie blue in 40% methanol and 10% acetic acid for 5 minutes. The stained materials were washed twice in tap water. Samples were viewed by bright-field microscopy. Pictures were taken by greyscale digital camera (Scion Corporation Model CFW-1310M).

2.2.2.4 Alizarin staining

2% Alizarin red stain (pH 4) was prepared by mixing 2 g of Alizarin red S with 100 ml of water and diluted ammonium hydroxide was added to adjust the pH. After 4 weeks of culture, the osteoprogenitors were fixed in 4% formaldehyde for 15 min at 37°C. Then they were stained with 2% alizarin red for 5 min before washing with tap water. Samples were viewed by bright-field optical microscopy. Pictures were taken by greyscale digital camera (Scion Corporation Model CFW-1310M).

2.2.2.5 Protein extraction and protein precipitation from cells cultured on microtopography

After 4 weeks culture, cell sheets were trypsinized from the PCL substrate and the cell suspension was collected by centrifugation at 1,400 rpm for 5 minutes. The cell pellet was re-suspended in 1 ml of DIGE lysis buffer (7M Urea, 2M Thiourea, 4% CHAPS and 30 mM Tris-base pH 8.0) with 1X final concentration of protease inhibitor cocktail (Sigma-Aldrich). The cell suspension was left at room temperature for 1 hour with vigorous mixing every 20 minutes. The suspension was then centrifuged at 2,100 rpm for 10 minutes to remove insoluble material. Proteins were then precipitated from the supernatant by addition of 4 volumes of 100% cold acetone (-20 °C). After centrifugation, the protein pellets were washed in 80% acetone and re-suspended in DIGE lysis buffer.

2.2.2.6 The Saturation labelling of protein extract from cells cultured on microtopography

Protein labelling was performed following the optimal protocol from 2.2.1.4. Briefly, 5 µg of the extracted proteins were added into sterile microfuge tubes. Protein in each tube was reduced with 1 µl of 2 mM TCEP. The reactions were incubated at 37°C in the dark for 1 hour. Protein in each tube was labelled with the required volumes of

Cy3 and Cy5 in the dark for 30 minutes. Equal volumes of 2X sample buffer (7M Urea, 2M Thiourea, 4% w/v CHAPS, 2% w/v PharmalyteTM, broad range pH 4-7 and 2% w/v DTT) were added to stop the reactions. Proteins labelled with Cy3 and Cy5 were mixed together. 2D-Gel electrophoresis was performed. Fluorescence images of the gels were obtained by scanning on a Typhoon 9400 scanner (GE Healthcare). Cy3 and Cy5 images were scanned at 532 nm/580 nm and 633 nm/670 nm excitation/emission wavelengths respectively at a 100 μ m resolution. Image analysis and statistical quantification of relative protein expression was performed using DeCyderTM 6.1 software (GE Healthcare). Spots that showed changes in protein expression were matched with preparative gel then protein identification was performed. The details of preparative gel and protein identification were presented separately in part III.

2.2.3 Part III The reference gel and protein identification by mass spectrometry

2.2.3.1 Preparative 2D gel (reference gel): Protein extraction was performed using the same method as described in 2.2.1. 175 μ g of protein extracted from osteoprogenitor cells was reduced by 3.5 μ l of 20 mM TCEP and then labelled with 30 μ l of Cy3 DIGE flour. After 2D Gel Electrophoresis was performed and fluorescence images of the gels were obtained by scanning on a Typhoon 9400 scanner (GE Healthcare). Cy3 images were scanned at 532 nm/580 nm excitation/emission wavelengths respectively at a 100 μ m resolution. Image analysis was performed using DeCyderTM 6.1 software (GE Healthcare), the preparative gel image was matched with analytical DIGE gel images and the spots of interest were selected for mass spectrometric analysis.

A pick list was generated, containing gel co-ordinates that were used to direct spot cutting. Gel spots were excised using an Ettan Spot Handling Workstation (Amersham Biosciences, UK) and each gel piece was placed in a separate well of a 96-well plate. Gel pieces were washed three times in 100 μ l of 50 mM ammonium

bicarbonate, 50% v/v methanol and then twice in 100 μ l 75% v/v acetonitrile, before drying. Gel pieces were rehydrated with trypsin solution (20 μ g trypsin/ml 20 mM ammonium bicarbonate), and incubated for 4 hours at 37°C. Peptides were extracted from the gel pieces by washing twice in 100 μ l of 50% v/v acetonitrile / 0.1% v/v trifluoroacetic acid, before being transferred in solution to a fresh 96-well plate and dried before mass spectrometric analysis.

2.2.3.2 Mass spectrometry and Data Analysis

(1) MALDI-TOF-TOF. Trypsinised peptide solutions were mixed at a 1:1 ratio with saturated α -cyano-4-hydroxycinnamic acid (CHCA) matrix in 0.3% TFA and spotted on stainless steel MALDI sample plates (Applied Biosystems, Framingham, MA). Peptide mixtures were then analyzed using MALDI/TOF/TOF (4700 Proteomics Analyzer, Applied Biosystems, Framingham, MA). MALDI-TOF spectra were collected from m/z 800 – 4,000 and up to 10 peaks were selected for MS/MS analysis. Protein identification was performed using Global Proteome Server Explorer software (Applied Biosystems, Framingham, MA) utilizing the NCBI Reference Sequence human protein database. The identification was assigned to a protein spot feature if the protein score was calculated to be greater than 50, correlating to a confidence interval of 95%. Protein identifications were assigned using the Mascot search engine, which gives each protein a probability based MOWSE score. In all cases variable methionine oxidation was used for searches. Only proteins identified with a significant score ($p = <0.05$) were included, corresponding to a MOWSE score greater than 66.

(2) ESI-Q-TOF: All peptide samples were separated on an LC system (Famos / Switchos / Ultimate, LC Packings) before being analysed by electrospray ionisation (ESI) mass spectrometry on a QSTAR® XL Hybrid LC/MS/MS System. Peptides were separated on a Pepmap C18 reversed phase column (LC Packings), using a 5 -

85% v/v acetonitrile gradient (in 0.5% v/v formic acid) run over 45 min. The flow rate was maintained at 0.2 μ l / min. Mass spectrometry analysis was performed using a duty cycle, consisting of a 3 second survey MS scan, followed by four MS/MS analyses of the most abundant peptides (3 second per peak). Data generated from the Q-STAR® XL hybrid mass spectrometer was analysed using Applied Biosystems Analyst QS (v1.1) software and the automated Matrix Science Mascot Daemon server (v2.1.06). Protein identifications were assigned using the Mascot search engine, which gives each protein a probability based MOWSE score. In all cases variable methionine oxidation was used for searches. Only proteins identified with a significant score ($p = <0.05$) were included, corresponding to a MOWSE score greater than 44.

2.3 Results

2.3.1 Part I: Optimisation of DIGE for osteoprogenitor cells.

2.3.1.1 Protein assay

The standard curve showed that at protein concentration range 0-50 μ g/ml the graph had a linearity of absorbance (figure 2.3). The absorbance of the protein extracts was determined and the standard curve was used to calculate the amount of protein in the extract. 500 μ g of protein extract was needed for 2D gel electrophoresis.

2.3.1.2 Protein extraction and protein separation by 2D gel electrophoresis

500 μ g of protein extract from the flask was separated using 2D gel electrophoresis. From figure 2.4 the total pH range of the IPG strip used was 3-10, however, high resolution protein separation could be observed only the inner part of the 2D gel image (marked with line AB). The gels showed a poor resolution at the margins. This result suggested that the pH range of IPG strip should be narrowed to pH 4-7.

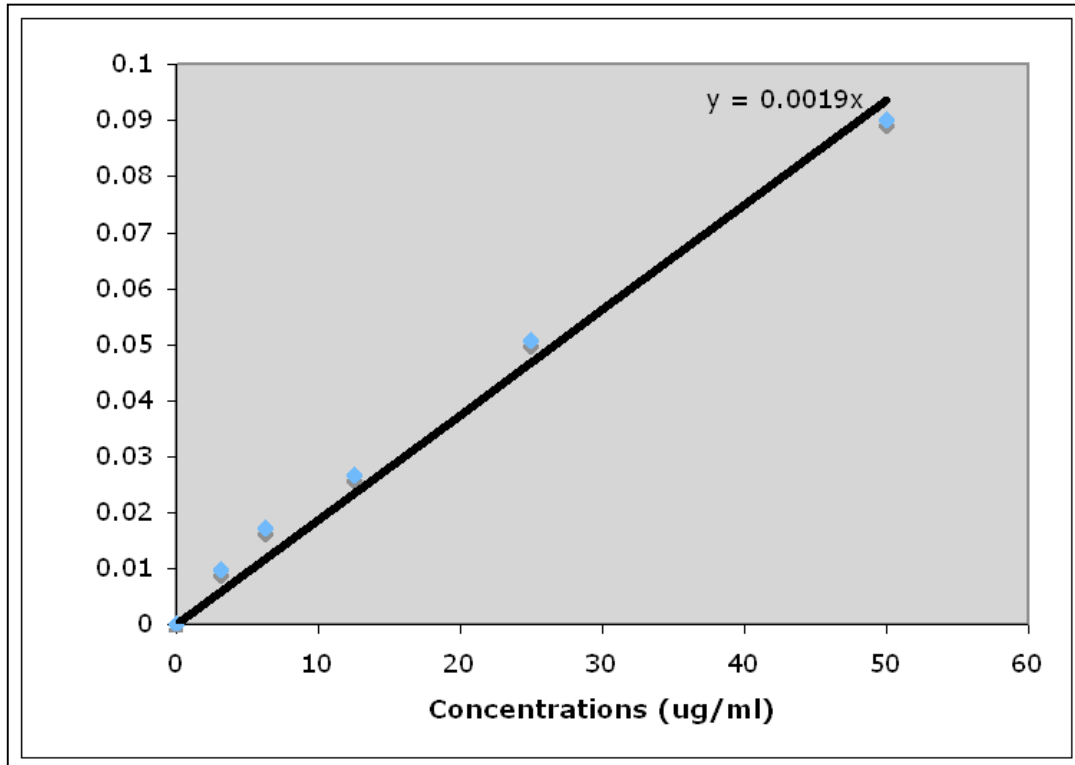


Figure 2.3 Standard curve of protein assay. The standard curve showed the linearity in the range of concentration 0-50 $\mu\text{g/ml}$ with R^2 value = 0.9852.

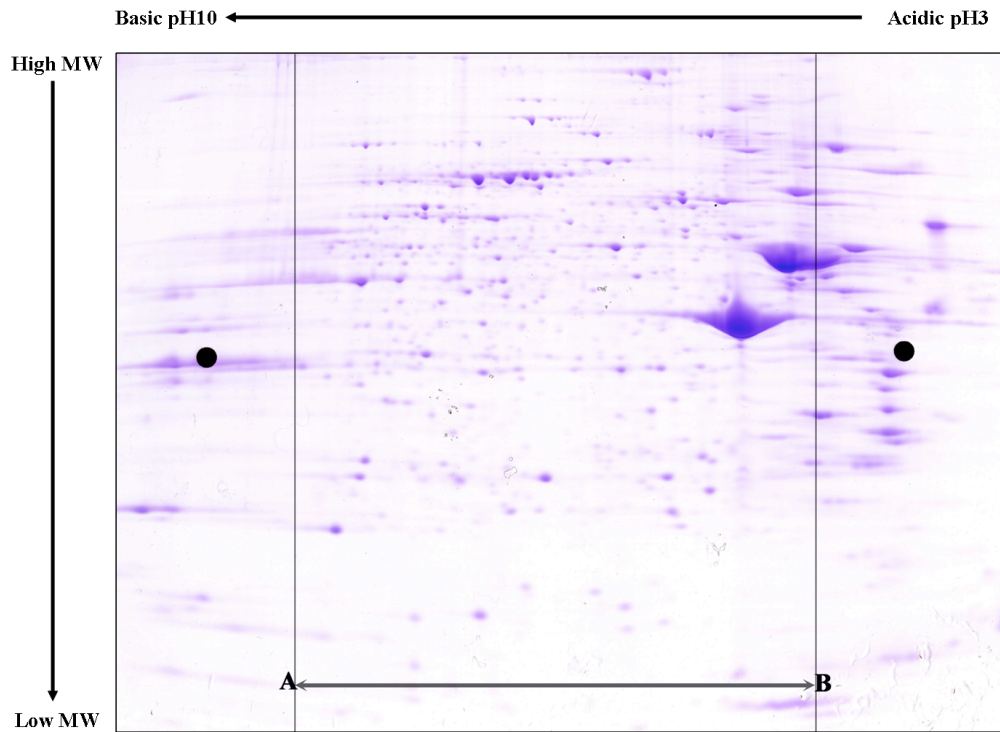


Figure 2.4 The 2D SDS-PAGE of protein extract from tissue culture flask. The protein extract was separated by standard protocol using IPG strip pH range 3-10. The best resolution can be observed only for the inner part of gel (line AB). Horizontal streaks were observed at both margins of gel.

2.3.1.3 Optimisation of saturation labelling

The optimal conditions for saturation labelling were selected from the 2 trial conditions, A and B (as illustrated in table 2.1). Proteins labelled by both conditions were subjected to further 2D electrophoresis. The pH 4-7 IPG strips were used in this step to allow higher protein resolution to be achieved. The results shown in figure 2.5 indicate that protein labelled by condition A had similar outcome to protein labelled by condition B; both conditions provided good resolution and labelling. Thus, condition A was chosen to use in this thesis as less reagent was required to produce a similar outcome.

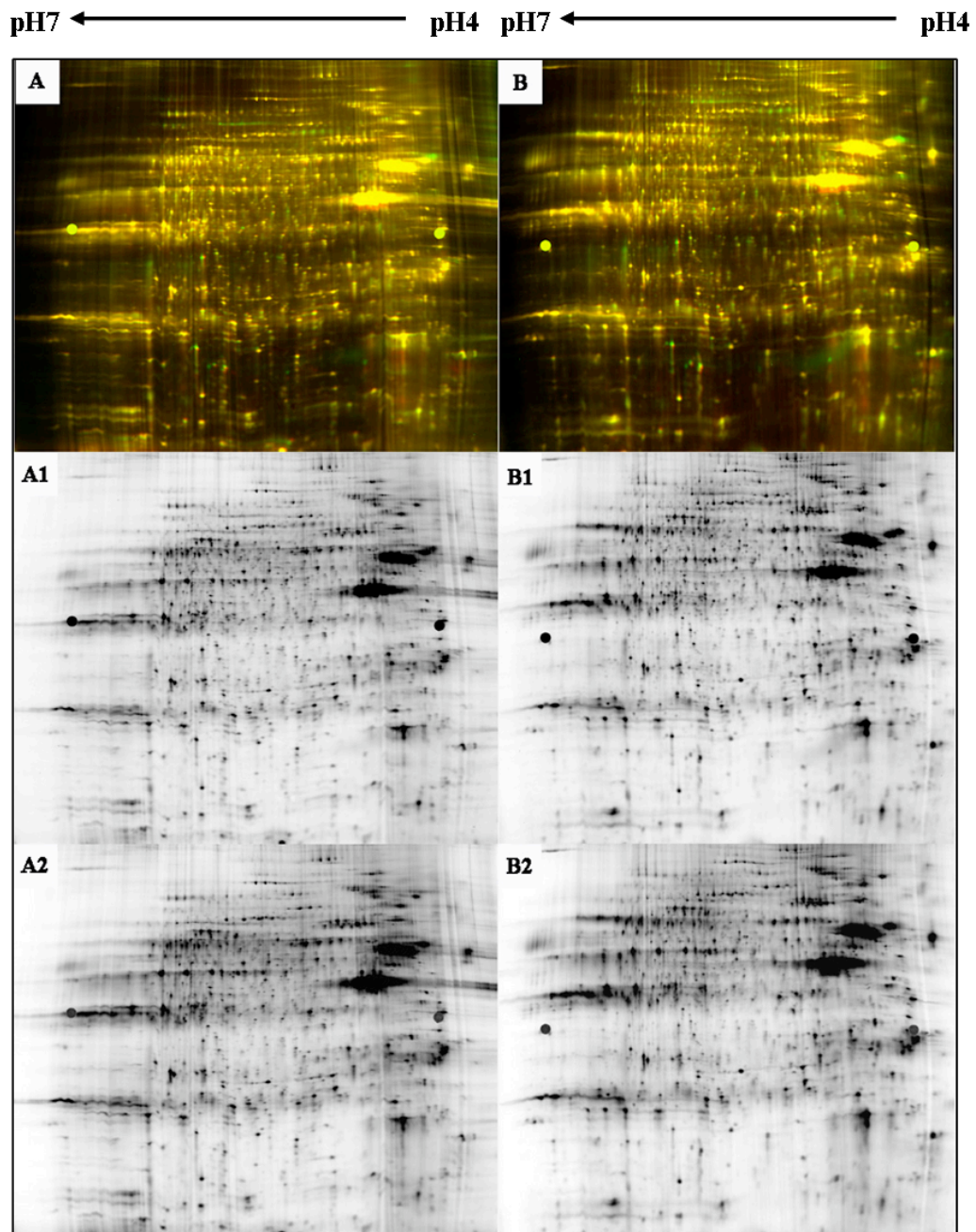


Figure 2.5 Saturation labelling optimisation. Image results of condition A compared against condition B on 2D SDS-PAGE with pH4-7 IPG strips. A&B are the fluorescent images of condition A and B respectively. A1&B1 are the images of proteins labelled by Cy3 whilst A2&B2 are the images of proteins labelled by Cy5 using condition A and B respectively.

2.3.2 Part II: Application of DIGE for topographical matrices.

2.3.2.1 Materials

The fabricated PCL sheet was analysed by Atomic force microscopy. AFM images showed firstly that the control materials had a Ra value of 28.406 nm and also the successful embossing of the grooves at 2 μm deep and 12.5 μm pitch (figure 2.6).

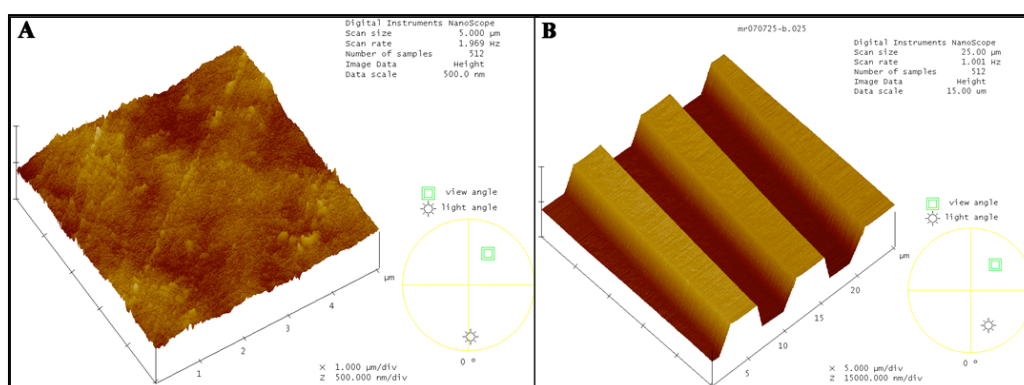


Figure 2.6 Atomic Force Microscopy. Ra values for the roughness of flat-PCL and AFM of grooved-PCL topography are shown: (A) in an area of 34.085 μm^2 , the Ra value for flat-PCL is 28.406 nm; (B) the AFM of the grooved-PCL sheet showed that the grooved pattern was successfully embossed.

2.3.2.2 Histology

After 5 days, osteoprogenitor cells on the grooved material were observed to align along the grooves while osteoprogenitor cells on control substrates were observed to spread randomly on the flat surface (figure 2.7 A&B). After 4 weeks of static culture, confluent cell layers (80-90%) were observed on both control and test substrates. However, the patterns of osteoprogenitor cell growth were different with tissue layers forming in the direction of groove orientation as opposed to random growth observed on the flat controls (figure 2.7 C & D). As a consequence of the limited number of replicates that can be cultured in the bioreactor tissue containers, no image of

bioreactor grown cells are presented and rather protein extraction provides evidence of cell growth.

Alizarin red staining of calcium was observed after 4 weeks culture on both grooved and control surfaces (figure 2.8 A&B). Whilst nascent nodules could be seen on both materials, it was only on the grooves that the osteoprogenitor cells were seen to produce dense mineral nodules.

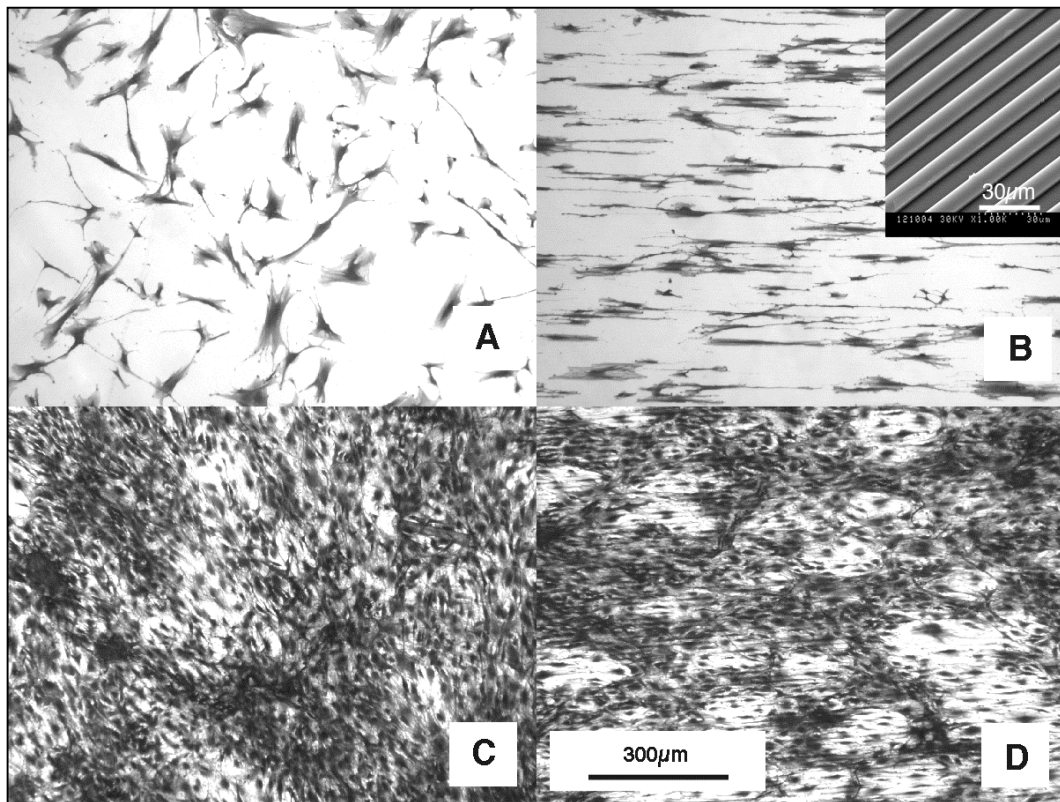


Figure 2.7 Osteoprogenitor cells (OPGs) cultured on PCL substrates in static culture. A. 5 days on flat surface, B. 5 days on grooved surface (inset is SEM image of the grooves), C. 4 weeks on flat surface, D. 4 weeks on grooved surface. Note that cells on the grooves at day 5 are elongated in the groove direction.

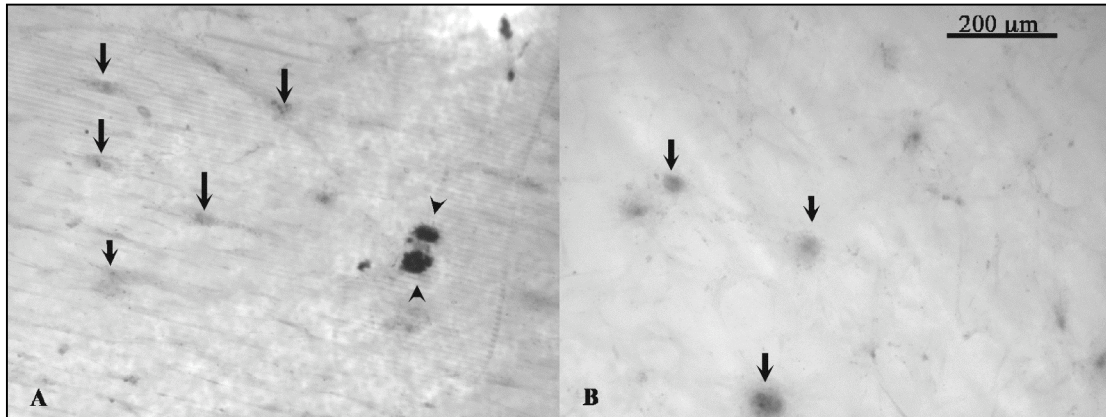


Figure 2.8 Alizarin red staining for calcium accumulation After 4 weeks culture in static culture, positive calcium staining (arrow) could be seen on both test (A) and control materials (B). However, only on the grooves were mature, very dense, nodules noted (arrow heads).

2.3.2.3 Cell culture in the flow condition

When comparing flat and grooved materials under either static or flow, there was no difference between the treatment in terms of amount of protein extracted (indicating similar cell numbers on both the flat and grooved materials). However, when considering static versus flow, enhanced tissue mass was observed using the flow system bioreactor as confirmed by the Bradford protein assay (approximately 4-fold increase, figure 2.9).

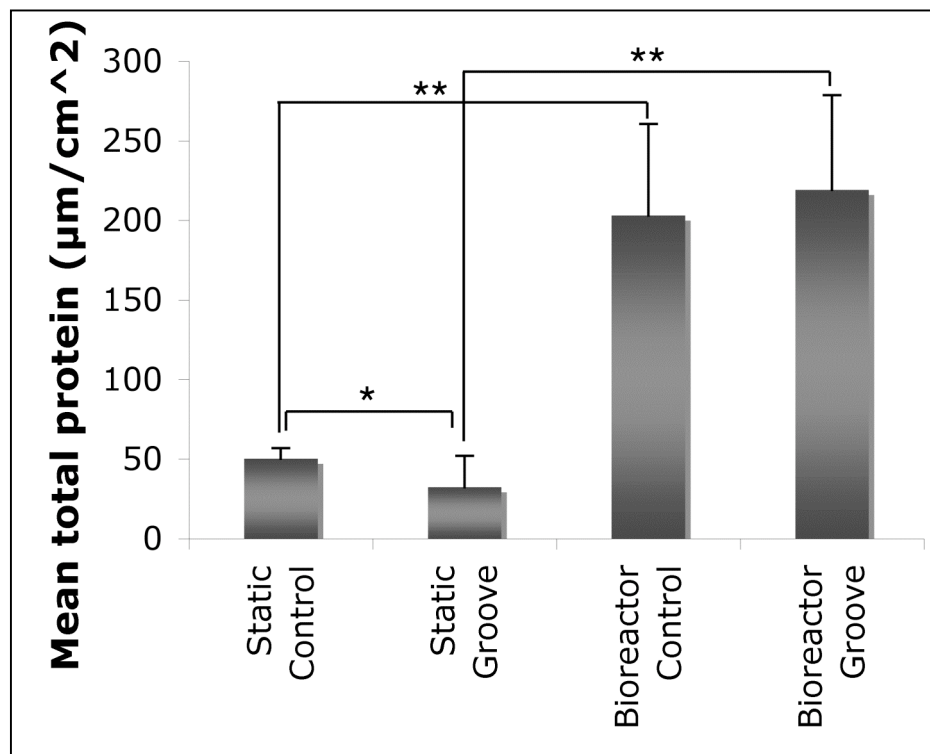


Figure 2.9 Quantification of protein extracts from static and fluid-flow culture.

Graph showing the amounts of protein extracted from each material indicated that the flow system used in this study could generate more tissue mass than the conventional static culture could ($p < 0.01$). *Student's pair-t-test* indicated that there was no difference between the amounts of protein extracted from cells cultured on the grooved and flat materials in the bioreactor ($p > 0.05$) but there was a difference between the amounts of protein extracted from cells cultured on the grooved and flat materials in static culture ($p < 0.05$). Graph shows mean \pm SD for 3 replicates, *= $p < 0.05$, **= $p < 0.001$).

2.3.2.4 DIGE

Optimized DIGE conditions were employed in the evaluation of differences in proteome expression between the micro-grooved topography and the flat control. DIGE showed expression changes for a number of proteins when osteoprogenitor cells were grown on the grooved materials compared to control (Figure 2.10). The results of 3 replicates from the bioreactor and 2 replicates from static culture are summarised in Table 2.2. For ease, results are presented as significant electrophoretic areas as this is how the software compares the fluorescence of the control and test proteins in the gels. A balance of up- and down-regulations were seen.

2.3.3 Part III The reference gel and protein identification by mass spectrometry.

2.3.3.1 Reference gel and protein identification

From figure 2.10, areas that showed degrees of difference in protein expression (≥ 2 -fold) were highlighted by Differential In-gel Analysis (DIA) (DecyderTM) and xml files were generated automatically. The xml images were opened in Biological Variation Analysis (BVA) software, which enables matching between analytical gels and reference gels (figure 2.11 A&B). After gel matching was performed, a picklist was generated from the reference gel and protein identification was performed. Names of the identified proteins were annotated to the corresponding spots on reference gel using the BVA module and those annotated protein names were also appeared on the matched spots on the analytical gels (figure 2.11 C&D).

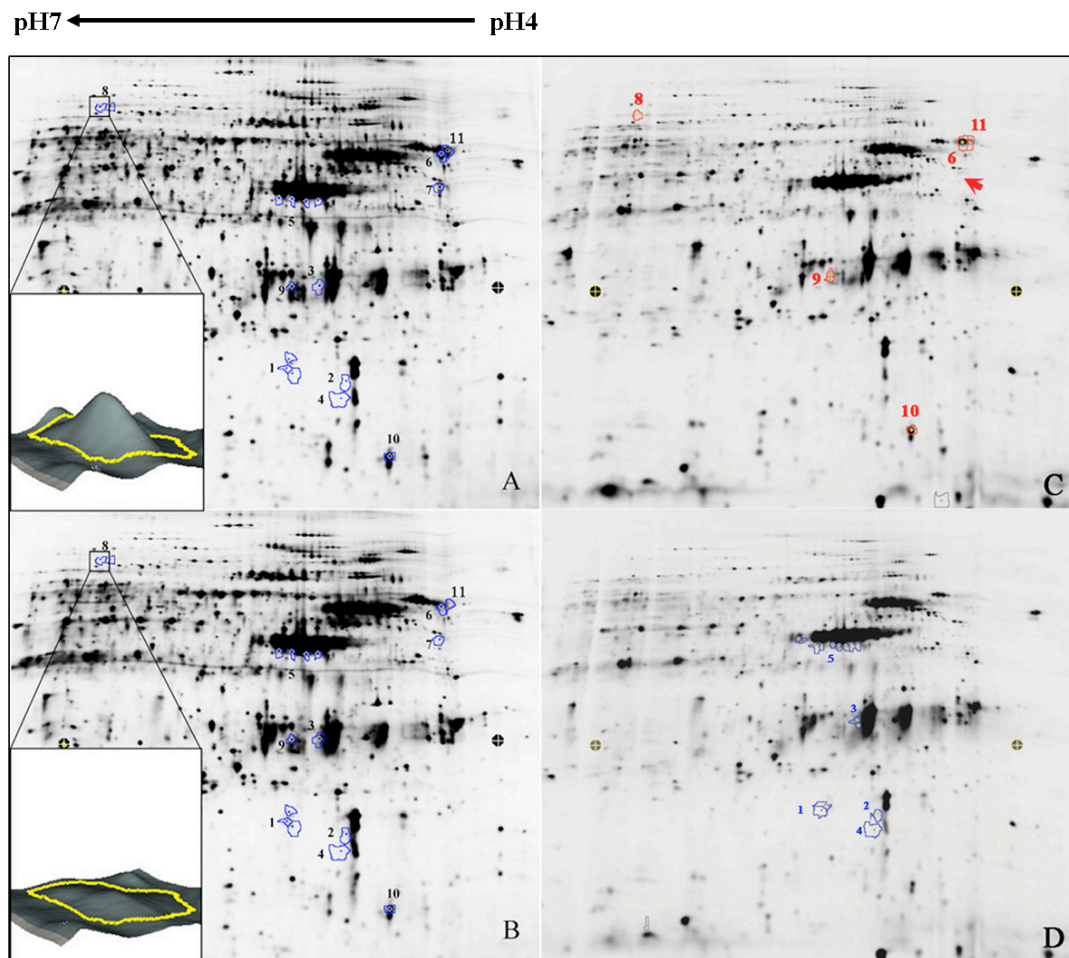


Figure 2.10 Typical DIGE images. DIGE images were analyzed by DeCyder™ Image Analysis Software for (A) the control proteins (Cy3) and (B) the proteins for cells cultured on topography (Cy5) from flow condition. Peak volumes of each spot were compared against each other as demonstrated by the inserts. 2.0-fold difference in peak volume was used as a cut-off to determine the difference of protein expression between test and control. In all DIGE gels there were areas showing results of up and down-regulation. The electrophoretic regions of interest, as considered in the results section, are labelled numerically. Note that the control protein (C) and the proteins for cells cultured on topography (D) from the static condition showed the same result as cells cultured in the flow condition except that no osteonectin expression was observed in static culture (red arrow).

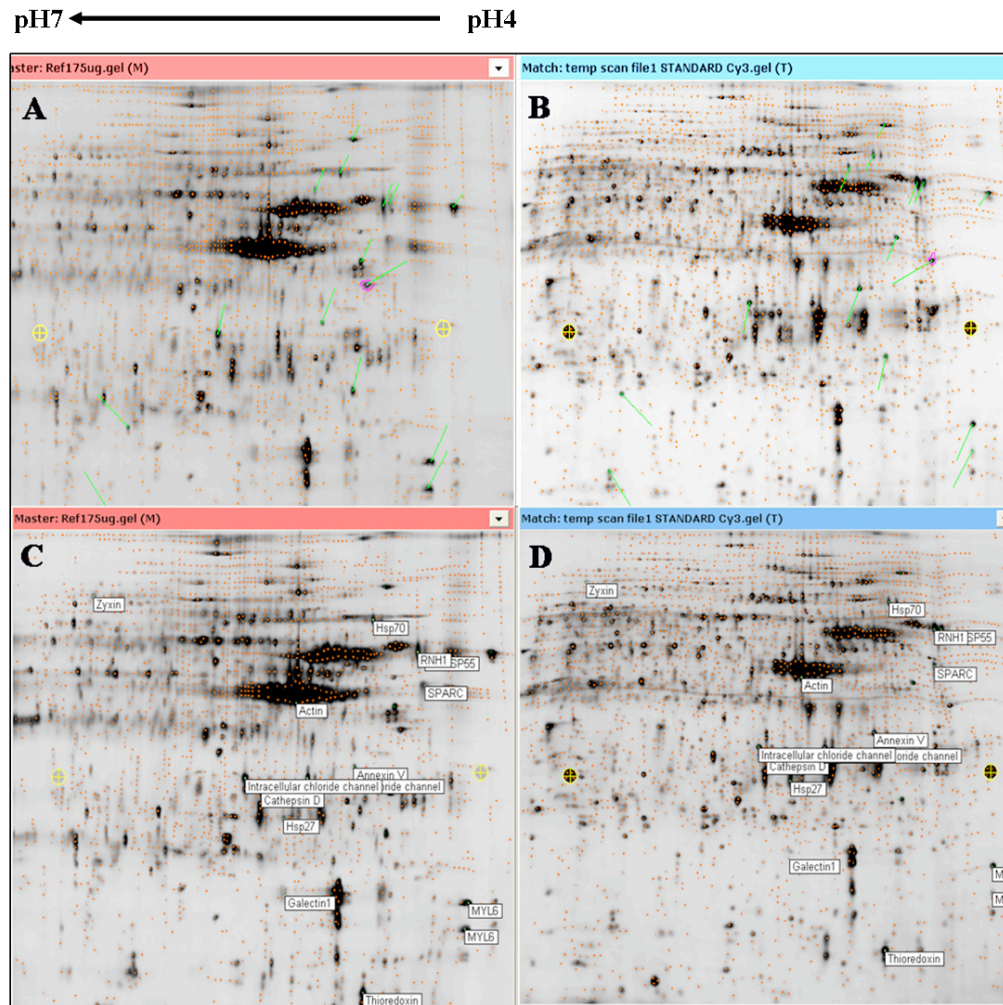


Figure 2.11 BVA images and gel matching. BVA image of reference gel (A) was matched with BVA image of analytical gel (B). After protein identification, protein names were annotated to the corresponding spot on reference gel (C) and protein names also appeared on coordinating spots on analytical gel (D).

2.3.3.2 This allowed the identification of modulated proteins thus:

Electrophoretic area 1 and 2: Up-regulation of beta-galactoside-binding lectin precursor (galectin precursor) and galectin-1 were found. These results may indicate increased osteospecific differentiation on the grooves as galectin-1 is associated with the nuclear matrix in differentiated osteoblasts and presented throughout osteoblast

differentiation by binding to nuclear matrix of the differentiated osteoblast (Choi et al., 1998). The other isoform of galectin is also presented during osteoblast differentiation as expression of galectin-3 in skeletal tissue is controlled by Runx2 during the matrix maturation stage of osteoblastic development (Stock et al., 2003).

Electrophoretic area 3: Tumor protein D52-like, intracellular chloride channel (p64) and Ran-binding protein1 (RanBP1) were shown to be up-regulated. Tumor protein D52-like plays a physiological role in vesicle trafficking and exocytotic secretion (Boutros et al., 2004). It is known that cells can respond to their topographic environment through increased endocytotic activity and vesicle formation (Dalby et al., 2004). Chloride ion channels (CLIC) are typically involved in several crucial cellular processes including apoptosis and cell cycle regulation, membrane potential, signal transduction, and acidification of organelles. Recently, it was found out that membrane CLICs are regulated by actin to modify solute transport at key stages during cellular events such as apoptosis, cell and organelle division and fusion, cell-volume regulation, and cell movement (Singh et al., 2007).

Also found was Ran-binding protein1 (RanBP1) co-expression in this area. Ran binding protein 1 (RanBP1) is a binding partner of the Ras-related nuclear protein. It has an important role in controlling nucleocytoplasmic transport (Nishimoto, 1999).

Electrophoretic area 4: The ubiquitin-like family (SUMO/SMT3) precursor was found up-regulated. SUMOylation infers proteins stability, nuclear-cytosolic transport or transcriptional regulation (Verger et al., 2003, Bae et al., 2004, Ghioni et al., 2005, Chen et al., 2006).

Notably, most of the up-regulated proteins in area 3 and area 4 are related to nuclear-cytosolic trafficking. It is considered that the transport machinery itself may be regulated in ways that contribute to cell differentiation and development (Dernburg and Misteli, 2007).

Electrophoretic area 5: Actin isoforms were found up-regulated. The aggregation of actin along grooves is a primary driving event in determining the orientation of cells on microgrooved substrata (Wojciak-Stothard et al., 1995). Focal adhesions and actin microfilament bundles are found to align along micrometer-sized grooves and ridges, however, cells and cytoskeletal elements did not display any preferred orientations on flat substrates (Britland et al., 1996, den Braber et al., 1998, Matsuzaka et al., 2000, Loesberg et al., 2006). The generation of tension by actin stress fibers is necessary for the formation of focal adhesions (Chrzanowska-Wodnicka and Burridge, 1996) and signal transduction (Pavalko et al., 1998).

Electrophoretic area 6: Ribonuclease/angiogenin inhibitor 1 (RNH1) was seen to be down-regulated. RNase activity is inhibited by formation of a complex with an inhibitor (such as RNH1). *In vivo* more than 95% of ribonuclease is complexed with an inhibitor and the inhibitor/RNase ratio is elevated in proliferating tissues (Schneider et al., 1988). Thus, it may be that this result indicates the lower proliferative activity of the cells on the grooves (compared to control) as a consequence of differentiation to matrix secreting cells.

Electrophoretic area 7: SPARC/osteonectin was seen to be down-regulated. It is a matricellular protein expressed by osteoblasts (Yan and Sage, 1999, Alford and Hankenson, 2006). SPARC binds to type I collagen to form a nucleator of hydroxyapatite (Termine et al., 1981a, Termine et al., 1981b). It is likely that as osteonectin levels are known to drop intracellularly after 21 days of culture in highly differentiating osteoblasts (switch from matrix production to mineralization) (Stein and Lian, 1993) and that this study only looked at intracellular proteins, it is to be expected more mature osteoblasts would express less of this protein by this late time point.

Electrophoretic area 8: Zyxin is one of LIM domain proteins at focal adhesion plaques (Wang and Gilmore, 2003). Zyxin is a phosphoprotein localized at sites of cell-substratum adhesion and also plays a role as an intracellular signal transducer.

Zyxin and its partners have been implicated in the spatial control of actin filament assembly as well as in pathways important for cell differentiation (Beckerle, 1997). This group of proteins also shuttle through the nucleus and may regulate gene transcription by interaction with transcription factors (Wang and Gilmore, 2003).

Electrophoretic area 9: Heat shock protein 27 (Hsp27) controls the balance between differentiation and apoptosis (Arrigo, 2000) and was down-regulated by the topography. Hsp27 has been found to be up-regulated during bone cell development previously. However, the previous study was carried out at 7, 11, 14 and 18 days. The highest Hsp27 mRNA level was shown on day 14 but decreased on day 18 (Shakoori et al., 1992). In this study, the proteomic analysis was performed after 4 weeks culture, the expression of Hsp27 is again stage-specific (Shakoori et al., 1992, Leonardi et al., 2004). Hsp27 is also known to modulate cell functions via interaction with the actin cytoskeleton. Hsp27 overexpression increased FAK phosphorylation and focal adhesion formation, depending on integrin-mediated actin cytoskeleton polymerization (Lee et al., 2008).

Electrophoretic area 10: Thioredoxin (TRX) was down-regulated compared to control. It plays important roles in cell growth, cell cycle, gene expression, apoptosis and maintenance of the redox balance. As well as Hsp27, thioredoxin was found up-regulated in differentiating cells in a previous study at earlier time points (Schutze et al., 1998) but down-regulated in this study (4-week culture). However, decrease in expression of thioredoxin in this study might be the consequence of the decrease in expression of Hsp27 as Hsp27 also plays a role in maintaining intracellular levels of reduced glutathione (Preville et al., 1999). There is an overlap in the nature of the GSH–glutaredoxin and thioredoxin systems because thioredoxins function together with Glutathione reductase (Glr1) to maintain the high intracellular GSH:GSSG ratio (Trotter and Grant, 2003).

Electrophoretic area 11: Golgi reassembly stacking protein 2 (GRASP55) plays a mitogen-activated protein kinase kinase /extracellular-activated protein kinase

(MEK/ERK)-regulated role in Golgi ribbon formation and cell cycle progression (Feinstein and Linstedt, 2008). Down-regulation of golgi reassembly stacking protein 2 (GRASP55) might indicate the decreasing of proliferative activity.

Protein expression profiles of osteoprogenitor cells cultured in static and flow systems were compared to each other. The protein expression profiles of both systems were similar. This indicated that fluid flow did not affect protein expression of cells culture on the micro-grooved surface. Furthermore, when considering the fold regulation of each protein, no significant change was noted.

Table 2.2 Protein expression profiles. Names and mean fold values for proteins modulated by the microgrooved topography. Changes of greater than 2.0-fold up/down changes in regulation in all 3 gels were considered significant for this study.

Electrophoretic area	Name	Expression resulting from bioreactor culture	Expression resulting from static culture
1	Beta-galactoside-binding lectin precursor and Galectin1	+3.41±0.53	+2.46±1.05
2	Beta-galactoside-binding lectin precursor and Galectin1	+3.67±0.86	+3.26±0.61

Table 2.2 Protein expression profiles (continue). Names and mean fold values for proteins modulated by the microgrooved topography. Changes of greater than 2.0-fold up/down changes in regulation in all 3 gels were considered significant for this study.

Electrophoretic area	Name	Expression resulting from bioreactor culture	Expression resulting from static culture
3	1. Tumor protein D52-like 2 2. Similar to chloride intracellular channel 1 (p64 CLCP) 3. Similar to Ran-specific GTPase-activating protein (Ran-binding protein1) (RanBP1)	+2.75±0.24	+2.86±0.74
4	SMT3A protein Small ubiquitin-related modifier 3 precursor	+4.56±1.84	+2.73±0.29
5	Actin isoforms	+3.23±1.25	+2.58±0.50
6	Ribonuclease/angiogenin inhibitor 1	-3.15±0.63	-2.35±0.78
7	ECM Protein (Sparc molecule/osteonectin)	-2.97±0.4	-2.17±0.08

Table 2.2 Protein expression profiles (continue). Names and mean fold values for proteins modulated by the microgrooved topography. Changes of greater than 2.0-fold up/down changes in regulation in all 3 gels were considered significant for this study.

Electrophoretic area	Name	Expression resulting from bioreactor culture	Expression resulting from static culture
8	Zyxin	-3.85±0.57	-2.26±0.50
9	Heat shock protein 27 (Hsp27)	-2.74±0.40	-2.21±0.54
10	Thioredoxin (TRX)	-2.24±0.37	-1.72±0.36
11	GRASP55	-3.24±0.96	-3.13±0.1

2.4 Discussion

The application of comparative proteomics to biomaterials embossed with surface topography for bone tissue engineering was performed for the first time in this chapter. The small size of the fabricated surfaces due to the limitations of fabrication meant that small sample techniques had to be employed. Furthermore, for bone related biomaterials, a highly sensitive technique is required because as cells differentiate into bone-forming cells *in vitro* they tend to form discrete nodules rather than confluent sheets and thus low protein yields are expected. In fact, for most academic scale biomaterials research, when considering either genomics or

proteomics, sensitivity is a key issue due to the sample areas normally provided is typically 1 -2 cm².

The optimised protocol was developed from protein extraction, protein quantifying, protein separating and protein labelling using cells cultured in tissue culture flasks. In the next step, cells were cultured on fabricated biomaterials in both static culture and in flow conditions and the trial methodology was employed with success. This indicated that comparative proteomics can apply to tissue engineering and biomaterials research.

Cell morphology is influenced by surface topography; a phenomenon known as contact guidance. In this study, cells stretched along the grooved surfaces but were observed to spread randomly on the flat surface. Four weeks after cell seeding, it was shown that cells, particularly on the grooved surfaces, formed areas of dense aggregation surrounded by more cell sparse areas reminiscent of nascent nodule formation (figure 2.7 & 2.8), characteristic of bone formation (Woll et al., 2006). Furthermore, dense nodules were only produced by cells cultured on the grooves. These observations tie in with previous histological observations (immunolocalisation of osteocalcin and osteopontin) in human osteoprogenitor cells cultured on grooves (Dalby et al., 2006b).

Changes in cell morphology, such as contact guidance, typically imply changes in the organisation of the cytoskeletal network. Previous studies have indicated the importance of cytoskeletal organization arising from changes in cell morphology (Dalby et al., 2007a, Dalby et al., 2007c). This chapter indicates that as well as considering the main cytoskeletal proteins themselves (actin, tubulin and with these cells, vimentin), linker proteins such as caldesmon should be considered. This may be especially the case at late time-points, where the cells are active in producing bone and where perhaps stabilization of the cytoskeleton is important.

Changes in cell adhesion generate mechanical forces that affect cell cytoskeletal polymerization which can be seen here in the form of changes in expression of some transducer proteins such as zyxin and hsp27. Previous studies have indicated that mechanical forces affected focal adhesions in a zyxin-dependent manner (Yoshigi et al., 2005, Lele et al., 2006, Hirata et al., 2008). Both zyxin and hsp27 plays roles in the FAK pathway (Brancaccio et al., 2006, Lee et al., 2008). FAK activation depends on actin cytoskeleton and integrin signalling (Lee et al., 2008). Additionally, down-regulation of GRASP55 implicated the involvement of MEK/ERK signaling. It is possible that changes in cell proteome and ultimately cell differentiation seen in this study were driven by the ERK-FAK signaling cascade.

In this chapter, a bioreactor was used to increase tissue mass for (A) tissue engineering goals and (B) to deliver sufficient protein for proteome analysis. In order to generate sufficient tissue for clinical use, bioreactors and long-term culture are a requirement; here perfusion and 4 weeks of culture were used and the cells assessed at this meaningful time-point (i.e. post-nodule formation). Since the bioreactor provides increased nutrient supply, the tissue growing rate compared to static culture was increased similarly for flat and grooved materials. Moreover, the highlighted protein changes could be sensibly related to osteogenic activity through database assessment of protein activities.

In the next step the techniques and protocols used in this chapter will be applied to the tissue culture on nanoscale topography. The use of nanoscale topography as a modulator of bone tissue engineering is the overall goal of this thesis.

CHAPTER III The optimisation of the DIGE protocol to study the effect of disordered nanopits on osteoprogenitor cell differentiation

3.1 Introduction

The main focus of this thesis is to follow proteomic changes in the osteoprogenitor populations on bioactive (osteogenic) nanotopographical surfaces using DIGE.

The previous chapter demonstrated an optimal methodology which could be successfully applied to evaluate differential protein expression of osteoprogenitors on micro-grooved surfaces compared to flat controls. However, as the nanotopographical materials used in this chapter had smaller areas than the microtopographies used in the previous chapter, protein extraction needed to be modified. On the microgrooves, cell sheets were trypsinised from the surfaces prior to protein extraction and this excluded endogenous extracellular matrix proteins on the material surfaces, which are important in tissue development. This will be addressed within Chapter III.

3.2 Disordered nanoscale topography (NSQ50)

A particularly interesting nanoscale topography that has similar levels of osteoconversion of progenitor cells to treatment with dexamethasone and ascorbate has recently been reported and thus forms a natural focus for this thesis (Dalby et al., 2007b).

Previous studies have implicated roles for nanoscale topography in skeletal cell differentiation and implications therein for bone tissue engineering (Dalby et al., 2006b, Dalby et al., 2006a, Dalby et al., 2007d). When considering nanopits (120 nm diameter, 100 nm depth) fabricated by electron beam lithography, it was seen that changes in pit spacing by as little as ± 20 nm could strongly influence bone osteoid formation *in vitro*. Pits in an absolute square arrangement with 300 nm centre-to-centre spacing showed little production of bone osteoid, whereas by adding degrees

of controlled disorder (near square) strongly induced osteoid formation, to an optimum of ± 50 nm (NSQ50). Totally random pit placing resulted in a low degree of bone matrix formation (Dalby et al., 2007d). This shows the exquisite level of control that can be elicited on progenitor cells and stem cells by control and manipulation of their nanoenvironment.

The same pits were also seen to strongly affect the formation of focal adhesions in human osteoblasts. The square arrangement leads to a shift in distribution of focal complexes (<2 μm), focal adhesions (2-5 μm) and super-long adhesions (>5 μm) towards the transient focal complexes. However, the near-square topography caused a shift in the opposite direction, towards an increased density of super-long adhesions (Biggs et al., 2007b). A study of fibroblasts cultured on the absolute square pits used immuno-transmission electron microscopy to show that the cells could not form adhesions over the pits and thus the surface area available to the cells to form adhesions was reduced (Dalby et al., 2007a). However, the results studying adhesion length (Biggs et al., 2007b) suggest this is otherwise in cells cultured on the near-square pits; i.e. the pits rather induce adhesion formation in bone cells.

Larger pit systems, more similar in size to osteoclast resorption pits, produced by photolithography, with pits of 362 nm depth and 40 μm diameter, have also been observed to promote induction of bone osteoid and expression of the osteoblast-specific extracellular matrix proteins (osteocalcin and osteopontin) (Dalby et al., 2006a). Nanopits have further been shown to affect integrin expression in human foetal osteoblast (hFOB) cells and to induce differences in expression of integrin-mediated cell signalling molecules e.g. focal adhesion kinase (FAK) in osteoblastic cells (Lim et al., 2007). These results suggest roles for biomimicry in the fabrication of biomaterial topographies. That is, when techniques such as electron beam lithography are employed to produce nanosurfaces, perhaps a biological level of disorder must be included, or perhaps natural features (such as resorption pits in bone) should be incorporated.

In this chapter, the novel near square nanopits arrays embossed in the biodegradable polymer polycaprolactone (PCL, approved for use in the body) has been further considered with respect to their influence on osteoprogenitor proteome. Coomassie blue and alizarin red have been used to observe the cellular morphology of the human osteoprogenitors in order to validate DIGE results.

3.3 Materials and methods

3.3.1 Nanotopographical Fabrication

Samples were made in a three-step process of electron beam lithography (EBL), nickel die fabrication and hot embossing. Silicon substrates were coated with ZEP-520A resist to a thickness of 100 nm. After the samples were baked for a few hours at 180 °C, they were exposed in a Leica LBPG 5-HR100 beamwriter at 50 kV. We have developed an efficient way to pattern a 1 cm² area with 1–10 billion pits. Three different pit sizes were made using different spot sizes. An 80 nm spot size was used finally resulting, after embossing, in pits with a diameter of 120 nm. The pitch between the pits was set to an average of 300 nm with a ± 50 nm error (in x and y) written into the placement of the pits at the centre of the square. After exposure the samples were developed in *o*-xylene at 23 °C for 60 s and rinsed in copious amounts of *iso*-2-propanol.

Nickel dies were made directly from the patterned resist samples. A thin (50 nm) layer of Ni–V was sputter coated on the samples. This layer acted as an electrode in the subsequent electroplating process. The dies were plated to a thickness of ca. 300 μ m. A diagram of the EBL process is shown as figure 3.1.

Polymeric replicas were made in polycaprolactone (PCL; Sigma-aldrich) sheets. PCL sheets were cut into 1 cm² squares before being cleaned with 75% ethanol following by deionized water and blown to dry with cool air. The PCL substrates were heated

by light until they started to melt. Either the nickel die or flat slides were embossed onto the PCL substrates. PCL substrates were cooled down and the moulds were removed. The samples were denoted as being near square ± 50 nm (NSQ 50) (figure 3.2).

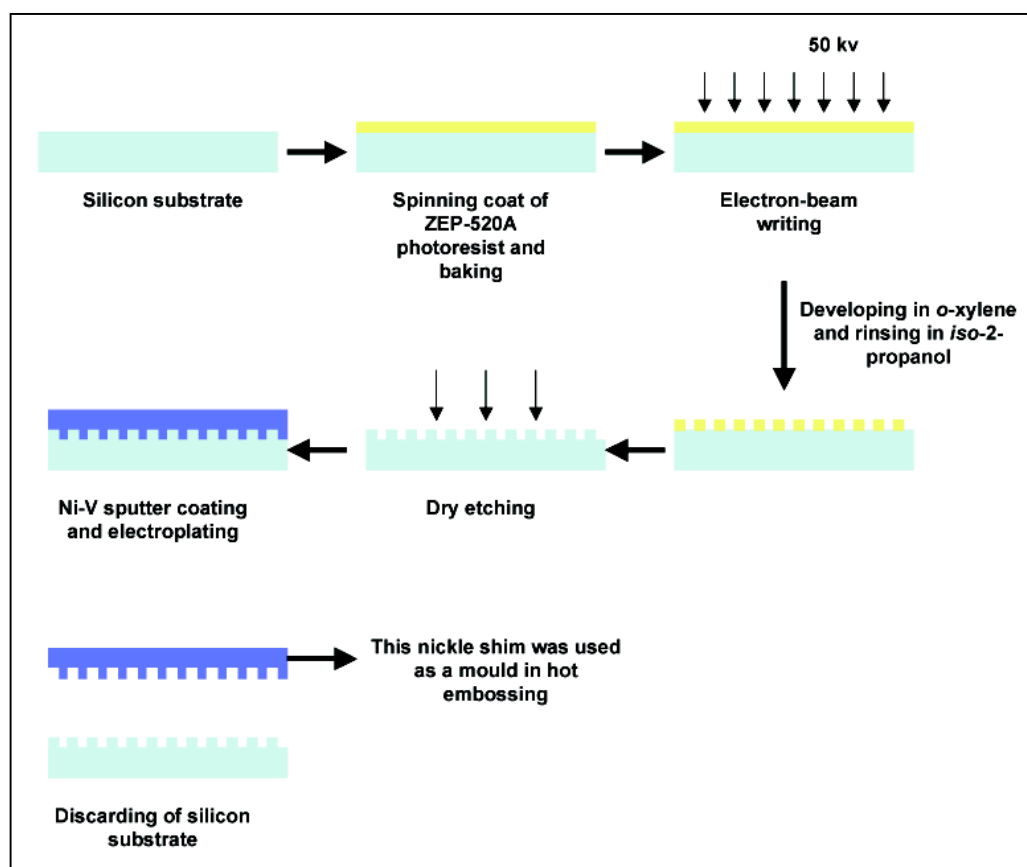


Figure 3.1 Electron Beam lithography. The diagram of NSQ50 fabrication using Electron Beam Lithography.

3.3.2 Cell Culture

Human osteoprogenitor cells were obtained from haematologically normal patients undergoing routine surgery. Only tissue that would have been discarded was used with the approval of the Southampton & South West Hants Local Research Ethics Committee. Primary cultures of bone marrow cells were established as previously described (Oreffo et al., 1999b).

Human osteoprogenitor cells were cultured in 75 cm² tissue culture flasks at passage 2. Culture was maintained in basal media (α -MEM containing 10% FCS and 2% Antibiotics) at 37 °C, supplemented with 5% CO₂. Confluent cell sheets were trypsinized and 1x10⁵ cells were seeded onto NSQ50 and control flat PCL sheets. The cells were maintained as a static culture and media was changed twice per week.

3.3.3 Histology

Coomassie blue was used to monitor cell morphology at two time-points (1 and 3 weeks, selected to allow viewing of individual cells and nascent bone nodules). PCL sheets with cultured cells were fixed in 4% formaldehyde in PBS for 15 minutes at each time point. Cell staining was performed using 5% Coomassie blue in 40% methanol and 10% acetic acid for 5 minutes. The stained materials were washed twice in tap water. Samples were viewed by bright-field microscopy. Pictures were taken by greyscale digital camera (Scion Corporation Model CFW-1310M).

3.3.4 Scanning Electron Microscopy (SEM)

Cells were fixed with 1% glutaraldehyde (Sigma, UK) buffered in 0.1 M sodium cacodylate (Agar, UK) (4 °C, 1 h) after a 3-week culture period to allow the viewing of any nascent bone nodules. The cells were then post-fixed in 1% osmium tetroxide (Agar, UK) and 1% tannic acid (Agar, UK) was used as a mordant, dehydrated through a series of alcohol from 20 to 70%, stained in 0.5% uranyl acetate, followed

by further dehydration in 90, 96, and 100% alcohol. The final dehydration was in hexamethyl-disilazane (Sigma, UK), followed by air-drying. Once dry, the samples were sputter coated with gold before examination with Hitachi S800 field emission SEM.

3.3.5 Alizarin staining

2% Alizarin red stain (pH 4) was prepared by mixing 2 gms of Alizarin red S (Sigma) with 100 ml of water and diluted ammonium hydroxide was added to adjust the pH. After 3 weeks of culture in order to view nascent nodules, the osteoprogenitors were fixed in 4% formaldehyde for 15 min at 37 °C. Then they were stained with 2% alizarin red for 5 min before washing with water. Samples were viewed by bright-field optical microscopy. Pictures were taken by greyscale digital camera (Scion Corporation Model CFW-1310M).

3.3.6 Protein Extraction and Protein Precipitation

After 5 weeks culture, to ensure sufficient levels of protein for analysis, cell sheets were lysed 1 ml of DIGE lysis buffer (7M Urea, 2M Thiourea, 4% CHAPS and 30 mM Tris-base pH 8.0) with 1X final concentration of general purpose protease inhibitor cocktail. Note that there was no trypsinisation step but lysis buffer was added directly onto materials. The cell suspension was left at room temperature for 1 hour with vigorous mixing every 20 minutes. The suspension was then centrifuged at 2,100 rpm for 10 minutes to remove insoluble material. Proteins were then precipitated from the supernatant by addition of 4 volumes of 100% cold acetone (-20 °C). After centrifugation, the protein pellets were washed in 80% acetone and re-suspended in DIGE lysis buffer. The Bradford protein assay was used to determine the amount of protein extracted from each material. Protein assay was performed as described in chapter II, section 2.2.1.

3.3.7 DIGE – analytical gels

The same method used in chapter II, section 2.2.1.4 was applied to analyse protein extract from NSQ50.

3.3.8 Preparative 2D gels

Osteoprogenitor cells (passage 2) were grown in a 75 cm² tissue culture flask until 80-90% confluent. The cells layer was rinsed with HEPES saline before 1 ml of DIGE lysis buffer was added (7M Urea, 2M Thiourea, 4% CHAPS and 30 mM Tris-base pH 8.0) with 1X final concentration of protease inhibitor cocktail (Sigma-Aldrich). The cell suspension was left at room temperature for 1 hour with vigorous mixing every 20 minutes. The suspension was then centrifuged at 2,100 rpm for 10 minutes to remove insoluble material. Proteins were then precipitated from the supernatant by addition of 4 volumes of 100% cold acetone (-20 °C). After centrifugation, the protein pellets were washed in 80% acetone and re-suspended in DIGE lysis buffer. 300 µg of the protein extracted was reduced by 6 µl of 20 mM TCEP and then labelled with 20 µl of Cy3 DIGE fluor. After this, 2D-Gel Electrophoresis was performed and the gel scanned as described above. The preparative gel image was matched with analytical DIGE gel images and the spots of interest were selected for further analysis.

A pick list was generated, containing gel co-ordinates that were used to direct spot cutting. Gel spots were excised using an Ettan Spot Handling Workstation (Amersham Biosciences, UK) and each gel piece was placed in a separate well of a 96-well plate. Gel pieces were washed three times in 100 µl of 50 mM ammonium bicarbonate, 50% v/v methanol and then twice in 100 µl 75% v/v acetonitrile, before drying. Gel pieces were rehydrated with trypsin solution (20 µg trypsin/ml 20 mM ammonium bicarbonate), and incubated for 4 h at 37 °C. Peptides were extracted from the gel pieces by washing twice in 100 µl of 50% v/v acetonitrile / 0.1% v/v

trifluoroacetic acid, before being transferred in solution to a fresh 96 well plate and dried before mass spectrometric (MS) analysis. The use of a preparative gel was required due to the detection limits of the MS and the protein yield from our small samples.

3.4 Results

3.4.1 Fabrication

Both SEM and AFM images indicated that the disordered nanopits were reproduced with good fidelity on the surface of embossed PCL sheets (SEM images are shown in figure 3.2). AFM was also used to evaluate the surface roughness of the flat PCL sheet which was used as a control surface (AFM images of NSQ50 and control are shown in figure 3.3).

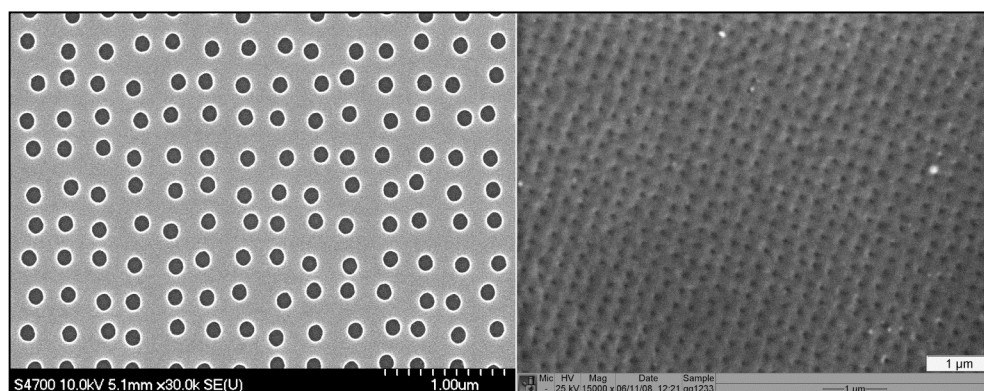


Figure 3.2 SEM image of NSQ50 nanopitted substrates. Near square nanopits with 120 nm diameter, 100 nm depth and with average 300 nm centre-centre spacing (300 nm spaced pits in square pattern, but with +/-50 nm disorder) on polycarbonate substrates produced by electron beam lithography and embossing (A). Embossed-PCL sheet analysed by atomic force microscope to confirm that the nanoscale topography was successfully transferred (B).

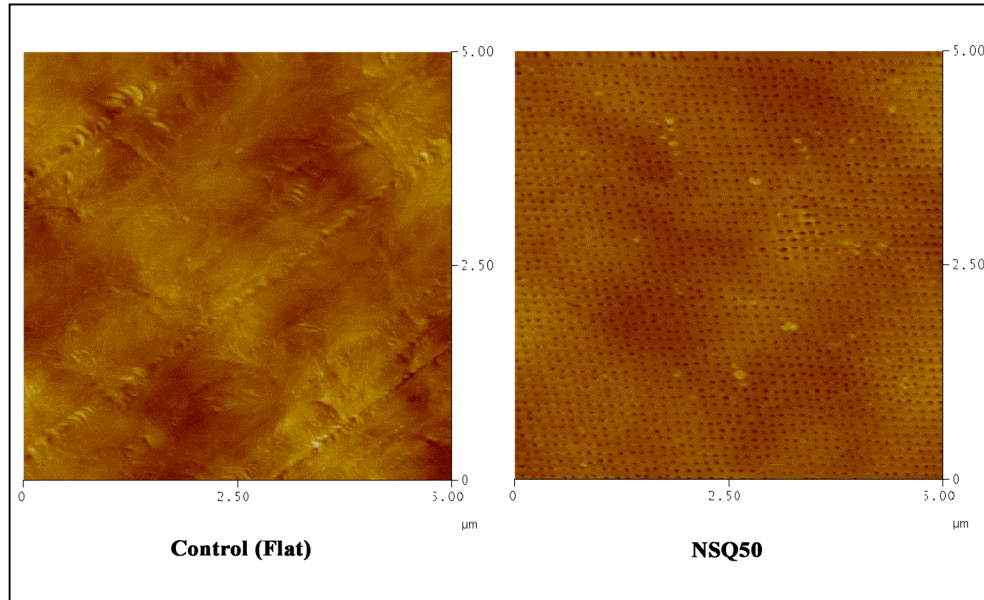


Figure 3.3 AFM image of flat control and NSQ50 nanopit substrates. Planar control and near square nanopits with 120 nm diameter, 100 nm depth and with average 300 nm center-center spacing (300 nm spaced pits in square pattern, but with +/-50 nm disorder) embossed into polycaprolactone (PCL) substrates showed good fidelity.

3.4.2 Cell morphology and histology

Coomassie blue staining after 5 days indicated that osteoprogenitor cells on the flat control were observed to be well spread, whilst osteoprogenitors on the NSQ50 test surface appeared less well spread (figure 3.4). Higher magnification observation, however, showed that similar cell numbers could be observed in each image-grab area and that the cells on the NSQ50 topography were indeed smaller (figure 3.5).

After 3 weeks of static culture, confluent cell layers (90%+) were observed on control. However, dense clusters of cells were noted on nanopit surface (figure 3.4) with the appearance of bone osteoid. Results from scanning electron microscopical evaluation confirmed these results with bone nodule-like structures only observed on NSQ50 (figure 3.6). Alizarin red staining of calcium was observed after 3 weeks

culture on both NSQ50 and control materials (figure 3.7). Dense aggregates with intense staining, however, were only observed on the NSQ50 test topography.

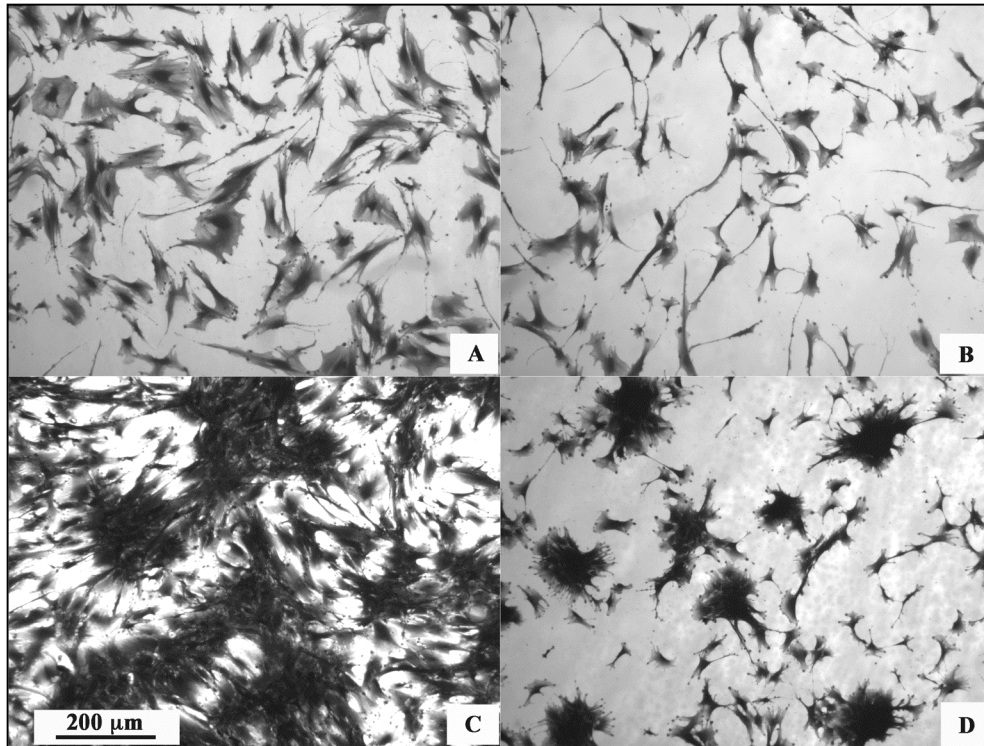


Figure 3.4 Osteoprogenitor cells (OPGs) cultured on PCL substrates in static culture. A. 5 days on flat surface, B. 5 days on NSQ50, C. 3 weeks on flat surface, D. 3 weeks on NSQ50. Note that cells on NSQ50 at day 5 are less spread compared to flat surface. By 3 weeks, dense aggregates appear on NSQ50, similar in appearance to bone nodules.

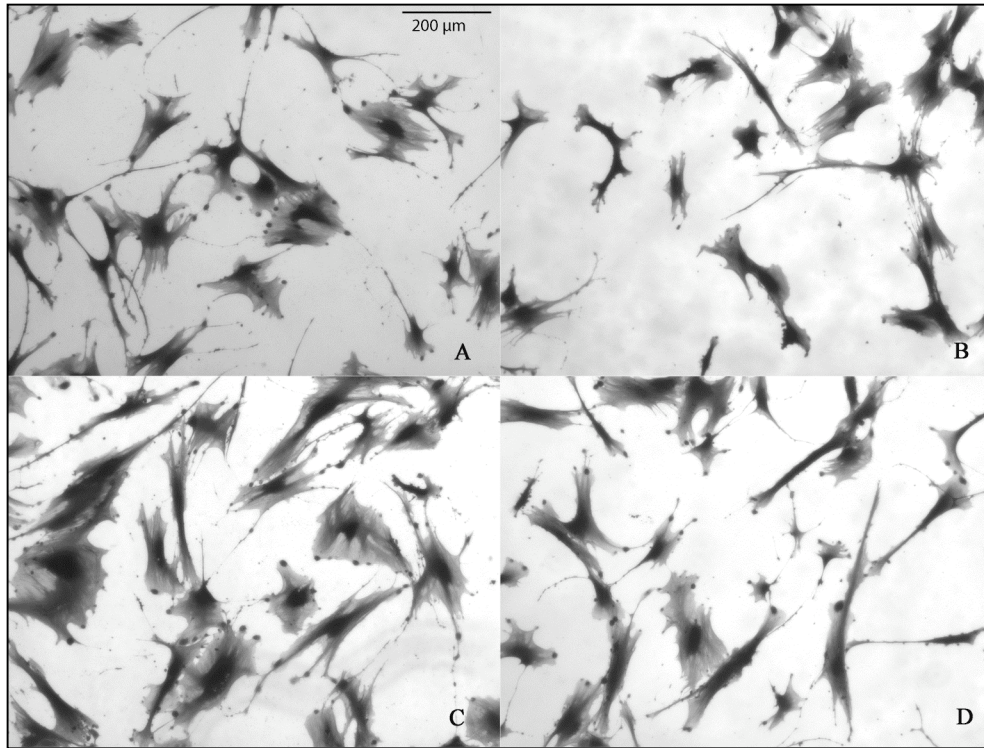


Figure 3.5 Higher magnification of Osteoprogenitor cell morphology. Higher magnification images of different areas on flat (A and C) and NSQ50 (B and D) after 5 days of culture showed that the number of osteoprogenitors adhered on both surfaces were similar.

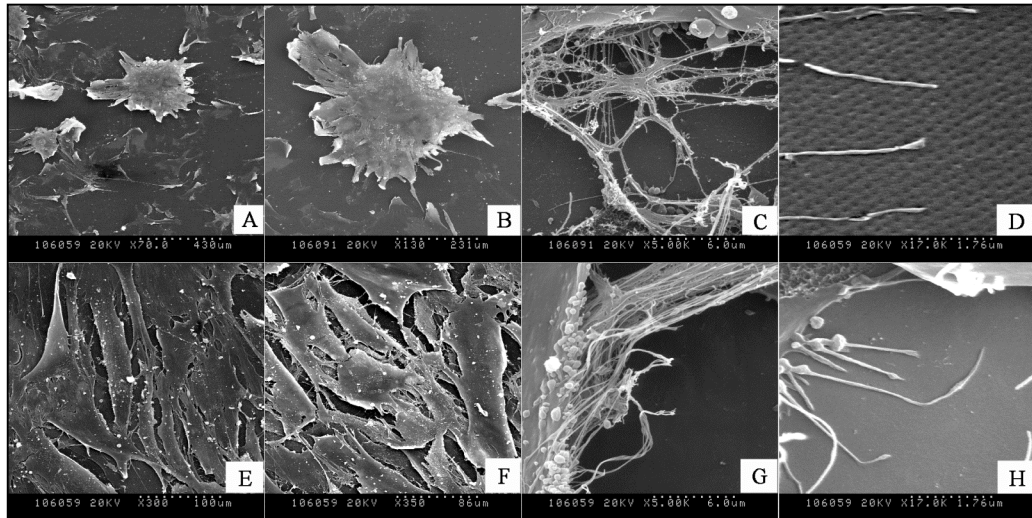


Figure 3.6 Scanning electron micrographs of osteoprogenitor interaction with NSQ50 nanopits compared to flat control. On the NSQ50 topography (upper row), cells could adhere and differentiate to form a dense aggregate of cells similar in appearance to bone nodules (A and B). Cells used their filopodia to sense nanopit topography surface (C and D). On the flat surface (bottom row), cells were fully spread and proliferated to form confluent tissue layers (E and F). Also, cells using their filopodia to sense the substratum surface can be seen (G and H).

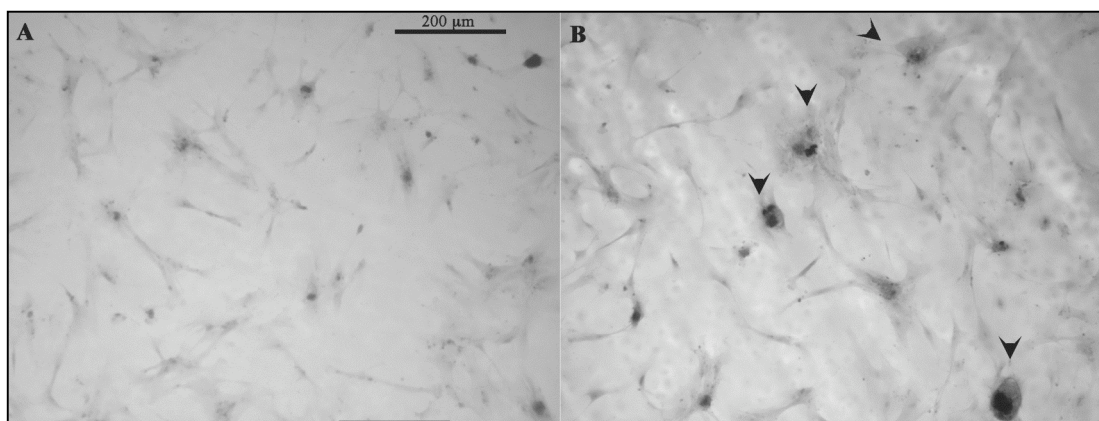


Figure 3.7 Alizarin red staining for calcium accumulation. Positive calcium staining could be seen 3 weeks after cell seeding on planar control and NSQ50. Dense aggregates of cells, bone nodules, however, were only observed on NSQ50 (B, arrowheads)

3.4.3 DIGE

After labelling, proteins were separated and analysed by DeCyder software. Areas that had the degree of difference more than 2 fold were matched with standard preparative gels and then the protein identifications were reported. DIGE showed that the expression of a number of proteins was significantly modulated following the culture of human osteoprogenitor cells on NSQ50 compared to those cultured on flat control (figure 3.8). The results, including name, direction and magnitude of regulation and at-a-glance function, of the identified proteins are shown in Table 3.1.

3.4.4 Preparative gel and protein identification

Areas that showed degrees of difference in protein expression on analytical gels (figure 3.8) were matched with the reference gel (figure 3.9). After gel matching was performed, a pick list was generated from the reference gel and protein identification was performed. Names of the identified proteins were annotated to the corresponding spots on reference gel using the BVA as previously described in chapter II.

Note that there was no step of cell sheet trypsinisation, thus the extracellular matrix proteins adsorbed to the flask surface will also have been extracted. As presented in figure 3.9, there were three areas that could not be detected in the previous work with lysates from trypsinised cell cultures (chapter II). These areas are marked by red arrowheads and numbers (Figure 3.9). Interestingly, area # 1 was identified as albumin which should come from fetal bovine serum in the medium. Area # 2 was identified as galectin-8 which is important for cell adhesion and cell survival and area # 3 was identified as hypothetical protein. However, protein identification of other areas on both reference gels (3.9 A) and analytical gel (3.9 B) had similar results as discussed in the previous chapter setion 2.3.3.1.

3.4.4.1 Proteins with Increased Expression

Significant up-regulations of actin isoforms, beta-galectin1, vimentin and procollagen-proline, 2-oxoglutarate 4-dioxygenase, prolyl 4-hydroxylase were noted.

Electrophoretic area 1: Procollagen-proline, 2-oxoglutarate 4-dioxygenase and Prolyl 4-hydroxylase are a group of enzymes that play critical roles in the maturation of collagen fibers (Pihlajaniemi et al., 1991). Hydroxyproline is involved in hydrogen bond formation which is important for the stabilization of collagen fibers (Ramachandran et al., 1973). Prolyl 4-hydroxylase catalyzes the formation of 4-hydroxyproline in collagens and the reaction catalyzed by prolyl 4-hydroxylase requires Fe^{2+} , 2-oxoglutarate, O_2 and ascorbate and involves an oxidative decarboxylation of 2-oxoglutarate (Kivirikko et al., 1989). The up-regulation of these enzymes suggests increasing collagen synthesis in cells cultured on nanopits.

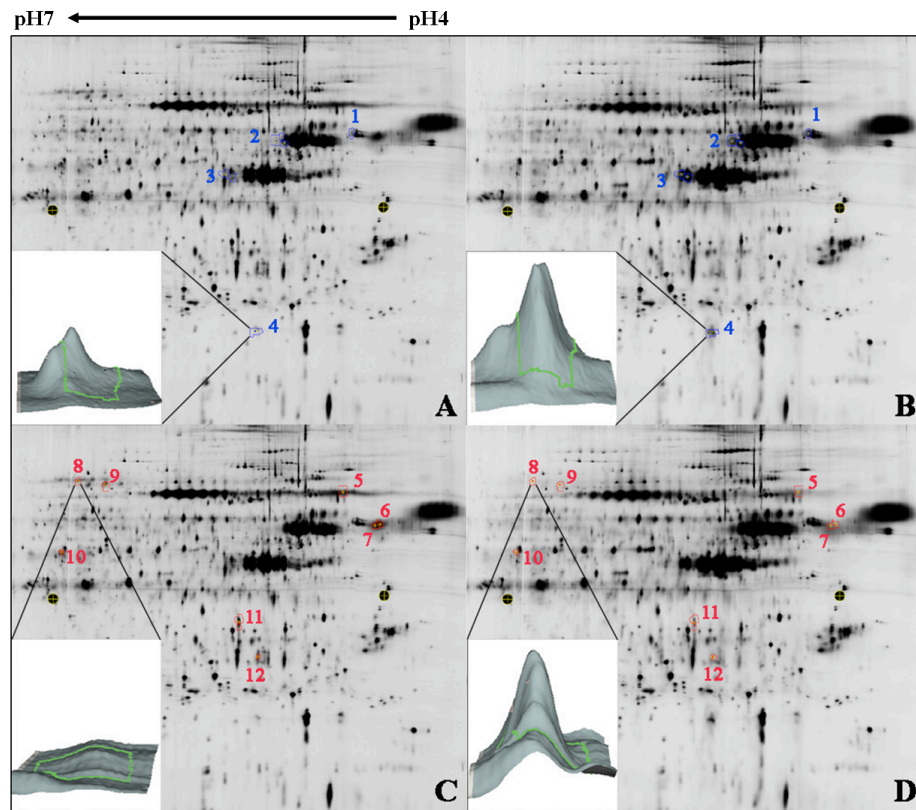


Figure 3.8 Typical DIGE images as were analyzed by DeCyder™ Image Analysis Software. Figure A&C were the images of proteins from control labelled by Cy3. Figure B&D were the images of proteins from NSQ50 labelled by Cy5. Figure A&B showed the areas of up-regulated proteins on NSQ50 (B) when compared control (A) whilst figure C&D showed the areas of down-regulated proteins on NSQ50 (D) when compared control (C). Peak volumes of each spot were compared against each other (insets). 2.0-fold difference in peak volume was used as a cut-off to determine the difference of protein expression between test and control. In all DIGE gels there were areas showing results of up and down-regulation and these spots were used for protein identification.

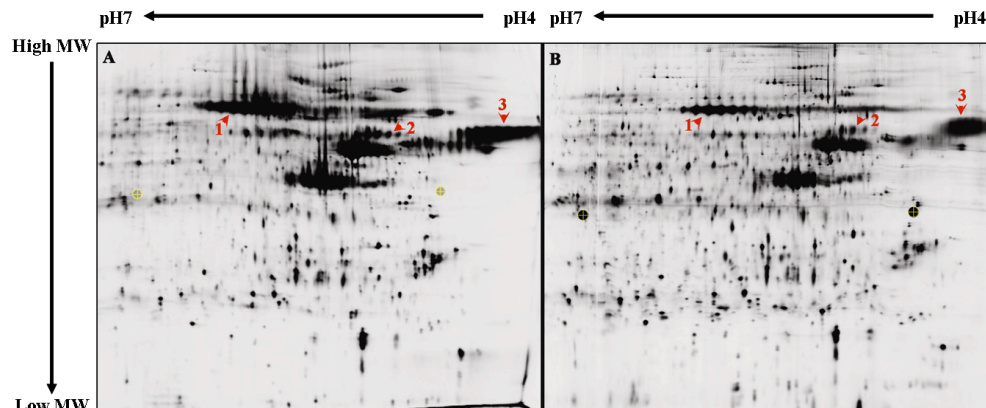


Figure 3.9 Spot matching and protein identification. Using the modified protein extraction method, three areas were found distinctively from the previously used method. These areas were detected on both reference gel (A) and analytical gel (B).

Electrophoretic area 2: Vimentin is the major skeletal intermediate filament cytoskeletal protein and is involved in a wide range of cellular activities. Intermediate filaments play an important role in supporting the location of the organelles (Katsumoto et al., 1990). Furthermore, intermediate filaments respond to mechanical stresses with great sensitivity (Thoumine et al., 1995) and have postulated roles in mechanosensitive signalling via e.g. cellular tensegrity (Ingber, 1997a, Wang et al., 1993). In previous study, the osteoblast-like cell line MC3T3-E1 showed higher expression of vimentin during the differentiation and mineralization phase than in the proliferation phase suggesting vimentin may have a role in bone maturation (Kitching et al., 2002).

Electrophoretic area 3: Actin is a cytoskeletal protein known to be important in topographical contact guidance (Wojciak-Stothard et al., 1995). Changes in actin organization have also been reported in response to nanoscale topographies (Dalby et al., 2003). Increase in well-organized actin stress fibres is associated with enhanced osteogenic activity (Titushkin and Cho, 2007). This may be through the generation of tension by actin stress fibres effecting the formation of focal adhesions which have critical roles in cell response to materials through transmembrane integrins linking the

extracellular matrix to the cytoskeleton. Such changes to cellular adhesion will change signalling from associated proteins such as focal adhesion kinase (FAK), extracellular receptor kinase (ERK) and Src family kinases. All of which interact during FAK autophosphorylation during adhesion maturation and stress fibre assembly (Chrzanowska-Wodnicka and Burridge, 1996, Dalby et al., 2008a).

Electrophoretic area 4: Up-regulation of beta-galactoside-binding lectin precursor (galectin precursor) and galectin-1 were found. These results may indicate increased osteo-specific differentiation on NSQ50 compared to control (Choi et al., 1998, Aubin et al., 1996, Colnot et al., 1999) as expression of galectin in skeletal tissue is controlled by Runx2 during the matrix maturation stage of osteoblastic development (Stock et al., 2003). Galectin-1 was found associated with the nuclear matrix in differentiated osteoblasts. It was detectable only in the nuclear matrix of differentiated osteoblasts (Choi et al., 1998)

3.4.4.2 Proteins with Decreased Expression

Significant down-regulations for enolase, caldesmon, zyxin, GRASP55, Hsp70, (BiP, GRP78), RNH1, cathepsin D and Hsp27 were found.

Electrophoretic area 5: Previous studies indicate that certain isoforms of Hsp70 were down-regulated. Heat shock 70-kDa protein 8 isoform 1 (HSPA8) is expressed on the cell surface of human embryonic stem cells and down-regulated upon differentiation (Son et al., 2005). Decrease in mtHSP70 is important for the induced differentiation of HL-60 promyelocytic leukemia cells (Xu et al., 1999). In contrast, other study showed an increasing in Hsp70 (GRP78/Bip) during differentiation (Nakai et al., 1995). In addition, Cotrupi and Maier have also suggested that cells in microgravity express Hsp70 in order to maintain their proliferative potential (Cotrupi and Maier, 2004). While little is understood yet about this group of proteins, it seems likely that heat shock proteins will be important in modulation osteoblastic proliferation and differentiation.

Electrophoretic area 6: Down-regulation of RNase inhibitor was also noted in a previous study (Kantawong et al., 2009) which considered progenitor cells on grooves. Activity of RNase is inhibited by formation of a complex with an inhibitor (such as RNH1). *In vivo* more than 95% of ribonuclease is complexed with an inhibitor and the inhibitor/RNase ratio is elevated in proliferating tissues (Schneider et al., 1988). Thus, it may be that this result indicates the lower proliferative activity of the cells on the NSQ50 (compared to control) as a consequence of differentiation to matrix secreting cells.

Electrophoretic area 7: Down-regulation of Golgi reassembly stacking protein 2 (GRASP55) might indicate the decreasing of mitotic activity of the cultured cells on disordered nanopits. GRASP55 plays a mitogen-activated protein kinase kinase /extracellular-activated protein kinase (MEK/ERK)-regulated role in Golgi ribbon formation and cell cycle progression (Feinstein and Linstedt, 2008). GRASP55 mediates assembly of Golgi stacks in an *in vitro* assay (Shorter et al., 1999).

Electrophoretic area 8: Zyxin is one of LIM domain proteins at focal adhesion plaques (Wang and Gilmore, 2003). Zyxin is a phosphoprotein localized at sites of cell-substratum adhesion and also plays a role as an intracellular signal transducer. Zyxin and its partners have been implicated in the spatial control of actin filament assembly as well as in pathways important for cell differentiation (Beckerle, 1997). This group of proteins also shuttle through the nucleus and may regulate gene transcription by interaction with transcription factors (Wang and Gilmore, 2003).

Electrophoretic area 9: Down-regulation of caldesmon can also be correlated to the previous proteomic study considering grooved topography (Kantawong et al., 2009). Caldesmon is an actin binding protein. In non-muscle cells it influences contractility by interfering with focal adhesion and stress fibre assembly (Helfman et al., 1999, Li et al., 2004). Thus, this result appears to fit well with the previous observation of increased actin isoform expression. This result is also in agreement with a further previous study (Inoue et al., 2000) which indicated that caldesmon is down-regulated

during osteoblastic differentiation.

Electrophoretic area 10: Down-regulation of alpha-enolase provides further evidence that culture cells on NSQ50 were differentiating (compared to control). Alpha-enolase was found up-regulated in proliferating human keratinocytes and down-regulated in differentiating cell types (Olsen et al., 1995).

Electrophoretic area 11: Cathepsin D is a well-characterized aspartic protease expressed ubiquitously in lysosomes. The enzyme has broad substrate specificity at acidic pH. Cathepsin D is important in bone degradation due to a role in extracellular matrix degradation. Cathepsin D has also been implicated in cell growth and apoptosis and expressed as a marker for osteoclast differentiation. Osteoclasts are macrophage-derived cells developed from the haematopoietic lineage. This suggested that protein expression during cell differentiation depends on individual cell types.

Electrophoretic area 12: Heat shock protein 27 is a downstream regulator of actin filament structure and dynamics (Landry and Huot, 1995). Heat shock protein 27 is involved in regulation of actin polymerization and stability (Benndorf et al., 1994, Huot et al., 1996) and participates in the cell proliferation and differentiation during tissue development (Wang and Gilmore, 2003, Takahashi-Horiuchi et al., 2008, Matalon et al., 2008). In contrast, HSP27 expression was decreased in this study. HSP27 overexpression has been shown to increase FAK phosphorylation and focal adhesion formation, depending on integrin-mediated actin cytoskeleton polymerization (Lee et al., 2008).

Table 3.1 Names and functions of proteins modulated by the NSQ50 topography.

The cut-off used in this study was changes greater than 2.0-fold up/down regulation.

Area	Name	Function summary	Expression resulting from static culture
1	Prolyl 4-hydroxylase	Collagen formation	+2.50±1.13
2	Vimentin	Cytoskeleton (Intermediate filament)	+2.93±0.51
3	Actin	Cytoskeleton (Microfilament)	+3.55±1.57
4	Galectin-1	Regulation of cell adhesion	+3.63±0.82
5	Hsp70 and GRP78 (BiP)	Chaperone	-2.39±0.29
6	GRASP55	Reassembling of golgi apparatus	-2.81±0.82
7	RNase inhibitor	RNA degradation inhibition	-2.77±0.77
8	Zyxin	Focal adhesion forming	-2.83±0.89
9	Caldesmon	Calmodulin and actin binding protein	-5.03±0.99
10	Alpha-enolase	Enzyme in glycolytic pathway	-2.58±0.31
11	Cathepsin D	Lysosomal protease	-2.23±0.31
12	Heat shock protein 27 (Hsp27)	Chaperone	-4.23±0.39

3.5 Discussion

The application of optimal protocols from chapter II was used successfully to evaluate the different of protein expression between cells cultured on NSQ50 and control. In this chapter most of the protocols used were exactly the same as those used in chapter II. However, the method of protein extraction was modified to be suitable for a smaller areas of the nanopitted material (2 cm² of grooves compared to 1 cm² of nanopits).

This chapter has examined the differential osteoblast proteomic profiles of cells cultured on an osteogenic nanotopography, NSQ50, and flat control over a 36 day time frame and demonstrated significant regulation of a number of matrix, cytoskeletal, heat shock and molecular and biochemical players.

Chapter II considered DIGE of osteoprogenitor cells cultured on microtopography (grooves) and showed that microgrooved topography altered the cell morphology and induced changes in protein expression profiles. It could be theorised, from linking to previous studies, that these changes are induced by changes in the arrangement of the cytoskeletal network (Dalby et al., 2007a, Dalby et al., 2007c). The cytoskeleton is thought to act as an integrated network transducing changes in cellular tension to the nucleus via the close relationship of the cytoskeletal intermediate filaments (e.g. vimentin) and the nucleoskeletal intermediate filaments, the lamins (Ingber, 2003a). Furthermore, lamins have been described as being intimate with interphase chromatin (Bloom et al., 1996).

It has been reported that nanoscale topographies can induce changes in cell adhesion complex formation (Biggs et al., 2007a, Biggs et al., 2008b), cell morphology (Biggs et al., 2007b), cytoskeleton network and nuclear organization (Dalby et al., 2007c). This chapter investigates whether such changes translate to the proteome on a highly novel nanotopography for which gene expression has also been investigated; the protein expression profile provides definitive evidence of transcriptional protein

changes as a consequence of alterations to the gene expression. Here, protein profiles in long-term culture have been studied (5 weeks). As observed, with cells on microgrooves, the regulation of the cytoskeleton, is of central importance.

The influence of microscale features on cytoskeletal filaments and tubules are easier to appreciate due to the scale of the features compared to the cell; i.e. they are in the same order of magnitude. However, nanoscale features are far smaller than the cell, corresponding in size to features such as filopodia, and thus it seems likely that nanotopography will change cell behaviour through alteration in adhesion formation rather than mechanical constraint. In this study, the novel osteogenic nanotopography, NSQ50, resulted in changes in protein expression profiles of the cultured osteoprogenitor cells confirming nanotopography can direct cell differentiation with implications therein in the future design of scaffolds and biomaterials for reparative approaches.

In recent publications looking at nanoscale topographies (including NSQ50) and genomic regulations (Dalby et al., 2007d, Dalby et al., 2008a), it has been shown that there are several canonical (well-defined) signalling pathways that appear to be specifically triggered by nanotopography. These include actin related signalling and integrin related signalling. The proteomic observation of cytoskeletal and regulatory protein changes suggests translation of these pathways from the genome to the proteome. This is critical for expression of phenotype from genomic regulations.

NSQ50 has previously been shown to modulate osteoid formation *in vitro* in basal media, whilst osteoprogenitor cells grown on flat control appear to have a more fibroblastic morphology (Dalby et al., 2007d). It is clear that NSQ50 attenuates cell adhesion as shown in the down-regulation of zyxin and Hsp27 which will affect focal adhesion kinase (FAK) signalling downstream. These changes will have effects on cell cytoskeleton and subsequent cellular trafficking. Since Cathepsin D is involved in protein trafficking and protein degradation, it might be postulated that the down-regulation of this enzyme results from changes in cellular trafficking activity. The

maturation of cathepsin D depends on the clathrin-mediated trafficking of TGN-derived cargo which is regulated via actin assembly (Carreno et al., 2004, Poupon et al., 2008).

The most important change influenced by NSQ50 is the attenuation of cell proliferation as shown in the down-regulation of Golgi reassembly stacking protein (GRASP55), the downstream regulator of the mitogen-activated protein kinase kinase (MKK)/extracellular-activated protein kinase (ERK) pathway (Jesch et al., 2001). Down-regulation of RNH1 also agrees that the proliferation rate of cells on NSQ50 should be decreased. Changes in expression of galectin and procollagen-proline, 2-oxoglutarate 4-dioxygenase and prolyl 4-hydroxylase, all infer changes in the maturational state of the progenitor cells and thus the results presented in this chapter suggest that the balance of these proteins could be important in topographically induced bone cell differentiation and bone formation.

Disordered nanopits imprinted onto a PCL substrate are a stimulator of human osteoprogenitor cell differentiation. This chapter demonstrates a differential proteomic technique to study the cells response to nanotopography and shows a number of significant changes in protein expression. The changes implicate modulation of focal adhesions and the cytoskeleton as having central roles in inducing cell differentiation on nanotopography.

The development of materials that can elicit desired responses in stem cell and progenitor cell populations will underpin tissue engineering where a key drive is the formation of complex tissues in the laboratory. This requirement for complex nanostructures indicates the need to further elucidate the mechanisms and disordered structures implicated in stem cell differentiation and potential therein for developing innovative strategies to tissue repair.

Chapter IV Temporal proteomic analysis of novel disordered nanopit topography

4.1. Introduction

The aims of this chapter is to firstly monitor changes in expression of proteins for osteoprogenitor cells cultured on the osteogenic NSQ50 nanopography at different time points. The second aim is to compare static and flow conditions using proteomics for cells cultured on NSQ50.

In the previous chapter, disordered nanopits (NSQ50) were shown to direct osteoprogenitor cell differentiation. Osteoprogenitor cells cultured on NSQ50 started to form nascent nodules three weeks after cell seeding but proteomic profiles were analysed two weeks later (five weeks after cell seeding). It was postulated that cells on NSQ50 had lower proliferative activity when compared to flat surface but a higher differentiative ability. To build on this, here, proteomic analysis of osteoprogenitor cells was performed at 3, 4, 5 and 6 weeks after cell seeding to explore how NSQ50 modulates mineral nodule formation.

In this chapter, two proteomic approaches were used, firstly DIGE and secondly dimethyl labelling. DIGE was used to monitor the expression of the proteomic profile at 3, 4, 5 and 6 weeks after cell seeding and dimethyl labelling was used to confirm and expand the protein expression profile after 6 week culture.

Dimethyl labelling uses isotopic and non-isotopic formaldehyde to tag the protein extracts from test and control materials respectively. Then, the differential protein expression between test and control can be quantified by liquid chromatographical separation of isotopic against non-isotopic forms and mass spectrophotometric analysis (Hsu et al., 2003). Highly hydrophobic proteins are rarely to be found on 2D gel separations of whole cell lysates (Wilkins et al., 1998) because of precipitation of many of these proteins during first-dimension, isoelectric focusing (Fandino et al.,

2005). LC-MS/MS allows the possibility of enhanced hydrophobic protein detection compared to 2D gel electrophoresis by allowing the analyses of complete complexes and preventing protein aggregation of hydrophobic regions during electrophoresis (Fandino et al., 2005).

Histology has been used alongside the proteomic techniques to confirm growth and differentiation. Previous histological analysis of osteoblast adhesion formation on NSQ50 revealed that absolute order reduced adhesion size resulting in a shift (from focal adhesion formation (2-5 μm long adhesions)) to formation of small focal complexes (< 2 μm long), whilst introducing controlled disorder resulted in a shift to the formation of larger, super-mature, adhesions (> 5 μm long). This result implicated focal adhesion formation and the cytoskeleton in osteoblastic activity of the disordered topography. Gene array of progenitor cells indeed implicated integrin (including focal adhesion kinase, FAK) and cytoskeletal signaling (including small G-proteins responsible for filopodial, lamellipodial and stress fibre formation). However, also implied have been the mitogen activated protein kinase (MAPK) family especially extracellular signal-regulated (ERK) and p38 MAPK (Dalby et al., 2007d). Changes in these pathways have also been implied by genomic and histological studies with other topographies (Biggs et al., 2008b, Biggs et al., 2008a, Hamilton and Brunette, 2007).

ERK 1/2 (also known as MAPK3, MAPK1) is an interesting biochemical target as, as discussed in chapter III, it is linked to cell adhesion and is important in cellular proliferation, differentiation, and survival through modulation of transcription factors; this includes Runx 2 (runt related protein 2, the osteogenic master gene) (Phillips et al., 2006, Reilly et al., 2005). The ERK cascade (which involves FAK) is initiated by adhesion to the extracellular matrix, for example, activation of ERK following $\alpha_5\beta_1$ integrin binding at the cell surface to extracellular matrix proteins such as fibronectin (Yee et al., 2008).

4.2 Materials and methods

4.2.1 Cell Culture

Human osteoprogenitor cells (as used in the previous chapter) were cultured in 75 cm² tissue culture flasks until at passage 2 (to allow for expansion, but to retain multipotency). Culture was maintained in basal media (α -MEM containing 10% foetal bovine serum and 2% Antibiotics) at 37⁰C, supplemented with 5% CO₂. Cells were trypsinized and 1x10⁵ cells were seeded onto NSQ50 and control flat PCL sheets. The culture was maintained until week 3 then 5 pairs of material (5 controls, 5 tests) were harvested for protein extraction and histological staining. This was repeated also for weeks 4, 5 and 6 of culture. Media was changed twice per week. At 3 weeks of culture (NOTE: one time point only), fluid-flow bioreactor was used alongside the static culture. The cell culture plan is presented in figure 4.1.

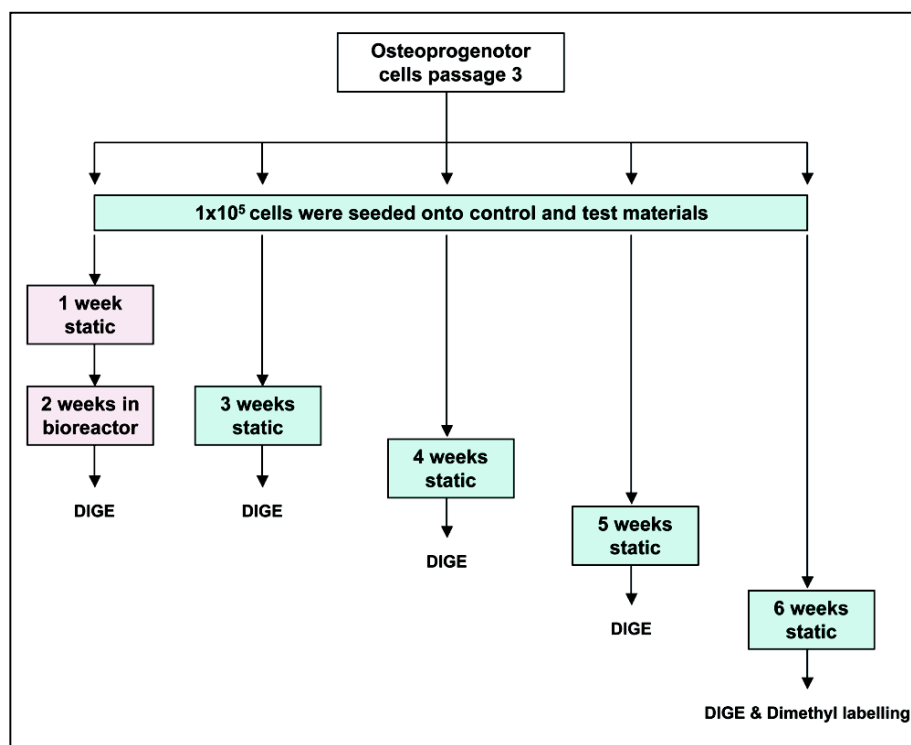


Figure 4.1 Cell culture plan. Five groups of cell culture were set and then stopped at different time point (3, 4, 5 and 6 weeks of culture) for differential proteomic analysis. At 3 weeks culture both static- and flow-system were used.

4.2.2 Histology

At similar time points (3, 4, 5 and 6 weeks of culture) to those used for protein extraction, cells were fixed for histology.

4.2.2.1 Coomassie Blue. PCL sheets with cultured cells were fixed in 4% formaldehyde in PBS for 15 minutes. Cell staining was performed using 5% Coomassie blue in 40% methanol and 10% acetic acid for 5 minutes. The stained materials were washed twice in tap water. Cell morphology was monitored at 3, 4, 5 and 6 weeks after cell seeding. Samples were viewed by bright-field microscopy. Pictures were taken by greyscale digital camera (Scion Corporation Model CFW-1310M).

4.2.2.2 Alizarin Red: 2% Alizarin red stain (pH 4) was prepared by mixing 2 gms of Alizarin red S (Sigma) with 100 ml of water and diluted ammonium hydroxide was added to adjust the pH. After 3, 4, 5 and 6 weeks of culture, the osteoprogenitors were fixed in 4% formaldehyde for 15 min at 37 °C. Then they were stained with 2% alizarin red for 5 minutes before washing with tap water. Samples were viewed by bright-field optical microscopy. Pictures were taken by greyscale digital camera (Scion Corporation Model CFW-1310M).

4.2.3 Protein Extraction and Protein Precipitation

After 3, 4, 5 and 6 weeks culture, cells on the materials were lysed in 1 ml of DIGE lysis buffer with 1X final concentration of general purpose protease inhibitor cocktail. The cell suspension was left at room temperature for 1 hour with vigorous mixing every 20 minutes. The suspension was then centrifuged at 2,100 rpm for 10 minutes to remove insoluble material. Proteins were then precipitated from the supernatant by addition of 4 volumes of 100% cold acetone (-20 °C). After centrifugation, the protein pellets were washed in 80% acetone and re-suspended in DIGE lysis buffer. The Bradford protein assay was used to determine the amount of protein extracted

from each material. Saturation labelling, 2D gel electrophoresis included preparative 2D gel and protein identification were performed as mentioned in the previous chapter.

4.2.4 Dimethyl labelling

4.2.4.1 Protein extraction: After 6 weeks of culture (only 1 time point used for this very new method), protein extraction was modified from the Eukaryotic Membrane Protein Extraction Kit protocol (Pierce). Six cultured materials (6 flat PCL vs 6 NSQ50) were rinsed in HEPES saline buffer. 150 μ l of reagent A was added to the cultured materials and incubated at room temperature for 10 minutes. 900 μ l of reagent B/C was added and incubated on ice for 30 minutes. The suspension was spun down at 10,000 g for 3 minutes. The insoluble debris was separated. The solubilised proteins fraction was used in phase partitioning at 37 $^{\circ}$ C for 10 minutes following by 10,000 g centrifugation for 2 minutes. The hydrophobic (bottom) and hydrophilic (top) fractions were separated from each other. Protein precipitation was performed by adding 4 volumes of cold acetone (-20 $^{\circ}$ C) into both fractions and leaving overnight at -20 $^{\circ}$ C. After centrifugation at 10,000 g for 10 minutes, protein pellets were washed in 80% cold acetone (-20 $^{\circ}$ C) and collected to use in the labelling later on.

4.2.4.2 Protein labelling: protein pellets were solubilised in SDS buffer. Protein quantification was performed using the Bradford Assay Kit (Bio-Rad, UK). 90 μ l of 100 mM Sodium acetate was added to the lysate. Differential labelling was performed with the addition of 10 μ l of 4% formaldehyde (control sample) or 4% deuterated formaldehyde (treated sample) to the lysate, followed by 10 μ l of 1M Sodium cyanoborohydride. The samples were vortexed to mix, and left at room temperature for 5 minutes. Following labelling, the control (light labelled) and test (heavy labelled) samples were mixed together, and the resulting mixture was

vortexed and spun down. The hydrophobic fraction of control was mixed with the hydrophobic fraction of test and the hydrophilic fraction of control was mixed with the hydrophilic fraction of test then both fractions were separated by SDS-PAGE.

4.2.4.3 SDS-PAGE & In-gel digestion: protein electrophoresis was performed following the NuPAGE Electrophoresis Protocols. The polyacrylamide gel was stained with 5% Coomassie blue. Protein bands were excised and placed in 96 well-plate. Gel pieces were washed in 25 mM ammonium bicarbonate for 30 minutes followed by a wash with 50% acetonitrile/100 mM ammonium bicarbonate for 30 minutes. Trypsin (Promega, UK) was reconstituted in 25 mM NH_4HCO_3 pH 8 to a final concentration of 0.2 $\mu\text{g}/\mu\text{l}$ and enough volume was added to cover the gel pieces. Proteins were allowed to digest overnight at 37 °C. Acetonitrile was added to the digest to give approximately 50% acetonitrile in the final volume and incubated for 20 minutes before centrifugation. Soluble peptides were transferred to a fresh 96-well plate. 1% formic acid was added to cover the gel pieces followed by the incubation at room temperature for 20 minutes. Acetonitrile was added to the gel pieces again to re-extract the remaining peptides. The soluble peptides were transferred to the same 96-well plate.

4.2.4.4 LC-MS/MS: Samples were separated by liquid chromatography using an UltiMate HPLC (Dionex, UK). Chromatography was performed using a PepMap C18 column (Dionex, UK), with a gradient running from 5% to 40% acetonitrile in 20 minutes followed by a wash at 72% acetonitrile for 5 minutes, and a reequilibration step at 5% acetonitrile for 6 minutes. Mass spectrometry was performed using a QStar pulsar i (Applied Biosystems, UK), with a scan range from 400 to 1500m/z, a collection rate of one spectrum per three seconds. For each survey scan collected, four precursors were selected for fragmentation, for a total duty cycle of 15 seconds.

4.2.4.5 Dimethyl Labelling Data Processing: Initial protein identification was performed using the Analyst software to pass data to the MASCOT software (Matrix Science, UK). Quantitative data processing was performed by passing each LC-MS/MS data file through the MZwiff program to generate an MZXML file which was combined with the MASCOT peak file for analysis by the XInteract (XPRESS) software (part of the Trans-Proteomic Pipeline).

4.3 Results

4.3.1 Histology

4.3.1.1 Cell morphology (Coomassie blue): Temporal analysis (3, 4, 5 and 6 weeks of culture) showed that the progenitor cells grew well on both the NSQ50 test surface and the flat control surface (figure 4.2).

4.3.1.2 Tissue mineralization (alizarin red): The progenitor population was seen to be highly osteogenic with dense bone nodules observed on both flat control and NSQ50 by 6 weeks of culture. However, whilst aggregates were seen on both the control and NSQ50 after 6 weeks of culture, progenitors cultured on NSQ50 were seen to form dense nodules 2 weeks prior to cells on control (NSQ50 nodules seen at 4 weeks, control nodules seen at 6 weeks) (figure 4.3).

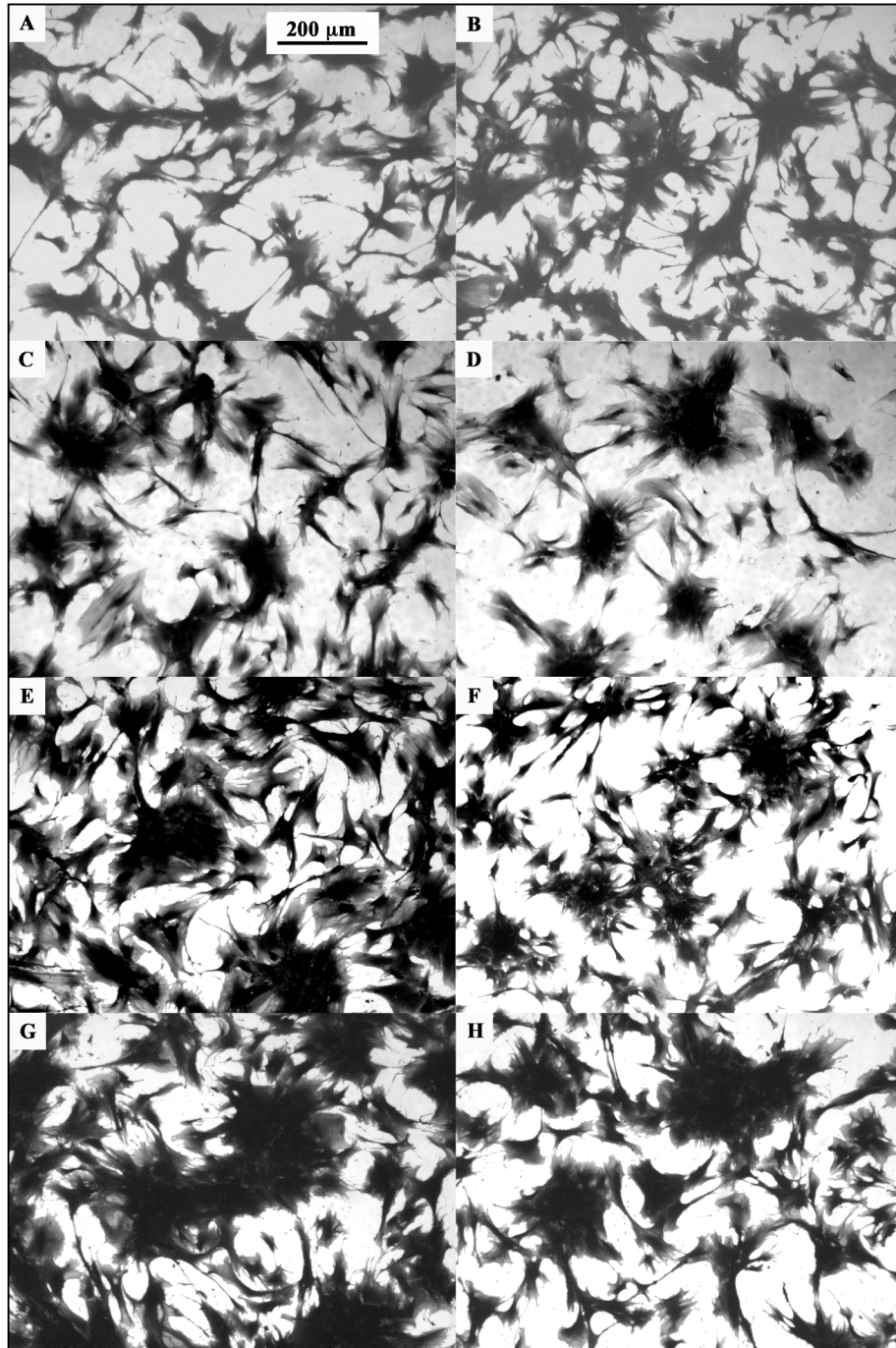


Figure 4.2 Coomassie blue staining of osteoprogenitor cells (OPGs) cultured on PCL substrates in static culture. A&B = 3 weeks on flat and NSQ50 surface, C&D = 4 weeks on flat and NSQ50 surface, E&F = 5 weeks on flat and NSQ50 surface and G&H = 6 weeks on flat and NSQ50 surface.

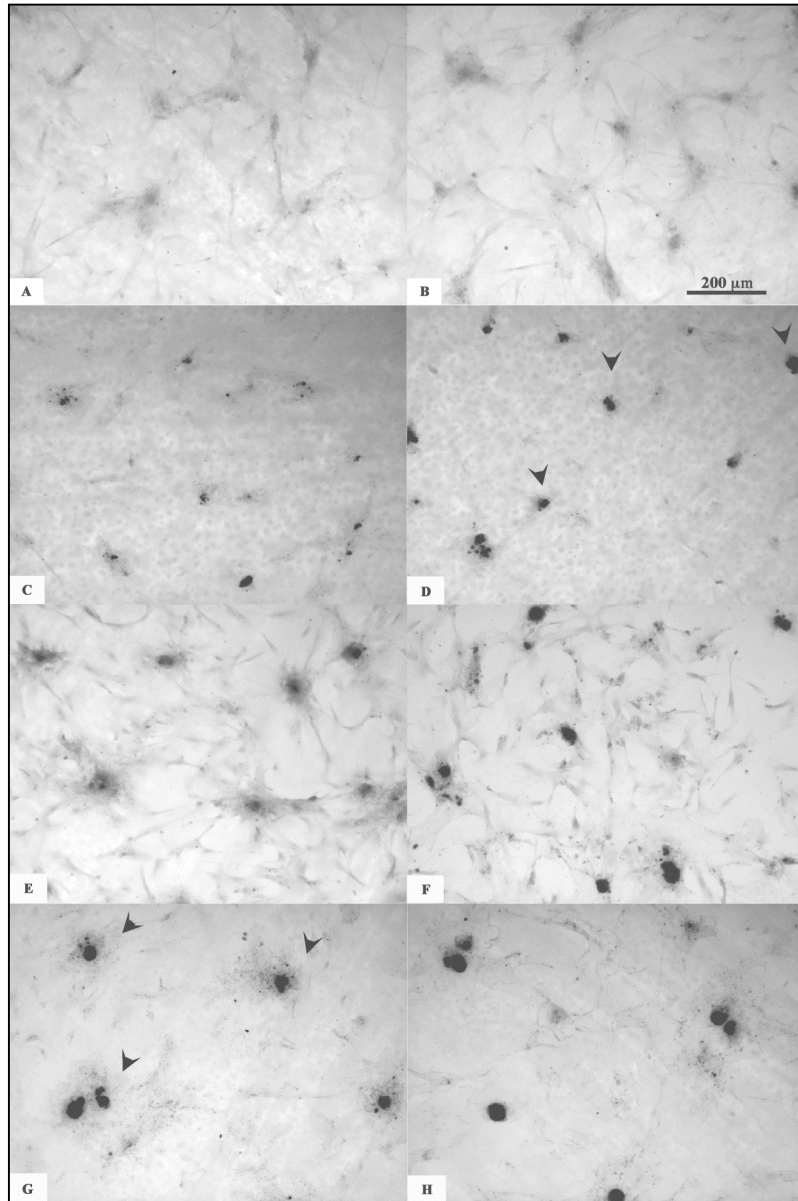


Figure 4.3 Alizarin red staining for calcium accumulation. Calcium staining was observed at 3- (A&B), 4- (C&D), 5- (E&F) and 6- (G&H) week culture. Positive calcium staining could be seen 3 weeks after cell seeding. Dense aggregates of cells, bone nodules, were observed on both flat and NSQ50. Note that, lower number of less dense aggregates appear on flat surface (A, C and E) while dense aggregates were formed on NSQ50 with higher number (B, D and F). Dense, mature, nodules were formed by cells on NSQ50 two weeks before observed on control (arrowheads).

4.3.2 Temporal DIGE

DIGE results showed the differential regulation of many proteins at each time point as derived from 2D gel images. The following is the list of proteins, together with their functions related to cell proliferation and differentiation. The spot areas of each protein in the list are shown in figure 4.4

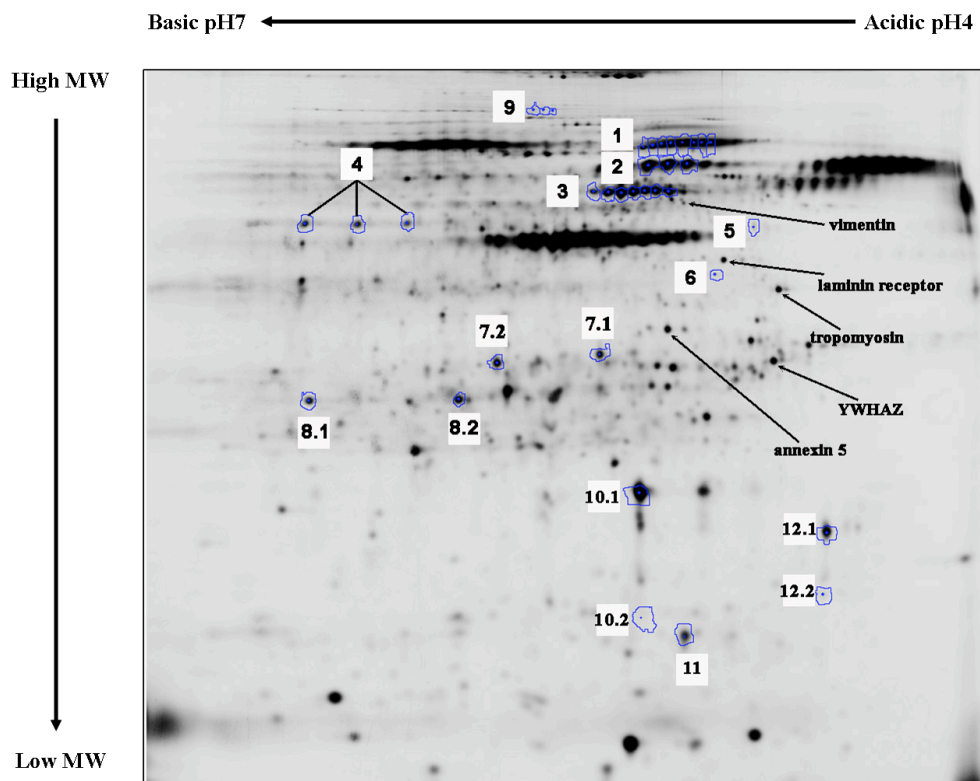


Figure 4.4 Typical DIGE images as were analyzed by DeCyder™ Image Analysis Software. The images of 2D gel showing areas of protein that up-/down-regulated. Peak volume of each spot was compared against each other. 1 = Hsp70, 2 = Gal-8, 3 = tubulin, 4 = α -enolase, 5 = vimentin, 6 = Npm1, 7.1&7.2 = p64, 8.1&8.2 = Hsp27, 9 = α -collagen, 10.1&10.2 = Gal-1, 11 = thioredoxin and 12.1&12.2 = MYL6.

Protein Expression of cells cultured in the static environment

Electrophoretic area 1 Heat shock protein 70 (GRP78 and BiP): The major role of Hsp70 is working as a chaperone, however, several Hsp70s were characterized as microtubule-associated protein (Liang and MacRae, 1997). In mammals there is an evidence that mitogen-activated protein kinases (MAPKs) of the ERK family alter Hsp70 transcription. The ERK signaling pathway induces expression of Hsp70 (Hung et al., 1998) and inhibition of ERK reduces Hsp70 expression in response to various stressors (Yang et al., 2004, Keller et al., 2008). Hsp70 was down-regulated (~3-fold) at 3-week culture, however, after 3 weeks the expression of Hsp70 was rising and had stabilized by 5 weeks (figure 4.5A).

Electrophoretic area 2 Galectin 8: Secreted galectin-8 inhibits adhesion of human carcinoma (1299) cells to plates coated with integrin ligands, and induces cell apoptosis (Hadari et al., 2000). When immobilized, it functions as a matrix protein in promoting cell adhesion by ligation and clustering of a selective subset of cell surface integrin receptors and triggers integrin-mediated signalling cascades such as Tyr phosphorylation of FAK and paxillin. In contrast, when present in excess as a soluble ligand, galectin-8 forms a complex with integrins that negatively regulates cell adhesion (Levy et al., 2001, Zick et al., 2004). There was no difference of galectin-8 expression between test and control at 3 weeks culture (~1-fold) but the expression continuously increased. At 6 weeks culture the expression of galectin-8 on NSQ50 was up-regulated significantly (~3.5-fold) when compared to control (figure 4.5B).

Electrophoretic area 3 Tubulin: Disruption of tubulin organization affects the kinetics of actin organization (Rodriguez et al., 2004). Tyrosinated alpha-tubulin is involved in specific regulation of cyclin B synthesis (Vee et al., 2001). Tubulin was up-regulated at 3 weeks culture, however, after that there was no difference of tubulin expression on NSQ50 compared to control (figure 4.5C).

Electrophoretic area 4 Enolase: Enolase is a multifunctional glycolytic enzyme (Kang et al., 2008) and a novel class of surface proteins which do not possess classical machinery for surface transport (Pancholi, 2001). It has an ability to serve as a plasminogen receptor on the surface of a variety of hematopoietic, epithelial and endothelial cells (Seweryn et al., 2007) and to function as a heat-shock protein and to bind cytoskeletal and chromatin structures. This indicates that enolase may play a crucial role in transcription (Keller et al., 2007). The induction of alpha-enolase is involved with ERK1/2 signalling (Mizukami et al., 2004, Sousa et al., 2005). Enolase was up-regulated on NSQ50 at 3 weeks (~2.5-fold). After that the expression of alpha-enolase on NSQ50 compare to control was not different (~1-fold). After 5 weeks the expression of alpha-enolase on NSQ50 decreased again and by 6 weeks it was down-regulated about 1.5-fold when compared to control (figure 4.5D).

Electrophoretic area 5 Vimentin: Vimentin and intermediate filaments were also used as a differentiation marker in many cell types. For example, the differentiation process of optic vesicle epithelium into neural retina is influenced by the amount of vimentin in epithelial cells (Iwatsuki et al., 1999). In the clonal osteoblast-like cell line MC3T3-E1, cDNAs for vimentin were upregulated in both differentiation and mineralization, compared with proliferation (Kitching et al., 2002). Vimentin expression could thus play a role at an advanced stage of osteogenesis (Rius and Aller, 1992). At 3 weeks the expression of vimentin on NSQ50 was massively higher than control ~6-fold (6.12 ± 2.13). After that (4 weeks onwards) there was no different of vimentin expression between NSQ50 and control.

Electrophoretic area 6 Nucleophosmin 1 (Npm1): Npm1 is an abundant and ubiquitously expressed phosphoprotein (Szebeni et al., 1995). It locates mainly in the nucleolus and shuttles between nucleus and cytoplasm (Borer et al., 1989). Some studies suggest that suppression of Npm1 expression in neural stem cells inhibits cell proliferation (Qing et al., 2008). The study by *Chou et al.* suggested that the novel protein kinase C-mitogen-activated protein kinase (PKC-MAPK)-induced

megakaryocytic differentiation is involved in the down-regulation of NPM/B23 during TPA-induced megakaryocytic differentiation of K562 cells (Chou et al., 2007). After 3 weeks culture the expression of Npm1 was down-regulated (~2.5-fold) when compared to control. After 3 weeks, the expression was stable and there was no difference between NSQ50 and control as it showed 1.5-, 1.5-, 1-fold up-regulation at 4, 5 and 6 weeks respectively (figure 4.5E).

Electrophoretic area 7 Chloride intracellular channel (p64): Chloride ion channels have been implicated in a number of crucial cellular processes including apoptosis, membrane potential, signal transduction, cell cycle regulation, and acidification of organelles. The regulation of intracellular chloride channels has been found to be associated with cell maturational state (Stein et al., 1990). Since an alkaline pH supports mineral deposition while an acidic pH promotes mineral dissolution (Yamaguchi et al., 1995). Two isoforms of p64 (chloride intracellular channel 1 and chloride intracellular channel 4) were identified and followed; the expression of both isoforms displayed similar patterns with down-regulation at 3 weeks culture followed by a peak at week 4 (Fig 4.5H).

Electrophoretic area 8 Heat shock protein 27: Heat shock protein 27 (Hsp27) has been suggested to participate in cell proliferation and differentiation during tissue development (Ciocca et al., 1993). During differentiation of mammalian osteoblasts and promyelocytic leukemia cells, the expression of hsp27 mRNA was 2.5-fold increased (Shakoori et al., 1992). Non-phosphorylated Hsp27 might contribute to the formation of a short, branched actin network at the leading edge, whereas phosphorylated Hsp27 might stabilize the actin network at the base of lamellipodia, which is composed of long, unbranched actin filaments (Pichon et al., 2004). Two isoforms of Hsp27 were followed in our experiments, however, the expression pattern of both isoforms were similar (figure 4.5G). At 3 weeks both isoforms were up-regulated and then continuously dropped.

Electrophoretic area 9 Collagen: Alpha1 chain of collagen was found in this area. The detection of collagen indicated that cell started to produce extracellular matrix protein. Collagen expression was found in many cell types differentiation i. e. the expression of collagen type VI was found during odontoblast-like differentiation of human dental pulp cells (Wei et al., 2008), chondrogenic differentiation of human mesenchymal stem cells (Xu et al., 2008, Quarto et al., 1993), expression of type I and III procollagen genes was found in embryonic chicken myoblast cell cultures (Gerstenfeld et al., 1984). These evidences supported that cells were differentiating upon the modulation of NSQ50. The peak of collagen expression on NSQ50 compared to flat surface was at 4 weeks culture (~2-fold up-regulation) at 4 week (Fig 4.5F).

Electrophoretic area 10 Galectin 1 (Gal-1): Within cells, Gal-1 is distributed diffusely in the cytoplasm (Liu et al., 2002). Choi et al. have identified Gal-1 as a component of the nuclear matrix in rat osteoblasts (Choi et al., 1998). Gal-1 is present both inside and outside cells and has both intracellular and extracellular functions (Camby et al., 2006). The presence of Gal-1 in ECM will modify the effects of ECM on cells. Some evidence suggested that Gal-1 was externalized during cell differentiation (Cooper and Barondes, 1990, Lutomski et al., 1997, Wang et al., 2004). Gal-1 inhibits the growth of stromal bone marrow cells (Andersen et al., 2003). Anti-proliferative effects result from the inhibition of the Ras-MEK-ERK pathway (Fischer et al., 2005). Gal-1 is a homodimer linked together by non-covalent bond. Both dimeric (dGal-1) and monomeric gal-1 (mGal-1) can be found in culture systems. In this study two forms of Gal-1 were found but could not be distinguished as dGal-1 or mGal-1. The expression of each form was seen to be in the opposite direction to each other. At 3 weeks the higher molecular weight form was down-regulated (~2-fold) (figure 4.6) but the lower molecular weight form was up-regulated (~2-fold) (figure 4.6). After 3 weeks both forms were present with no different between NSQ50 and control (figure 4.5I).

Electrophoretic area 11 Thioredoxin: Cytosolic thioredoxin (Trx) protein contains a redox-active dithiol residue (Arner and Holmgren, 2000). In resting cells, thioredoxin resides in the cytosol, but activation by a wide variety of stimuli leads to translocation to the nucleus or secretion of this compound (Nakamura et al., 1997, Rubartelli et al., 1992). In the extracellular milieu Trx acts as a chemokine and co-cytokine, stimulating cytokine secretion and cell proliferation (Schenk et al., 1996). Trx can act as a growth factor through use of a surface thiol group (Andersen et al., 1997). Three isoforms were found at 3 weeks culture but only one form was found at 4, 5 and 6 weeks with no difference between NSQ50 and control (figure 4.7). At 3 weeks culture, 3 isoforms (spot 1, 2 and 3 in figure 4.7) were expressed differently. Spot 1 was down-regulated (-2.5 ± 1.0) while spot 2&3 were up-regulated (3.32 ± 0.98).

Electrophoretic area 12 Myosin light chain 6 (MYL6): MYL is associated with the neck region of the myosin protein complex and important for structural stability of the alpha-helical lever arm domain of the myosin head (Hernandez et al., 2007). Myosin is known to play a critical role in the regulation of myosin-based contraction (Korn, 2000). Myosin VI has an unconventional characteristic as it moves to the plus end of actin. MYL6 was dominantly expressed in these spots (spot 3 and 4 in figure 4.6). MYL6 is a smooth muscle and non-muscle isoform. Changes in expression of isoform1 and isoform2 could be noted at 3 weeks culture (figure 4.5J).

Electrophoretic area 13 Annexin V (AnxV): Annexin V was up-regulated in three out of five gels at 3-week culture. AnxV is a calcium-dependent phospholipid binding protein which functions as a Ca^{2+} selective ion channel. It has the ability to interact with both extracellular matrix proteins and cytoskeletal elements. Overexpression of annexin V also resulted in up-regulation of annexin II, annexin VI, osteocalcin, and runx2 gene expression, expression and activity of ATPase, and ultimately stimulation of mineralization (Wang et al., 2005).

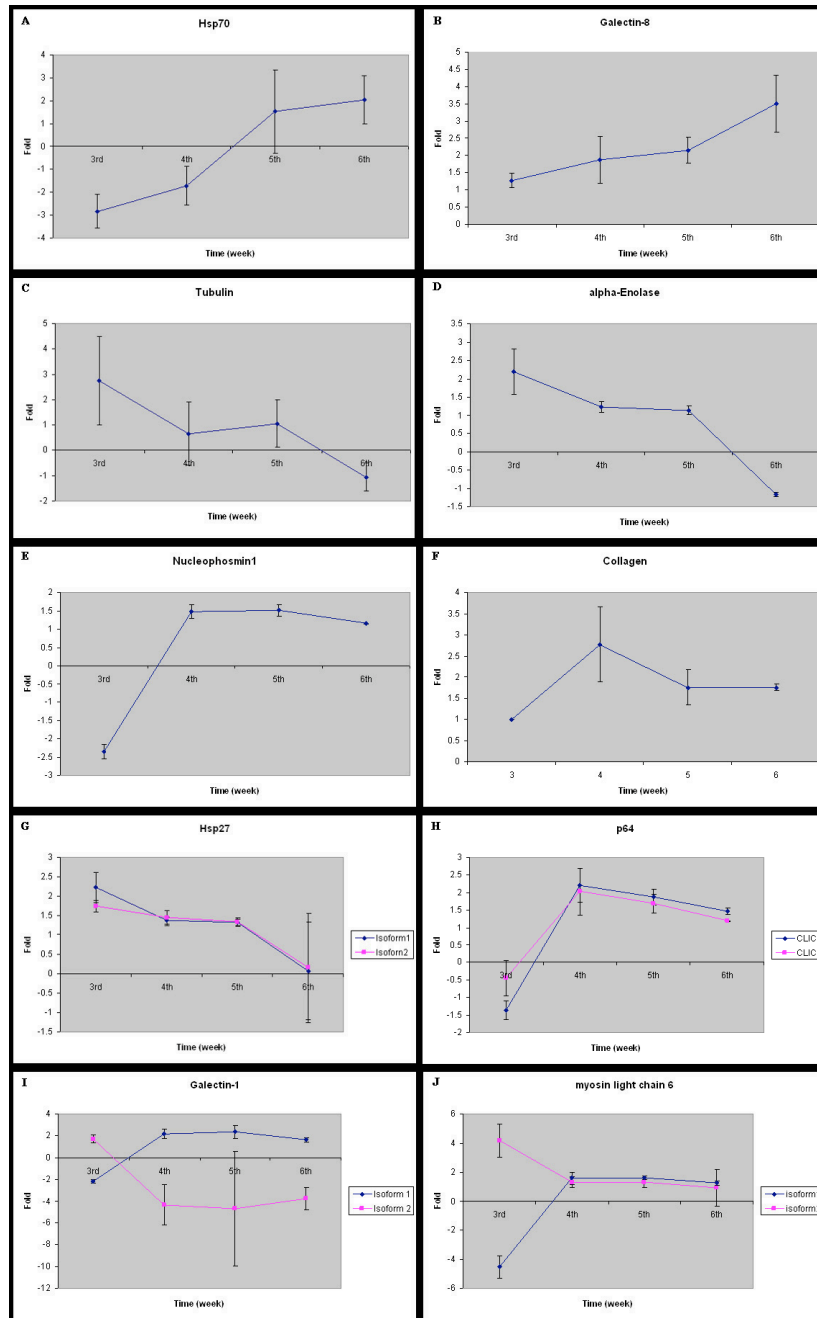


Figure 4.5 Temporal monitoring of protein expression. Change in expression of Hsp70 (A), Gal-8 (B), tubulin (C), alpha-enolase (D), Npm1 (E), α -collagen (F), Hsp27 (G), p64 (H), Gal-1 (I) and MYL6 (J) at 3, 4, 5 and 6 weeks culture. The presence of different isoforms were noticed for Hsp27 (G), p64 (H), Gal-1 (I) and MYL6 (J).

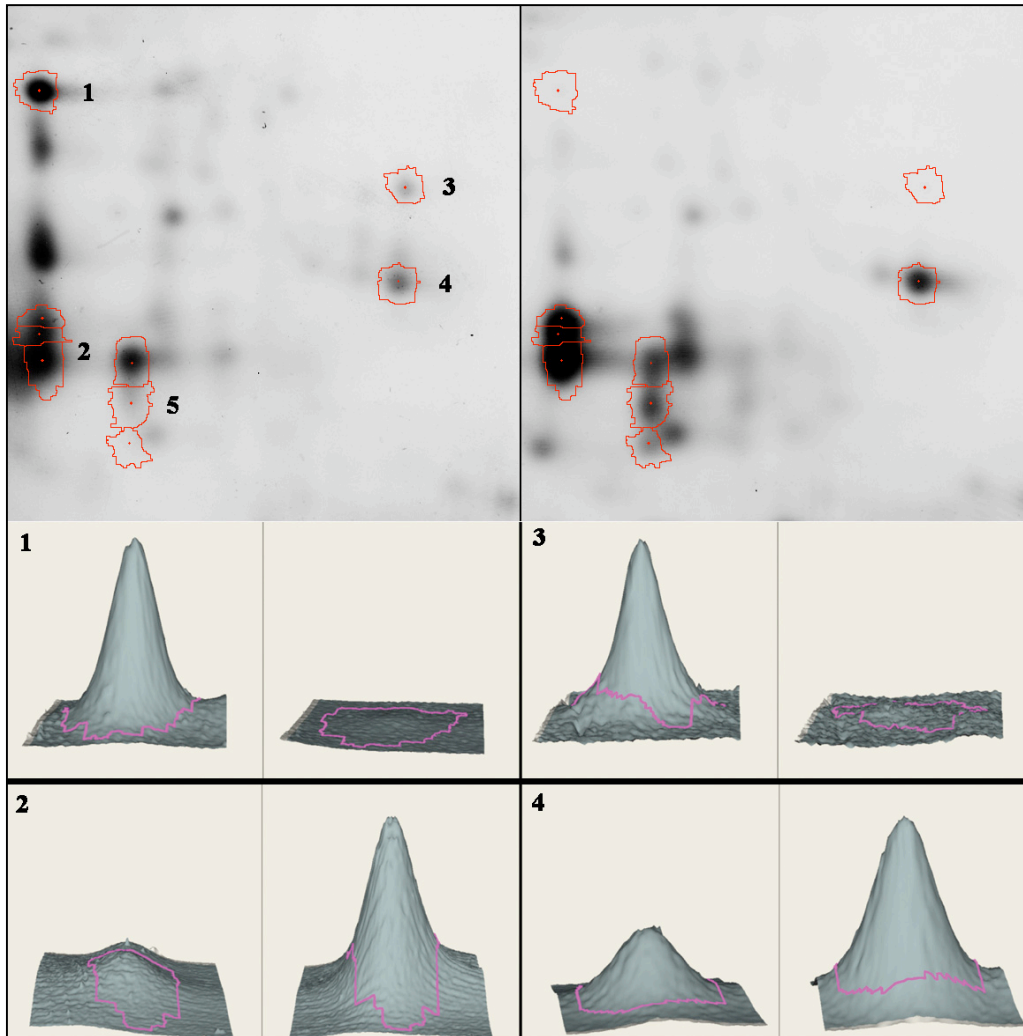


Figure 4.6 Differences in isomeric expression. Differences in expression of Gal-1 isoforms (1&2), and MYL6 isoforms (3&4) modulated by NSQ50 compared to control surface at 3 weeks culture is presented in this figure.

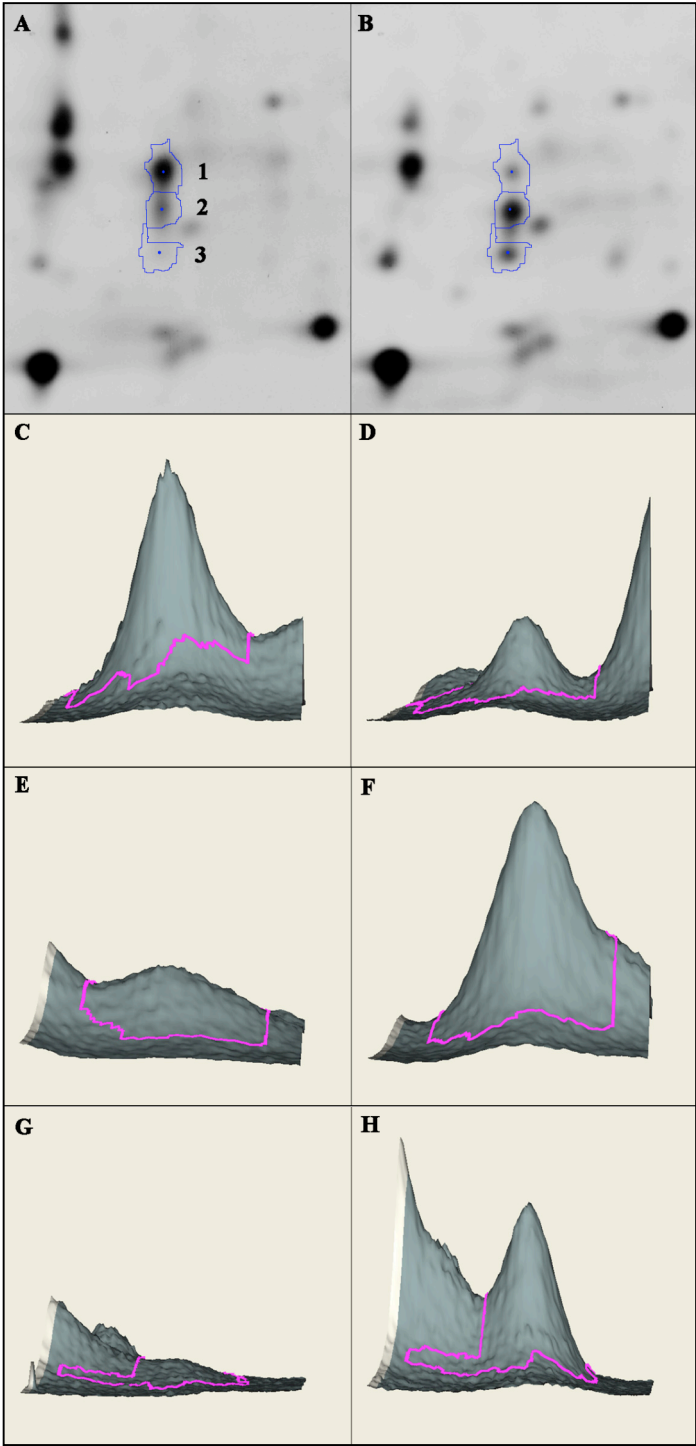


Figure 4.7 Differences in isomeric expression of Trx. thioredoxin modulated by NSQ50 compared to control surface at 3 weeks culture is presented in this figure.

4.3.3 Dimethyl labelling

The dimethyl gel image is shown in figure 4.8 and the results for differential protein expression are presented in table 4.1; there were some proteins that showed a remarkable up- and down-regulation as will be described.

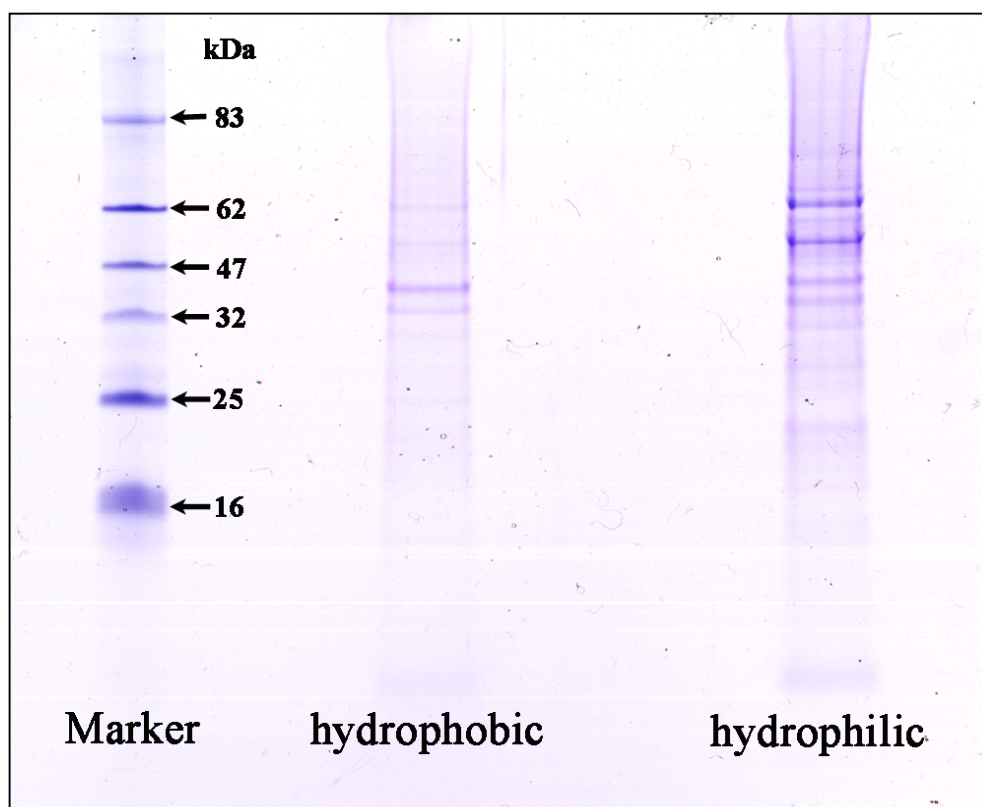


Figure 4.8 SDS-PAGE of proteins tagged by dimethyl labelling. SDS-PAGE was performed after dimethyl labelling to remove low molecular weight contaminants and to provide an additional dimension for separation. The gel was stained to visualise the lanes of separated proteins including marker, hydrophobic (mixed hydrophobic fraction of control and test) and hydrophilic (mixed hydrophilic fraction of control and test).

Table 4.1 Protein expression profile from dimethyl labelling. The table shows the regulation of a number of different proteins as determined by dimethyl labelling and mass spectrometric analysis. Data analysis was performed using Xpress software. Fold up-regulation (Xpress ratio) refers to the abundance of a particular protein in protein extract from NSQ50 against protein extract from control. Normalisation was performed against the median of all detected peptide ratios.

	Proteins	Protein probability	Xpress ratio (light/heavy)
1	Keratin1 isoform7	1	4.48
2	Pyruvate kinase 3	0.95	0.18
3	Annexin A2	0.98	0.35
4	Oligodendrocyte transcription factor 3	0.87	10.35
5	Beta-actin	0.85	0.59
6	Cytochrome b5 reductase	0.87	4.14
7	Helicase (DNA) B	0.95	10.78
8	Myosin regulatory light chain 2	1	0.6
9	Peroxiredoxin 1	0.99	-0.08
10	KIAA0120, transgelin 2	0.97	0.49
11	Chromosome 14 open reading frame1	0.97	0.27
12	Calmodulin-like 5	1	-1.57
13	Keratin 5 isoform 8	0.98	0.6
14	Actinin alpha	0.97	0.07
15	Keratin, type I cytoskeletal 14	1	0.05
16	Vimentin	1	0.79
17	Albumin	0.96	0.42
18	Gelsolin	0.91	1.74

Table 4.1 Protein expression profile from dimethyl labeling (continue). The table shows the regulation of a number of different proteins as determined by dimethyl labelling and mass spectrometric analysis. Data analysis was performed using Xpress software. Fold up-regulation (Xpress ratio) refers to the abundance of a particular protein in protein extract from NSQ50 against protein extract from control. Normalisation was performed against the median of all detected peptide ratios.

	Proteins	Protein probability	Xpress ratio (light/heavy)
19	Lamin A/C	0.99	0.08
20	Alpha-tubulin	0.96	-0.02
21	Eukaryotic translation initiation factor 4 gamma isoform 1	0.88	-2.04
22	TCR beta	0.9	4.12

Proteins with changes in expression

(1) Oligodendrocyte transcription factor 3: Olig family is a novel sub-family of basic helix-loop-helix transcription factors recently identified (Takebayashi et al., 2000). Olig3 was identified as the third member of Olig family (Takebayashi et al., 2002). 10-fold up-regulation of this protein demonstrated the possibility that there was neuronal differentiation occurring.

(2) Helicase (DNA) B: DNA B helicase is essential in DNA replication and able to stimulate primase (Frick and Richardson, 2001). In this study it was found 10-fold up-regulated on NSQ50 when compared to control. The expression of this protein could possibly be correlated with the up-regulation of oligodendrocyte transcription factor 3.

(3) Eukaryotic translation initiation factor 4 gamma isoform 1: eIF4G is a member of the class of translational initiation factors involved in mRNA recruitment to the 43S initiation complex (Keiper et al., 1999). The expression of this protein was about 2-fold down-regulated which might indicate the lower translation rate at 6 weeks culture.

(4) T-cell receptor (TCR) beta: TCRs are expressed on the surface of CD4⁺ or CD8⁺ T-cells (Armstrong et al., 2008). It was found up-regulated on NSQ50 4-times compared to control.

(5) Cytochrome b5 reductase: The expression of CBR is about a 4-fold up-regulation. It is an integral membrane protein with cytosolic active domains and short membrane anchors (Borgese et al., 1993). It also serves as an electron donor for cytochrome b5 and thus participates in a variety of metabolic pathways including steroid biosynthesis, desaturation and elongation of fatty acids, P450-dependent reactions, methaemoglobin reduction, etc. In agreement with this, the up-regulation of protein similar to a product of P450c21B gene, the truncated form of steroid 21-hydroxylase was found with time culture on NSQ50 compared to control (data not shown).

4.3.4 The effects of fluid flow bioreactor compared with static culture

4.3.4.1 The Histology of cells cultured in fluid-flow bioreactor

After 1 week in static culture and two weeks in fluid-flow bioreactor, the alizalin staining indicated that cells on NSQ50 in both flow and static culture had started to form nascent nodules (Fig 4.9A&B) and cell morphology observed by Coomassie blue staining of osteoprogenitors cultured on NSQ50 showed little difference between flow and static conditions.

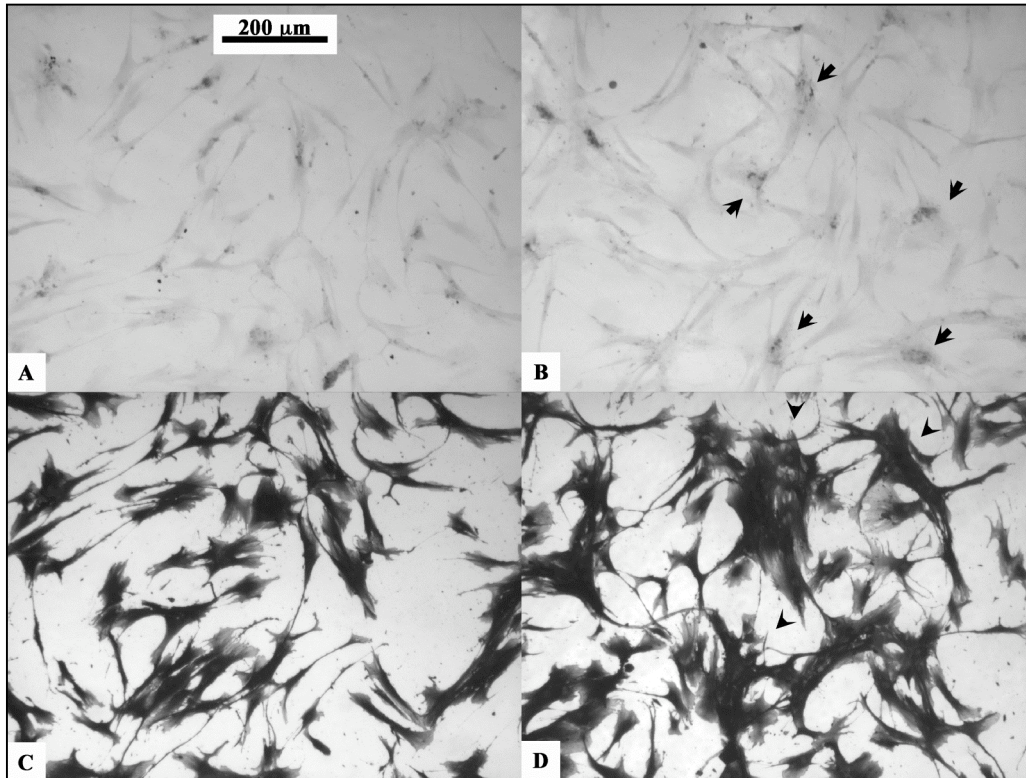


Figure 4.9 Cell morphology in fluid flow bioreactor. Alizarin staining of cells cultured on flat (A) and NSQ50 (B) indicated that cells started to aggregate on NSQ50 (arrows). Coomassie blue staining of cells cultured on flat (C) and NSQ50 (D) confirmed that cells on NSQ50 tended to form colonies (arrowheads).

4.3.4.2 DIGE analysis of cells cultured in the fluid-flow bioreactor

The proteomic profile of cells cultured in the fluid-flow bioreactor was, however, different from those cultured in static culture. It is noted that only two DIGE gels were successfully performed because of the small amount of protein extract that could be achieved. Hence only the name and function of proteins with change in expression more than 2-fold up-regulation were identified and reported. Protein expression profiles of cells cultured on NSQ50 in the static environment and fluid-flow bioreactor (3 weeks after cell seeding) are presented in table 4.2.

Table 4.2 A comparison between protein expression profiles from the fluid-flow bioreactor and static culture. By applying a 2-fold cut off, the protein expression profiles showed the difference between two systems which indicated that increased medium supply to osteoprogenitor cells cultured on NSQ50 from the bioreactor affected cell growth (NC represented no change in protein expression).

Number	Name	Regulation (static)	Regulation (bioreactor)
1.	Heat shock protein 70	Down	NC
2.	Galectin-8	NC	NC
3	Tubulin	Up	Up
4	Enolase	Up	NC
6	Nucleophosmin	Down	NC
7	Chloride intracellular channel (p64)	Down	NC
8	Heat shock protein 27	Up	NC
9	Alpha 1 collagen	NC	NC
13	Annexin 5	Up	Up
14	Vimentin	Up	Up
15	Laminin receptor	NC	Up
16	Cofilin	NC	Up
17	YWHAZ	NC	Up
18	Tropomyosin	NC	Up
19	Actin	NC	Up

4.3.4.3 Explanation of protein expression for cells cultured in the fluid-flow bioreactor

NOTE: All the below were up-regulated in bioreactor culture for cells grown on NSQ50 compared to static culture (except for vimentin that was up-regulated in both systems).

(1) Vimentin: Vimentin and intermediate filaments in general are used as a differentiation marker in many cell types. The differentiation process of optic vesicle epithelium into neural retina is reflected by the amount of vimentin in epithelial cells (Iwatsuki et al., 1999). The clonal osteoblast-like cell line MC3T3-E1 cDNAs for vimentin have higher normalized hybridization intensities in both differentiation and mineralization than in proliferation (Kitching et al., 2002). Vimentin expression could thus play a role at an advanced stage of bone formation (Rius and Aller, 1992).

(2) Laminin binding protein (laminin receptor): The laminin binding protein is one of the matrix receptors (Gloe and Pohl, 2002). A previous study in endothelial cells suggested that the mechanical forces acting on endothelial cells may be sensed in part by cell-matrix connections (Gloe et al., 1999).

(3) Cofilin: The RhoA/ROCK/LIM/cofilin pathway regulates actin cytoskeleton assembly and thereby effects cellular adhesion and migration (Kuzelova and Hrkal, 2008).

(4) Tyrosine 3-monooxygenase/tryptophan 5-monooxygenase (YWHAZ): YWHAZ belongs to the 14-3-3 family proteins. Cofilin also appears to be regulated by interactions with 14-3-3zeta (DesMarais et al., 2005). The 14-3-3zeta proteins may play a dynamic role in the regulation of cellular actin structures through increasing of phosphocofilin levels (Gohla and Bokoch, 2002).

(5) Tropomyosin: Tropomyosin competes with cofilin for accessibility of actin filament populations in different regions of the cell (DesMarais et al., 2005). The functional specificity of tropomyosins is related to the collaborative interactions of the isoforms with different actin binding proteins such as cofilin (Gunning et al., 2008).

(6) Actin: Actin contraction and stress fiber formation are controlled by RhoA. Increased actin polymerization results in smooth muscle cell differentiation and increased actin expression (Mack et al., 2001). Changes in actin assembly are regulated by controlling the balance between polymerized and non-polymerized actin. Stabilization of polymerized actin results in a significant increase in actin synthesis (Bershadsky et al., 1995).

4.4 Discussion

Whilst nascent nodules could be observed in progenitors cultured on NSQ50 at three weeks of culture, mature nodules were not noted until week 4; this is two weeks before the observation of mature nodules on flat control. That the cells did form nodules in basal media on the flat control demonstrates that whilst only at passage two, the cells already had high osteogenic capacity as we had not noticed this previously, but we note that the stem cells will vary in differentiative capacity from batch-to-batch; this is the nature of primary cell culture and the result clearly held that NSQ50 supported mature nodule formation significantly faster than flat control.

This chapter shows that at three weeks after cell seeding – i.e. pre-mineralisation, the protein expression profile indicates, in agreement with genomic studies (Biggs et al., 2008b, Biggs et al., 2008a), that progenitors on NSQ50 may be modulated by ERK1/2. It thus might be postulated at this time point that as the cells stop proliferating and prepare for mineralisation, they were switching in response to ERK signalling.

Evidence for this comes from a number of protein regulatory changes. Firstly, the expression profile of Hsp70 indicated that ERK signaling or p38 MAPK must be involved as expression of Hsp70 is controlled by ERK or p38 MAPK signaling (Hung et al., 1998). Hsp70 expression was seen to increase from week 3 suggesting that critical levels of ERK signalling had been achieved.

Ligation of integrins by galectin-8 is associated with activation of integrin-mediated signaling cascades (ERK and phosphatidylinositol-3-kinase) that are more effective and have longer duration than those induced upon cell adhesion to fibronectin (Levy et al., 2003). In this chapter the expression of galectin-8 was decreased on NSQ50 at 3 weeks but it increased continuously through out the experiment. The increasing of Gal-8 might reflect the temporal increase of extracellular matrix (ECM) as the cells produce their own, endogenous, ECM. Protein extraction was performed without trypsinisation thus the ECM will have been extracted and present in the analysed total protein. Protein extraction by trypsinisation of the cell sheet from the PCL sheet provided reduced detection of galectin-8 (data not shown). It can thus be postulated that most of the detected galectin-8 would be extracellular galectin-8 (and would thus only increase with time) which is required for the activation of the ERK cascade.

Previous studies have reported the down-regulation of tubulin as cells commit to differentiation e.g. β -tubulin expression in embryonic stem cells decreased significantly upon commencement of differentiation in TGF- β -supplemented media (Murphy and Polak, 2002). Decrease in α -tubulin expression can be observed along with monocytic differentiation of leukemic HL60 cells (Herblot et al., 1997). ERK2 is emerging as an important regulator of the control of cyclin B expression (Dangi et al., 2006) and we note here that tubulin has a role in the regulation of cyclin B synthesis (Vee et al., 2001). Also, a relationship between the level of tubulin and alpha B-crystallin related Hsp has been reported (Sakurai et al., 2005). Here, results showed time-related up-regulation of tubulin and alpha B-crystallin related Hsp but they are not reported as only two out of five gels showed the up-regulation. In the

experiments, tubulin levels peaked prior to mineralization and dropped pre-terminal differentiation, thus perhaps suggesting a role as a modulator of ERK signalling rather than a target.

Alpha-enolase was also up-regulated at the 3 week, pre-mineralisation time point. As noted, the induction of alpha-enolase is involved with ERK1/2 signalling (Mizukami et al., 2004, Sousa et al., 2005). Thus, raised levels may suggest that it is helping maintain ERK signalling pre-terminal differentiation before dropping off (as with tubulin, again suggesting an effector role).

It has been reported that Gal-1 modulates cell growth in a dose-dependent manner. While high doses (~1 μ M) of recombinant Gal-1 inhibit cell proliferation, low doses (~1 nM) of Gal-1 are mitogenic and thus increase proliferation (Adams et al., 1996, Vas et al., 2005). The paradoxical positive and negative effects of Gal-1 on cell growth are highly dependent on cell type and cell activation status, and might also be influenced by the relative distribution of monomeric versus dimeric, or intracellular versus extracellular, forms (Camby et al., 2006). Concentration is the factor which controls the formation of dimer. In high concentration Gal-1 has a tendency to form the dimer which will dissociate in low concentration. In this study, different forms of Gal-1 were identified and expressed differently in progenitor cells cultured on NSQ50 and flat control. The higher molecular weight (spot 1 in figure 4.6) was down-regulated but the lower one (spot 2 in figure 4.6) was up-regulated. In this study, it was observed that the spot 2 decreased with time and the spot 1 increased with time, thus suggesting a shift from low to high molecular weight and a slow-down in proliferation in cells on NSQ50 compared to control. The shift between the two forms needs further experimentation.

In agreement with this was the lowered expression, compared to control, of nucleophosmin1 (Npm1) in osteoprogenitors cultured on NSQ50 at 3 weeks. Npm1

indicated the lower proliferative activity of cells on NSQ50 at 3 weeks culture as suppression can inhibit proliferation (Wang et al., 2006, Qing et al., 2008).

Inhibition of the MEK/ERK pathway can enhance the ATP-stimulated dephosphorylation of myosin light chain (MYL) (Klingenberg et al., 2004). Unfortunately, the protein analysis software could not clearly distinguish the phosphorylated from dephosphorylated form so it could not be concluded whether the MEK/ERK was inhibited from the change of MYL, but is suggestive that it could be. The detection of MYL6 is interesting since it is dominantly expressed in smooth muscle e.g. blood vessel and could thus indicate multiple differentiation.

Thioredoxin (Trx) truncated at its carboxyl terminal (Trx80) was shown to induce differentiation of human CD14(+) monocytes by induction phosphorylation of p38 MAPK and c-Jun N-terminal kinase (JNK) (Pekkari et al., 2005). Three isoforms of Trx were reported; Trx1 (cytoplasm), Trx2 and Trx3 (mitochondria). From figure 4.7, it seemed like changes in the Trx isoforms may affect cell proliferation/differentiation. In previous studies, activation of mitochondrial Trx has implicated involvement with cell proliferation (Kim et al., 2003) and TRX-1 enhanced viability of cells exposed to nitrosothiols through up-regulation of the survival signaling pathways mediated by the ERK1/2 MAP kinases (Arai et al., 2008). At 3 weeks, spot 1 was down-regulated whilst spot 2&3 were up-regulated. Because of the limitation of isoform identification, this result still needs the further investigation before firm conclusions can be made.

For this study, DIGE was performed with the whole cell proteome, which has helped to understand cell differentiation through nanotopographical cell manipulation. In the future, studies of the proteomic profiles in each compartment would provide better understanding of the changes in isoform expression and the importance of such changes.

Regulatory changes of α -enolase, tubulin Hsp70, Hsp27, Trx, extracellular and

matrix-galectin-8 indicated significant ERK modulation while changes in Npm1, galectin 1, collagen, chloride intracellular channel, vimentin and SPARC (osteonectin) showed proliferative slow-down and enhancement of osteospecific matrix formation prior to mineralization (shown by alizarin red) in cells on the novel NSQ50 before cell culture on the control flat topography. It could be postulated by tying in with several pathway analyzing genomic studies (Dalby et al., 2007d, Biggs et al., 2008b, Biggs et al., 2008a, Dalby et al., 2008a) implicating ERK, that ERK is a major signalling mediator in the onset of osteogenesis. That said, there is need for further, interventionalist, study before this is clear.

The dimethyl study showed that by 6 weeks of culture there were relatively few changes; this concurs with DIGE results, where most differences and changes were seen in / from weeks 3 to 4. However, it can be noted that up-regulation of oligodendrocyte transcription factor might suggest the presence of neural cells. From a tissue engineering perspective, this is interesting and when tied with the observation of possible smooth muscle related proteins (MYL6) could indicate the formation of nerve and vascular tissue on the construct. Both are critical in the formation of a complex bone tissue in the laboratory. This result concurs with previous genomic data that reported the presence of endothelial differentiation on nanotopography and thus, the possible formation of vasculature as well as bone (Dalby et al., 2008a). From a mechanistic standpoint, however, the dimethyl study would have been better placed at weeks 3 and 4.

Results from osteoprogenitor growth on NSQ50 in flow and static culture indicated that bioreactor culture induced further up-regulations of some key proteins. The cell morphologies observed from the flow system indicated that cells on NSQ50 started to form nascent nodules as found in the static environment, and the proteomic expressions showed some similarities e.g. up-regulation of tubulin and annexinV and no change in extracellular matrix proteins such as collagen and galectin-8 were found at this time point. However, the group of proteins that related to the stability of actin cytoskeleton such as cofilin, YWHAZ, tropomyosin and actin were found up-

regulated and their function was related to the Rho family. Up-regulation of vimentin was also found and this indicated that the bioreactor influenced cytoskeletal organization in general.

It is possible that constant provision of media from the fluid-flow bioreactor modulated osteoprogenitor cells on NSQ50 through some different signalling pathway from NSQ50 stimulation alone; it can be speculated from these results that cytoskeletal and G-protein signaling was altered. The use of the fluid-flow bioreactor combined with the disordered nanopits topography provides a promising method for enhanced culture of osteogenic cells on nanosubstrates, but it still needs a lot of optimization i.e. the flow rate needs to be adjusted and the cell seeding needs to be improved.

Chapter V General Discussion

5.1 Introduction

This thesis has two main components. Firstly, the development of comparative proteomics techniques, DIGE and dimethyl labelling, for biomaterials research – specifically for nanomaterials and progenitor cells. Then, secondly, application of these techniques to help understand how the osteogenic nanotopography, NSQ50, elicits osteoconversion of progenitor cells in static and bioreactor culture. The general discussion section is thus divided into technical developments, biological observations and ideas for future research.

5.2 Technical developments

5.2.1 DIGE: DIGE was, for the first time, employed in biomaterials evaluation and it has been shown that only 5 µg of protein, extracted from restricted sample sizes that are commonly used in academic scale experiments, can successfully be analysed. DIGE allowed the observation of post-translationally modified isoforms of proteins such as CLIC 1&4, Hsp27 and enolase. Isoform expression is important in the interpretation of results i.e. phosphorylation of Hsp27 can help in the prediction of actin filament dynamics (Chen et al., 2009). An extension of this study to look at differential isoform expression could provide extra new data and will be discussed in the future work section.

5.2.2 Dimethyl labelling: This method was also for the first time applied to biomaterials research. The main goal was to evaluate changes in expression of membrane proteins that are typically under-represented in 2D gel-based analyses such as DIGE. This aim was achieved, as demonstrated by the identification of chromosome 14 open reading frame1 (Veitia et al., 1999) and TCR-beta. In LC-MS/MS, proteins are processed to peptides prior to analysis, allowing the analysis of a wider variety of protein types (Washburn et al., 2001). LC-MS/MS also allows for

the analysis of a greater proportion of lower abundance proteins than 2D gel electrophoresis. In this study, both the hydrophobic and the hydrophilic fractions were analysed simultaneously. Many important hydrophobic and hydrophilic proteins were identified but when compared between test and control, only a few significant differences between flat control and NSQ50 were found because the investigation was performed at 6-week culture at which time, both cells on control and test were already differentiated. A small group of proteins that showed a degree of difference when compared between NSQ50 and flat surface were oligodendrocyte transcription factor 3, helicase (DNA) B, eukaryotic translation initiation factor 4 gamma isoform 1, T-cell receptor (TCR) beta and cytochrome b5 reductase. This group of proteins might indicate proliferation or differentiation of a sub-population (Spits et al., 1998), but needs more supporting data from future work.

5.2.3 Bioreactor: In order to increase protein output from small sample sizes, the fluid-flow bioreactor was used to maintain the culture material before protein extraction and gel electrophoresis. The results from chapter II indicated that the continuous feeding increased the quantity of proteins extracted on micro-grooved PCL. However when the same conditions were applied to NSQ50, it was shown that the fluid-flow condition used did not significantly enhance the amount of protein extracted. It was likely that the extra supply of nutrients and the highly osteogenic nature of this topography curtailed the proliferative stages in order to enter into cell differentiation more rapidly (proliferation gives way to differentiation and a confluent cell layer is not required for bone nodule formation) (Stein and Lian, 1993). This is supported by the observation of a greater number of functional up-regulations seen in cells cultured on NSQ50 in the bioreactor compared to static culture.

5.3 Nanotopography and biological observations

This study has shown that surface topographies such as micro-grooves and nanopits can initiate contact guidance and induce bone formation in osteoprogenitor cells producing large-scale changes in the cell proteome. Topographical features can

modulate cell behaviours such as proliferation, migration, differentiation and apoptosis (Zhu et al., 2004, Kim et al., 2005a, Yim et al., 2005). Biochemical mechanotransduction implies the conversion of mechanical forces (e.g. changes in cell spreading and morphology from changing surface topography) into biochemical signals via biomolecules. Still, little is known concerning which pathways may be directly involved in cell response to changes in the material surface. A number of pathways have been implicated using focused studies of ‘selected’ biomolecules rather than a global analysis of signal pathways.

Here, we used DIGE to study osteoprogenitor cell response to contact guidance in grooves, firstly in order to optimise protocols and then to investigate the novel, osteogenic, NSQ50 topography. Furthermore, chromatography based dimethyl labelling was employed to analyse progenitor proteome changes in response to the NSQ50 topography. A number of distinct proteins were observed to exhibit significant changes in expression. These changes in protein expression suggest that the cells respond to topographies with alterations in their proteome that are correlated with changes in osteoprogenitor phenotype.

Many of the proteins that were found to be changed in expression form part of the extracellular signal-regulated kinase (ERK1/2) pathway. ERK1/2 is important for mesoderm formation (Nishimoto and Nishida, 2006). As described in chapter I, section 1.2, bones develop from mesodermal tissue (Olsen et al., 2000). Extracellular signal-regulated kinase 1 and 2 (ERK1/2) was first observed by Boulton et al (Boulton et al., 1990) And were shown to have the ability to phosphorylate microtubule-associated protein-2 (Boulton et al., 1991, Boulton and Cobb, 1991).

ERK1/2 mitogen-activated protein (MAP) kinase pathway plays a central role in cell proliferation control (Kato et al., 1998, Meloche and Pouyssegur, 2007). The regulation of G1- to S-phase transition is governed by the concerted action of cyclin-dependent kinases (Cdks) and their regulatory cyclin subunits. Strong activation of ERK1/ERK2 by conditionally active Ras or Raf causes cell cycle arrest in established

cell lines by inducing the expression of the Cdk inhibitor p21. Sustained ERK1/2 activation throughout G1 is required for S phase entry (Lefloch et al., 2009). Additionally, different growth factors generate different profiles of ERK pathway activation. These findings have historically complicated our understanding of ERK activity and are the reason why many studies about ERK1/2 and the cell cycle have been controversial; some studies indicate that ERK activation mediates cell cycle arrest e.g. (Tang et al., 2002, Kim et al., 2008) whilst some suggested the sustained ERK pathway activation promotes proliferation e.g. (Sharrocks, 2006). However, it seems that ERK is regulated by a negative feedback loop and thus may be critical to both initiation and cessation of proliferation (Yeung et al., 2000, Zeliadt et al., 2008, von Kriegsheim et al., 2006).

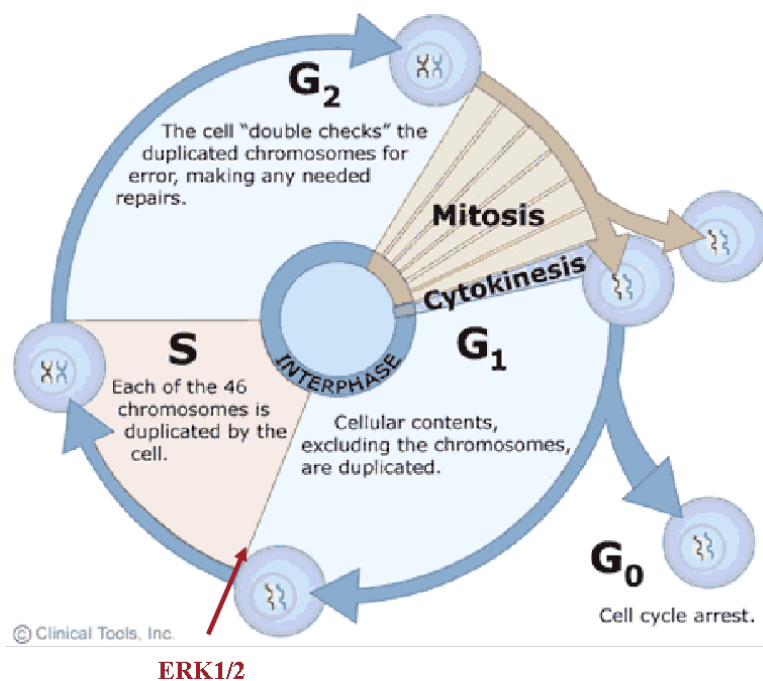


Figure 5.1 Cell cycle and ERK1/2: ERK1/2 is a key regulator of cell cycle of G1 to S-phase transition via cyclin D kinase. Adapted from (<http://www.le.ac.uk/ge/genie/vgec/sc/cellcycle.html>)

Changes in expression of many proteins in this study strongly indicates that ERK signaling was activated on NSQ50 (compared to flat control) and this has implications for ERK in stem cell differentiation as well as proliferation. In fact, it must be considered that cells must rapidly proliferate to recruit cell numbers for bone repair / formation and then stop almost completely to allow differentiation / bone formation. Thus, perhaps, proliferative control is critical to the whole process and, furthermore, both positive and negative control may be required.

Examples of ERK related events observed in this thesis include:

ERK signaling pathway induces expression of Hsp70 (Hung et al., 1998) and inhibition of ERK reduces Hsp70 expression (Chen et al., 2001, Yang et al., 2004, Taylor et al., 2007). In this study Hsp70 expression was seen to increase through all time points on the osteogenic NSQ50 topography.

Gal-8 was up-regulated on NSQ50 (compared to control) and binding of gal-8 to integrins can activate ERK signaling (Carcamo et al., 2006).

Enolase, which is influenced by ERK signalling, has regularly been used as a neuronal differentiation marker (Chang et al., 2005) and was initially up-regulated in this study. However, the major cell population response on NSQ50 is differentiated into bone. This could be due to the immature stem cell population of the progenitor cells forming neural cells as well as osteoblastic cells. The mesenchymal stem cells are multipotent and have been shown to be able to form neurons (Engler et al., 2006). The formation of multiple lineages on the same material could have positive implication for tissue engineering of complex, functional, organs.

Some studies have suggested a role for p38 in the induction of hsp27 expression (Yu et al., 2008, Carlson et al., 2007). However, the activation of p38 can be a side effect of ERK activation (Wang et al., 2002, Deng et al., 2004). It is proposed that in this study, the induction of hsp27 was an indirect effect of ERK signalling.

That enhanced differentiation is followed by a slow down in proliferation is evidenced by changes in expression of some proteins influenced by the osteogenic NSQ50 topography:

The cyclin-dependent kinase inhibitor (p21) is a critical regulator of cell cycle, and it is readily degraded by the proteasome through ubiquitin-dependent and -independent pathways. Nucleophosmin (NPM)/B23, is a multifunctional protein that binds p21 and contributes to its stability (Xiao et al., 2009). At the 3rd week of culture, NPM was down-regulated on NSQ50 (compared to flat) but at the 4th week it was up-regulated and maintained at that increased level until the 6th week. It could be postulated that p21 was stabilized by the rising level of NPM and caused cell cycle arrest.

Tubulin was up-regulated at the 3rd week (about 3-fold) but then became down-regulated on NSQ50. The decline of tubulin expression could be the result of a lower rate of microtubule formation (Ben-Ze'ev, 1990) as the pool of tubulin monomer controls its own expression (Cleveland et al., 1981) and this evidence supports a lower proliferation rate (Shi et al., 2009).

Enhanced differentiation should clearly be defined by changes in expression of extracellular matrix proteins. Changes in expression of some proteins in this study indicated that cells on NSQ50 started to produce extracellular matrix such as collagen, galectin-8 and CLIC1&4 to higher levels and more rapidly than cells on flat control, and this can be directly related to the result for mineralization from alizarin staining.

A key question is how does topography influence ERK signalling? It seems likely that mechanotransductive events arising from changes in cell morphology will be central. Percolation theory describes the cytoskeleton as being interconnected and connecting the cell nucleus to the extracellular environment through focal adhesions (Forgacs, 1995, Shafrir and Forgacs, 2002). Mechanotransduction in this case is

mainly indirect (i.e. biochemical signalling) as percolation itself does not explain how direct mechanical signals (in order to distort the nucleus) are transmitted to the nucleus.

However, for direct mechanotransduction to occur, and it is known that micro and nanotopography cause changes in nucleus morphology (Dalby et al., 2003, Dalby et al., 2007a, Dalby et al., 2007c) from changes in cell morphology, there needs to be an inhomogeneity in the cytoplasm and this points to the cytoskeleton (Wang et al., 1993, Wang and Suo, 2005). As discussed in chapter 1, section 1.6.1, the key theory as to how direct mechanical signals could be conveyed to the nucleus is the cellular tensegrity model (Ingber, 2008). Normally, proper attachment to the extracellular matrix is essential for cell survival. Detachment from the extracellular matrix results in an apoptotic process termed anoikis due to loss of survival signals following integrin disengagement (Collins et al., 2005). The idea of cell distortion-dependent switching between distinct cell fates as cells spread and grow - slightly retracted cells differentiate and fully round or detached cells undergo apoptosis (Ingber, 2003b) - was supported by the way NSQ50 modulated cell shape, reducing proliferation and encouraging differentiation through slightly reduced spreading.

The tensegrity cell models predict that living cells are hard-wired to respond immediately to external mechanical stresses (Ingber, 2003a). This hard-wiring exists in the form of discrete cytoskeletal filament networks that mechanically couple specific cell surface receptors, such as integrins (Ingber, 1997a). When integrins are pulled, stresses are altered across integrins and this alters intracellular biochemistry. The theory is developed from engineering principles (Fuller, 1961) and relies firstly on the cells being pre-stressed (actin stress fibres acting upon adhesions) and then the cytoskeleton containing components under compression (tubulin microtubules) and tension (actin microfilaments and vimentin intermediate filaments), all acting together and connecting to the nucleus.

From the result of protein expression profile, cell morphology and mineralization, it can be postulated that NSQ50 generates mechanotransduction by modulating cell adhesion and, in consequence, results in altered cell morphology, which in turn, affects cytoskeletal organisation. Changes in cytoskeletal organization are likely to generate forces applied against the substratum surface and also against its surface receptors i.e. integrins. From the receptors, hierarchical chemical reactions like phosphorylation/dephosphorylation are stimulated to control cellular processes i.e. cell cycle, proliferation, differentiation and apoptosis. To understand the influence of biomaterials on cellular biology, this thesis applied a novel strategy that brought the tools of comparative proteomics to bear on regenerative medicine.

5.4 Future work

This thesis points to several key areas to consider in immediate future development. Firstly, rather than considering the total proteome, studies focusing on discrete subcellular compartments could be very revealing and give more focus to the study. Next, it could be very interesting to consider methods to increase bioactivity – e.g. composite formulations and embossing.

5.4.1 Cell compartment proteome

2-DE and LC-MS/MS are both powerful methods for proteomic analysis but neither technique has the analytical power to resolve and analyse all proteins in the proteome. 2-DE has limited capacity to separate proteins of extreme hydrophobicity or *pI* and proteins of relatively low abundance (Wilkins et al., 1998, Taylor et al., 2003). A single 2D gel can resolve up to 3000 proteins from a complex sample, representing only a fraction of the whole cell proteome. LC-MS/MS, while in many respects a good complement to 2D electrophoresis, does not resolve the isoform variety and can be still more limited in resolution. Proteomic fractionation is thus widely used to increase our understanding of the proteome (Ho et al., 2006). The proteomic study of sub-cellular compartments may provide greater depth of understanding about how

mechanotransduction directs cell fate.

Subcellular proteomic analysis could include, but are not limited to:

(1) Nucleus: Nuclear proteins play a major role in controlling cell function, thus the investigation of nuclear proteome could provide valuable information of cell differentiation. Recently, two-dimensional gel electrophoresis and mass spectrometry analysis was used to define the modifications of the nuclear proteome occurring during the switch from the proliferation state to the differentiation state of embryonic rat ventricle H9c2 cells (Bregant et al., 2009). Furthermore, a method for isolation of highly purified nuclear fractions from stem cell populations that allowed examination of nuclear proteins critical for differentiation has also been reported (Woodbury et al., 2008). It would be very interesting to apply this technique to biomaterials research.

(2) Membrane and other organelles: Methods to isolate lysosomes from mouse liver for proteomic studies including a comparison of the soluble, luminal proteins obtained from each of the two preparations separated by 2D gel electrophoresis was recently introduced (Zhang et al., 2008). It showed promising results that should be applied to the future work of this thesis. Furthermore, cathepsin D, a lysosomal enzyme, showed a correlation between the level of procathepsin D translation and the proliferative potential (Fusek and Vetvicka, 2005) and it would be interesting to focus on as this enzyme showed degree of up-regulation in some experiment of this study. The application of the subcellular fractionation could be a key to increasing focusing on protein such as this.

(3) Mitochondrial: The differential expression of mitochondrial proteins has very recently been investigated by DIGE (Jiang et al., 2009) and this could be modified to use in the biomaterials field in the near future.

(4) Extracellular matrix and Secretome: A proteomic approach was used to identify a total of 73 proteins from the secretome of human multipotent adipose-

derived stem cells in an investigation of early stage commitment to adipocytes and osteoblasts (Chiellini et al., 2008). Furthermore, methods used to isolate and enrich ECM constituents and secreted vesicles from bone-forming osteoblast cells, enabling comprehensive profiles of their proteomes to be obtained by mass spectrometry, was reported by Xiao et al (Xiao et al., 2008).

5.4.2 Phosphoproteomics

Activation of ERK 1/2 induces phosphorylation of the runx2/cbfa-1 transcription factor that controls osteogenic gene expression (Salaszyk et al., 2007). It has been hypothesized that FAK mediated signaling pathways supply a link between cell surface integrin-ECM binding and activation of ERK 1/2 (Salaszyk et al., 2007). Serine/threonine phosphorylation of runx2/cbfa-1 is emerging as a key target in this respect.

Additionally, Smad1 could be another interesting target since cooperation of BMP-Smads with Runx2/Cbfa1 among the Runx/PEBP2/Cbf family is particularly important for osteoblastic differentiation and both of them are critical transcription factors in osteoblastogenesis (Suzawa et al., 2002).

Other targets include:

Hsp27: Hsp27 phosphorylation may play a key role in actin filament remodeling required for smooth muscle cell migration and contraction (Meier et al., 2001). The p38 MAPK/MAPK-activated protein kinase 2/Hsp27 pathway is involved in F-actin alternations (Kostenko et al., 2009). In this thesis, changes in expression of Hsp27 isoforms were reported so it is possible that further study focusing on the expression of Hsp27 will provide interesting information.

MYL: Phosphorylation of myosin light chain (MYL) plays a part in many signalling pathways to modulate cell proliferation and differentiation i.e. the signaling pathways

involved in Myosin Light Chain Kinases (MLCK) plays a crucial role in cell migration through reciprocal cross-talk with activated ERK1/2 (Zhou et al., 2008), phosphoinositol-Akt-mammalian target of rapamycin-p70S6 kinase (PI3K/Akt/mTOR/p70S6K) pathway activation regulates VSMC differentiation from MSCs (Hegner et al., 2009).

5.4.3 Adding bioactive composites to the polymers being embossed with the osteogenic nanotopographies

In bone repair, the addition of bioactive fillers has been studied for a number of years. Bone itself is a composite material containing a collagen polymer and apatite mineral. Addition of synthetic hydroxyapatite to polymers such as polyethylene has produced promising results and methods to improve bioactivity are under study (Rea et al., 2004, Gibson and Bonfield, 2002, Patel et al., 2005). Furthermore, the use of drug-impregnated composite biomaterials has been previously studied with various bioactive agents e.g., bone morphogenic protein (Li et al., 2007) and the antibiotics vancomycin (Kim et al., 2005b) and tetracycline (Kim et al., 2004). In work related to this thesis, compositing has been initially trialled with the Chinese herb; *Puerariae radix* (the root of *Pueraria lobata* and *Pueraria mirifica*). This has been composited with micro-grooved PCL. *Puerariae* powder was pressed into melted PCL-sheets at one side, then the other side was embossed with grooved slide (12.5 μm width, 2 μm dept). The inclusion of *Puerariae* did not seem to have cytotoxic effects when 2% w/w was impregnated into grooved-PCL. Furthermore, impregnation of *Puerariae* powder did not affect subsequent embossing of topographic features into the other side of PCL sheet. The detection of isoflavones (e.g. methoxypuerarin, daidzin and daidzin) from *Puerariae radix* extract has been accomplished by HPLC-UV and it is suspected that these are the osteogenic component of the *Puerariae* (Jiang et al., 2005). In a preliminary study using topography, HPLC has shown the release of isoflavones. Mass spectrometry of *puerariae* crude extract showed 3 major peaks of 413.21, 417.02 and 429.16 m/z. The previous study, and Massbank records, indicate that 4'-methoxypuerarin, daidzin and daidzin have mass of 417.12 and formononetin

has a mass of 430 (Sun et al., 2008). Thus, the peak of 417.02 m/z could be the peak of 4'-methoxypuerarin, daidzin and daidzin (Kantawong, 2009).

These preliminary results provide a significant contribution to the application of alternative herbal medicine in biomaterial field and it can be applied to NSQ50 in the future.

5.5 Conclusion.

For the first time, global proteomics has been applied to the study of bone formation on topographies (micro and nanoscale). Previous genomic studies have indicated large scale regulatory changes of the genome, and here it is shown that this results in large-scale changes in the proteome. Specifically implicated is ERK1/2 and it's possible influence of the proliferation / differentiation balance. Proteomic profiles might provide the basic knowledge cell differentiation *in vivo*. This information can be use as a clue for biomaterial design in the future.

The thesis highlights topography as a biomaterials / tissue engineering strategy. It further indicates that combining with bioreactor culture could be used in tissue engineering. Such constructs that could be envisaged include, as a first step, the production of viable, mineralizing, biodegradable graft material produced from autologous progenitor cells for e.g. impaction grafting.

Work is underway in the Centre for Cell Engineering (Riehle group) for the fabrication of 3D nanostructures and this permits speculation that larger graft application could be met in the near future.

VI. Appendix**6.1 Culture medium**

Reagent	Quantity	Final concentration
Alpha-MEM	440 ml	-
FCS	50 ml	10%
antibiotic	10 ml	2%

6.2 Trypsin-versine solution

Reagent	Quantity	Final concentration
Trypsin	0.7 ml	
Versine	20 ml	

6.3 Frozen medium

Reagent	Quantity	Final concentration
Culture medium	7 ml	-
Fetal bovine serum	2 ml	20% (v/v)
DMSO	1 ml	10% (v/v)

6.4 Cell lysis buffer

Reagent	Quantity	Final concentration
Tris (1 M not pH)	3.0 ml	30 mM
Thiourea (MW 76.12)	15.22 g	2 M
Urea (MW 60.06)	42.0 g	7 M
CHAPS (MW 614.89)	4 g	4% (w/v)
Adjust pH to 8.0 with diluted HCl		
Make up to 100 ml with distilled water		

6.5 2x Gel loading buffer

Reagent	Quantity	Final concentration
Tris (1 M, pH 6.8)	12 ml	120 mM
Glycerol (87% v/v)	23 ml	20% (v/v)
SDS	4 g	4% (w/v)
DTT	3g	200 mM
Bromophenol Blue	A few grains	Trace
Make up to 100 ml with distilled water		

6.6 12.5% Acrylamide gel

Reagent	Quantity for 100 ml of a 12.5% gel
Acrylamide/Bis 40% (w/v)	32.0 ml
Tris (1.5 M, pH8.8)	25.0 ml
10% (w/v) SDS	1.0
10% (w/v) APS	1.0
TEMED	40 μ l
Make up to 100 ml distilled water	

6.7 1% (w/v) Agarose gel sealant

Reagent	Quantity	Final concentration
1x running buffer	100 ml	-
Low melting agarose	0.5 g	1% (w/v)
Make up to 100 ml with distilled water		

6.8 10x Running buffer

Reagent	Quantity
Tris (MW 121.14)	30.3 g
Glycine (MW 75.07)	144.0 g
SDS	10.0 g
Make up to 1 L with distilled water	

6.9 Displacing solution

Reagent	Quantity	Final concentration
Tris (1.5 M, pH 8.8)	25 ml	375 mM
Glycerol (87% v/v)	57.5 ml	50% (v/v)
Bromophenol Blue	A few grains	Trace
Make up to 100 ml with distilled water		

6.10 Water saturated butanol

Reagent	Quantity
Butanol	50 ml
Distilled water	50 ml or more until two layers are visible

6.11 2x Rehydration buffer stock

Reagent	Quantity	Final concentration
Urea (MW 60.06)	10.5 g	7 M
Thiourea (MW 76.12)	3.8 g	2 M
CHAPS (MW 614.89)	1 g	4% (w/v)
Make up to 25 ml with distilled water		

6.12 Rehydration buffer

Reagent	Quantity	Final concentration
2x Rehydration buffer stock	2.5 ml	-
pharmalyte™ broad range pH 4-7	25 µl	1% (v/v)
DTT (MW 154.2)	5 mg	0.2% (w/v)

6.13 Stock equilibration buffer

Reagent	Quantity	Final concentration
Tris (1.0 M, pH8.0)	20 ml	100 mM
Urea (MW 60.06)	72.07 g	6 M
Glycerol (87% v/v)	69 ml	30% (v/v)
SDS (MW 288.33)	4 g	2% (w/v)
Make up to 200 ml with distilled water		

6.14 Equilibration buffer

Reagent	Quantity	Final concentration
Stock equilibration buffer	100 ml	-
DTT (MW 154.2)	0.5 g	0.5% (w/v)

6.15 Colloidal coomassie staining1. Coomassie stock

5% Coomassie Blue G-250 in water. Shake before use.

2. Colloidal coomassie dye stock

- 50 g Ammonium sulphate
- 6 ml of 85% Phosphoric acid
- Add water to make up the volume to 490 ml

- 10 ml coomassie stock

Shake well before use.

3. Colloidal coomassie stain

- 200 ml colloidal coomassie dye stock

- 50 ml methanol

(Prepare fresh for each use)

- Fix gel 1-2 hrs in 40% ethanol, 10% acetic acid

- Wash gel 10 mins in water twice.

- Stain gel in freshly prepared colloidal solution for upto 1 week. Overnight maybe sufficient but sensitivity may improve by extending staining for several days.

- Rinse gel in several changes of water.

References

- ABOUSLEIMAN, R. I. & SIKAVITSAS, V. I. (2006) Bioreactors for tissues of the musculoskeletal system. *Adv Exp Med Biol*, 585, 243-59.
- ADAMS, L., SCOTT, G. K. & WEINBERG, C. S. (1996) Biphasic modulation of cell growth by recombinant human galectin-1. *Biochim Biophys Acta*, 1312, 137-44.
- ALFORD, A. I. & HANKENSON, K. D. (2006) Matricellular proteins: Extracellular modulators of bone development, remodeling, and regeneration. *Bone*, 38, 749-57.
- ANDERSEN, H., JENSEN, O. N., MOISEEVA, E. P. & ERIKSEN, E. F. (2003) A proteome study of secreted prostatic factors affecting osteoblastic activity: galectin-1 is involved in differentiation of human bone marrow stromal cells. *J Bone Miner Res*, 18, 195-203.
- ANDERSEN, J. F., SANDERS, D. A., GASDASKA, J. R., WEICHSEL, A., POWIS, G. & MONTFORT, W. R. (1997) Human thioredoxin homodimers: regulation by pH, role of aspartate 60, and crystal structure of the aspartate 60 --> asparagine mutant. *Biochemistry*, 36, 13979-88.
- ANDERSON, H. C. (1995) Molecular biology of matrix vesicles. *Clin Orthop Relat Res*, 266-80.
- ANDERSON, H. C. (2003) Matrix vesicles and calcification. *Curr Rheumatol Rep*, 5, 222-6.
- ARAI, R. J., OGATA, F. T., BATISTA, W. L., MASUTANI, H., YODOI, J., DEBBAS, V., AUGUSTO, O., STERN, A. & MONTEIRO, H. P. (2008) Thioredoxin-1 promotes survival in cells exposed to S-nitrosoglutathione: Correlation with reduction of intracellular levels of nitrosothiols and up-regulation of the ERK1/2 MAP Kinases. *Toxicol Appl Pharmacol*, 233, 227-37.
- ARMSTRONG, K. M., INSAIDOO, F. K. & BAKER, B. M. (2008) Thermodynamics of T-cell receptor-peptide/MHC interactions: progress and opportunities. *J Mol Recognit*, 21, 275-87.
- ARNER, E. S. & HOLMGREN, A. (2000) Physiological functions of thioredoxin and thioredoxin reductase. *Eur J Biochem*, 267, 6102-9.
- ARRIGO, A. P. (2000) sHsp as novel regulators of programmed cell death and tumorigenicity. *Pathol Biol (Paris)*, 48, 280-8.
- AUBIN, J. E., GUPTA, A. K., BHARGAVA, U. & TURKSEN, K. (1996) Expression and regulation of galectin 3 in rat osteoblastic cells. *J Cell Physiol*, 169, 468-80.
- BAE, S. H., JEONG, J. W., PARK, J. A., KIM, S. H., BAE, M. K., CHOI, S. J. & KIM, K. W. (2004) Sumoylation increases HIF-1alpha stability and its transcriptional activity. *Biochem Biophys Res Commun*, 324, 394-400.
- BECKERLE, M. C. (1997) Zyxin: zinc fingers at sites of cell adhesion. *Bioessays*, 19, 949-57.
- BELLOWS, C. G., JIA, D., JIA, Y., HASSANLOO, A. & HEERSCHKE, J. N. (2006) Different effects of insulin and insulin-like growth factors I and II on

- osteoprogenitors and adipocyte progenitors in fetal rat bone cell populations. *Calcif Tissue Int*, 79, 57-65.
- BEN-ZE'EV, A. (1990) Application of two-dimensional gel electrophoresis in the study of cytoskeletal protein regulation during growth activation and differentiation. *Electrophoresis*, 11, 191-200.
- BENNDORF, R., HAYESS, K., RYAZANTSEV, S., WIESKE, M., BEHLKE, J. & LUTSCH, G. (1994) Phosphorylation and supramolecular organization of murine small heat shock protein HSP25 abolish its actin polymerization-inhibiting activity. *J Biol Chem*, 269, 20780-4.
- BERSHADSKY, A. D., BALABAN, N. Q. & GEIGER, B. (2003) Adhesion-dependent cell mechanosensitivity. *Annu Rev Cell Dev Biol*, 19, 677-95.
- BERSHADSKY, A. D., GLUCK, U., DENISENKO, O. N., SKLYAROVA, T. V., SPECTOR, I. & BEN-ZE'EV, A. (1995) The state of actin assembly regulates actin and vinculin expression by a feedback loop. *J Cell Sci*, 108 (Pt 3), 1183-93.
- BIGGS, M. J., RICHARDS, R. G., GADEGAARD, N., MCMURRAY, R. J., AFFROSSMAN, S., WILKINSON, C. D., OREFFO, R. O. & DALBY, M. J. (2008a) Interactions with nanoscale topography: Adhesion quantification and signal transduction in cells of osteogenic and multipotent lineage. *J Biomed Mater Res A*.
- BIGGS, M. J., RICHARDS, R. G., GADEGAARD, N., WILKINSON, C. D. & DALBY, M. J. (2007a) The effects of nanoscale pits on primary human osteoblast adhesion formation and cellular spreading. *J Mater Sci Mater Med*, 18, 399-404.
- BIGGS, M. J., RICHARDS, R. G., GADEGAARD, N., WILKINSON, C. D. & DALBY, M. J. (2007b) Regulation of implant surface cell adhesion: characterization and quantification of S-phase primary osteoblast adhesions on biomimetic nanoscale substrates. *J Orthop Res*, 25, 273-82.
- BIGGS, M. J., RICHARDS, R. G., MCFARLANE, S., WILKINSON, C. D., OREFFO, R. O. & DALBY, M. J. (2008b) Adhesion formation of primary human osteoblasts and the functional response of mesenchymal stem cells to 330nm deep microgrooves. *J R Soc Interface*, 5, 1231-42.
- BLOOM, S., LOCKARD, V. G. & BLOOM, M. (1996) Intermediate filament-mediated stretch-induced changes in chromatin: a hypothesis for growth initiation in cardiac myocytes. *J Mol Cell Cardiol*, 28, 2123-7.
- BOIVIN, G. & MEUNIER, P. J. (2003) The mineralization of bone tissue: a forgotten dimension in osteoporosis research. *Osteoporos Int*, 14 Suppl 3, S19-24.
- BONK, T. & HUMENY, A. (2001) MALDI-TOF-MS analysis of protein and DNA. *Neuroscientist*, 7, 6-12.
- BOONEN, K. J., ROSARIA-CHAK, K. Y., BAAIJENS, F. P., VAN DER SCHAFT, D. W. & POST, M. J. (2009) Essential environmental cues from the satellite cell niche: optimizing proliferation and differentiation. *Am J Physiol Cell Physiol*, 296, C1338-45.
- BORER, R. A., LEHNER, C. F., EPPENBERGER, H. M. & NIGG, E. A. (1989) Major nucleolar proteins shuttle between nucleus and cytoplasm. *Cell*, 56, 379-90.

- BORGESE, N., D'ARRIGO, A., DE SILVESTRIS, M. & PIETRINI, G. (1993) NADH-cytochrome b5 reductase and cytochrome b5 isoforms as models for the study of post-translational targeting to the endoplasmic reticulum. *FEBS Lett*, 325, 70-5.
- BOULTON, T. G. & COBB, M. H. (1991) Identification of multiple extracellular signal-regulated kinases (ERKs) with antipeptide antibodies. *Cell Regul*, 2, 357-71.
- BOULTON, T. G., GREGORY, J. S. & COBB, M. H. (1991) Purification and properties of extracellular signal-regulated kinase 1, an insulin-stimulated microtubule-associated protein 2 kinase. *Biochemistry*, 30, 278-86.
- BOULTON, T. G., YANCOPOULOS, G. D., GREGORY, J. S., SLAUGHTER, C., MOOMAW, C., HSU, J. & COBB, M. H. (1990) An insulin-stimulated protein kinase similar to yeast kinases involved in cell cycle control. *Science*, 249, 64-7.
- BOUTROS, R., FANAYAN, S., SHEHATA, M. & BYRNE, J. A. (2004) The tumor protein D52 family: many pieces, many puzzles. *Biochem Biophys Res Commun*, 325, 1115-21.
- BRANCACCIO, M., HIRSCH, E., NOTTE, A., SELVETELLA, G., LEMBO, G. & TARONE, G. (2006) Integrin signalling: the tug-of-war in heart hypertrophy. *Cardiovasc Res*, 70, 422-33.
- BREGANT, E., RENZONE, G., LONIGRO, R., PASSON, N., DI LORETO, C., PANDOLFI, M., SCALONI, A., TELL, G. & DAMANTE, G. (2009) Down-regulation of SM22/transgelin gene expression during H9c2 cells differentiation. *Mol Cell Biochem*, 327, 145-52.
- BRINKLEY, W. (1997) Microtubules: a brief historical perspective. *J Struct Biol*, 118, 84-6.
- BRITLAND, S., MORGAN, H., WOJIAK-STODART, B., RIEHLE, M., CURTIS, A. & WILKINSON, C. (1996) Synergistic and hierarchical adhesive and topographic guidance of BHK cells. *Exp Cell Res*, 228, 313-25.
- BRYANT, Z., STONE, M. D., GORE, J., SMITH, S. B., COZZARELLI, N. R. & BUSTAMANTE, C. (2003) Structural transitions and elasticity from torque measurements on DNA. *Nature*, 424, 338-41.
- BURGER, E. H. & KLEIN-NULEND, J. (1999) Mechanotransduction in bone--role of the lacuno-canalicular network. *Faseb J*, 13 Suppl, S101-12.
- CAETANO-LOPES, J., CANHAO, H. & FONSECA, J. E. (2007) Osteoblasts and bone formation. *Acta Reumatol Port*, 32, 103-10.
- CALDERWOOD, D. A., FUJIOKA, Y., DE PEREDA, J. M., GARCIA-ALVAREZ, B., NAKAMOTO, T., MARGOLIS, B., MCGLADE, C. J., LIDDINGTON, R. C. & GINSBERG, M. H. (2003) Integrin beta cytoplasmic domain interactions with phosphotyrosine-binding domains: a structural prototype for diversity in integrin signaling. *Proc Natl Acad Sci U S A*, 100, 2272-7.
- CAMBY, I., LE MERCIER, M., LEFRANC, F. & KISS, R. (2006) Galectin-1: a small protein with major functions. *Glycobiology*, 16, 137R-157R.
- CAPLAN, A. I. (1994) The mesengenic process. *Clin Plast Surg*, 21, 429-35.
- CARCAMO, C., PARDO, E., OYANADEL, C., BRAVO-ZEHNDER, M., BULL, P., CACERES, M., MARTINEZ, J., MASSARDO, L., JACOBELLI, S.,

- GONZALEZ, A. & SOZA, A. (2006) Galectin-8 binds specific beta1 integrins and induces polarized spreading highlighted by asymmetric lamellipodia in Jurkat T cells. *Exp Cell Res*, 312, 374-86.
- CARLSON, R. M., VAVRICKA, S. R., ELORANTA, J. J., MUSCH, M. W., ARVANS, D. L., KLES, K. A., WALSH-REITZ, M. M., KULLAK-UBLICK, G. A. & CHANG, E. B. (2007) fMLP induces Hsp27 expression, attenuates NF-kappaB activation, and confers intestinal epithelial cell protection. *Am J Physiol Gastrointest Liver Physiol*, 292, G1070-8.
- CARRENO, S., ENGQVIST-GOLDSTEIN, A. E., ZHANG, C. X., MCDONALD, K. L. & DRUBIN, D. G. (2004) Actin dynamics coupled to clathrin-coated vesicle formation at the trans-Golgi network. *J Cell Biol*, 165, 781-8.
- CHANG, Y., QI, X., BU, L. S. & XU, Z. X. (2005) [Study on multipotential differentiation of human bone marrow mesenchymal stem cells in vitro.]. *Zhongguo Wei Zhong Bing Ji Jiu Yi Xue*, 17, 95-7.
- CHEN, A., WANG, P. Y., YANG, Y. C., HUANG, Y. H., YEH, J. J., CHOU, Y. H., CHENG, J. T., HONG, Y. R. & LI, S. S. (2006) SUMO regulates the cytoplasmic nuclear transport of its target protein Daxx. *J Cell Biochem*, 98, 895-911.
- CHEN, C. S., MRKSICH, M., HUANG, S., WHITESIDES, G. M. & INGBER, D. E. (1997) Geometric control of cell life and death. *Science*, 276, 1425-8.
- CHEN, H. F., XIE, L. D. & XU, C. S. (2009) Role of heat shock protein 27 phosphorylation in migration of vascular smooth muscle cells. *Mol Cell Biochem*, 327, 1-6.
- CHEN, Y. C., TSAI, S. H., SHEN, S. C., LIN, J. K. & LEE, W. R. (2001) Alternative activation of extracellular signal-regulated protein kinases in curcumin and arsenite-induced HSP70 gene expression in human colorectal carcinoma cells. *Eur J Cell Biol*, 80, 213-21.
- CHIELLINI, C., COCHET, O., NEGRONI, L., SAMSON, M., POGGI, M., AILHAUD, G., ALESSI, M. C., DANI, C. & AMRI, E. Z. (2008) Characterization of human mesenchymal stem cell secretome at early steps of adipocyte and osteoblast differentiation. *BMC Mol Biol*, 9, 26.
- CHOI, J. Y., VAN WIJNEN, A. J., ASLAM, F., LESZYK, J. D., STEIN, J. L., STEIN, G. S., LIAN, J. B. & PENMAN, S. (1998) Developmental association of the beta-galactoside-binding protein galectin-1 with the nuclear matrix of rat calvarial osteoblasts. *J Cell Sci*, 111 (Pt 20), 3035-43.
- CHOU, C. C., YUNG, B. Y. & HSU, C. Y. (2007) Involvement of nPKC-MAPK pathway in the decrease of nucleophosmin/B23 during megakaryocytic differentiation of human myelogenous leukemia K562 cells. *Life Sci*, 80, 2051-9.
- CHRZANOWSKA-WODNICKA, M. & BURRIDGE, K. (1996) Rho-stimulated contractility drives the formation of stress fibers and focal adhesions. *J Cell Biol*, 133, 1403-15.
- CIOCCA, D. R., OESTERREICH, S., CHAMNESS, G. C., MCGUIRE, W. L. & FUQUA, S. A. (1993) Biological and clinical implications of heat shock protein 27,000 (Hsp27): a review. *J Natl Cancer Inst*, 85, 1558-70.

- CIVITELLI, R. (2008) Cell-cell communication in the osteoblast/osteocyte lineage. *Arch Biochem Biophys*, 473, 188-92.
- CLEVELAND, D. W., LOPATA, M. A., SHERLINE, P. & KIRSCHNER, M. W. (1981) Unpolymerized tubulin modulates the level of tubulin mRNAs. *Cell*, 25, 537-46.
- COLLINS, N. L., REGINATO, M. J., PAULUS, J. K., SGROI, D. C., LABAER, J. & BRUGGE, J. S. (2005) G1/S cell cycle arrest provides anoikis resistance through Erk-mediated Bim suppression. *Mol Cell Biol*, 25, 5282-91.
- COLNOT, C., SIDHU, S. S., POIRIER, F. & BALMAIN, N. (1999) Cellular and subcellular distribution of galectin-3 in the epiphyseal cartilage and bone of fetal and neonatal mice. *Cell Mol Biol (Noisy-le-grand)*, 45, 1191-202.
- COOPER, D. N. & BARONDES, S. H. (1990) Evidence for export of a muscle lectin from cytosol to extracellular matrix and for a novel secretory mechanism. *J Cell Biol*, 110, 1681-91.
- COTRUPI, S. & MAIER, J. A. (2004) Is HSP70 upregulation crucial for cellular proliferative response in simulated microgravity? *J Gravit Physiol*, 11, P173-6.
- COTTER, R. J., GRIFFITH, W. & JELINEK, C. (2007) Tandem time-of-flight (TOF/TOF) mass spectrometry and the curved-field reflectron. *J Chromatogr B Analyt Technol Biomed Life Sci*, 855, 2-13.
- CURTIS, A. & RIEHLE, M. (2001) Tissue engineering: the biophysical background. *Phys Med Biol*, 46, R47-65.
- CURTIS, A. & WILKINSON, C. (1997) Topographical control of cells. *Biomaterials*, 18, 1573-83.
- CURTIS, A. S., DALBY, M. & GADEGAARD, N. (2006) Cell signaling arising from nanotopography: implications for nanomedical devices. *Nanomed*, 1, 67-72.
- CURTIS, A. S. & VARDE, M. (1964) Control Of Cell Behavior: Topological Factors. *J Natl Cancer Inst*, 33, 15-26.
- D'IPPOLITO, G., SCHILLER, P. C., PEREZ-STABLE, C., BALKAN, W., ROOS, B. A. & HOWARD, G. A. (2002) Cooperative actions of hepatocyte growth factor and 1,25-dihydroxyvitamin D3 in osteoblastic differentiation of human vertebral bone marrow stromal cells. *Bone*, 31, 269-75.
- DALBY, M. J., ANDAR, A., NAG, A., AFFROSSMAN, S., TARE, R., MCFARLANE, S. & OREFFO, R. O. (2008a) Genomic expression of mesenchymal stem cells to altered nanoscale topographies. *J R Soc Interface*, 5, 1055-65.
- DALBY, M. J., BERRY, C. C., RIEHLE, M. O., SUTHERLAND, D. S., AGHELI, H. & CURTIS, A. S. (2004) Attempted endocytosis of nano-environment produced by colloidal lithography by human fibroblasts. *Exp Cell Res*, 295, 387-94.
- DALBY, M. J., BIGGS, M. J., GADEGAARD, N., KALNA, G., WILKINSON, C. D. & CURTIS, A. S. (2007a) Nanotopographical stimulation of mechanotransduction and changes in interphase centromere positioning. *J Cell Biochem*, 100, 326-38.

- DALBY, M. J., GADEGAARD, N., CURTIS, A. S. & OREFFO, R. O. (2007b) Nanotopographical control of human osteoprogenitor differentiation. *Curr Stem Cell Res Ther*, 2, 129-38.
- DALBY, M. J., GADEGAARD, N., HERZYK, P., SUTHERLAND, D., AGHELI, H., WILKINSON, C. D. & CURTIS, A. S. (2007c) Nanomechanotransduction and interphase nuclear organization influence on genomic control. *J Cell Biochem*, 102, 1234-44.
- DALBY, M. J., GADEGAARD, N., TARE, R., ANDAR, A., RIEHLE, M. O., HERZYK, P., WILKINSON, C. D. & OREFFO, R. O. (2007d) The control of human mesenchymal cell differentiation using nanoscale symmetry and disorder. *Nat Mater*, 6, 997-1003.
- DALBY, M. J., HART, A. & YARWOOD, S. J. (2008b) The effect of the RACK1 signalling protein on the regulation of cell adhesion and cell contact guidance on nanometric grooves. *Biomaterials*, 29, 282-9.
- DALBY, M. J., MCCLOY, D., ROBERTSON, M., AGHELI, H., SUTHERLAND, D., AFFROSSMAN, S. & OREFFO, R. O. (2006a) Osteoprogenitor response to semi-ordered and random nanotopographies. *Biomaterials*, 27, 2980-7.
- DALBY, M. J., MCCLOY, D., ROBERTSON, M., WILKINSON, C. D. & OREFFO, R. O. (2006b) Osteoprogenitor response to defined topographies with nanoscale depths. *Biomaterials*, 27, 1306-15.
- DALBY, M. J., RIEHLE, M. O., YARWOOD, S. J., WILKINSON, C. D. & CURTIS, A. S. (2003) Nucleus alignment and cell signaling in fibroblasts: response to a micro-grooved topography. *Exp Cell Res*, 284, 274-82.
- DANGI, S., CHEN, F. M. & SHAPIRO, P. (2006) Activation of extracellular signal-regulated kinase (ERK) in G2 phase delays mitotic entry through p21CIP1. *Cell Prolif*, 39, 261-79.
- DATTA, H. K., NG, W. F., WALKER, J. A., TUCK, S. P. & VARANASI, S. S. (2008) The cell biology of bone metabolism. *J Clin Pathol*, 61, 577-87.
- DEN BRABER, E. T., DE RUIJTER, J. E., GINSEL, L. A., VON RECUM, A. F. & JANSEN, J. A. (1998) Orientation of ECM protein deposition, fibroblast cytoskeleton, and attachment complex components on silicone microgrooved surfaces. *J Biomed Mater Res*, 40, 291-300.
- DENG, Q., LIAO, R., WU, B. L. & SUN, P. (2004) High intensity ras signaling induces premature senescence by activating p38 pathway in primary human fibroblasts. *J Biol Chem*, 279, 1050-9.
- DERNBURG, A. F. & MISTELI, T. (2007) Nuclear architecture--an island no more. *Dev Cell*, 12, 329-34.
- DESMARIS, V., GHOSH, M., EDDY, R. & CONDEELIS, J. (2005) Cofilin takes the lead. *J Cell Sci*, 118, 19-26.
- DOTY, S. B. (1981) Morphological evidence of gap junctions between bone cells. *Calcif Tissue Int*, 33, 509-12.
- ELSEN, L. & CARELS, C. E. (2008) [Embryonic odontogenesis in vertebrates. A mini-review]. *Ned Tijdschr Tandheelkd*, 115, 71-7.
- ENGEL, E., MARTINEZ, E., MILLS, C. A., FUNES, M., PLANELL, J. A. & SAMITIER, J. (2009) Mesenchymal stem cell differentiation on

- microstructured poly (methyl methacrylate) substrates. *Ann Anat*, 191, 136-44.
- ENGLER, A. J., SEN, S., SWEENEY, H. L. & DISCHER, D. E. (2006) Matrix elasticity directs stem cell lineage specification. *Cell*, 126, 677-89.
- FALCONNET, D., CSUCS, G., GRANDIN, H. M. & TEXTOR, M. (2006) Surface engineering approaches to micropattern surfaces for cell-based assays. *Biomaterials*, 27, 3044-63.
- FANDINO, A. S., RAIS, I., VOLLMER, M., ELGASS, H., SCHAGGER, H. & KARAS, M. (2005) LC-nanospray-MS/MS analysis of hydrophobic proteins from membrane protein complexes isolated by blue-native electrophoresis. *J Mass Spectrom*, 40, 1223-31.
- FEINSTEIN, T. N. & LINSTEDT, A. D. (2008) GRASP55 regulates Golgi ribbon formation. *Mol Biol Cell*, 19, 2696-707.
- FERNANDEZ-TRESGUERRES-HERNANDEZ-GIL, I., ALOBERA-GRACIA, M. A., DEL-CANTO-PINGARRON, M. & BLANCO-JEREZ, L. (2006) Physiological bases of bone regeneration II. The remodeling process. *Med Oral Patol Oral Cir Bucal*, 11, E151-7.
- FISCHER, C., SANCHEZ-RUDERISCH, H., WELZEL, M., WIEDENMANN, B., SAKAI, T., ANDRE, S., GABIUS, H. J., KHACHIGIAN, L., DETJEN, K. M. & ROSEWICZ, S. (2005) Galectin-1 interacts with the $\alpha_5\beta_1$ fibronectin receptor to restrict carcinoma cell growth via induction of p21 and p27. *J Biol Chem*, 280, 37266-77.
- FITZGIBBON, M., LI, Q. & MCINTOSH, M. (2008) Modes of inference for evaluating the confidence of peptide identifications. *J Proteome Res*, 7, 35-9.
- FORGACS, G. (1995) On the possible role of cytoskeletal filamentous networks in intracellular signaling: an approach based on percolation. *J Cell Sci*, 108 (Pt 6), 2131-43.
- FRANCESCHI, R. T., GE, C., XIAO, G., ROCA, H. & JIANG, D. (2007) Transcriptional regulation of osteoblasts. *Ann NY Acad Sci*, 1116, 196-207.
- FRICK, D. N. & RICHARDSON, C. C. (2001) DNA primases. *Annu Rev Biochem*, 70, 39-80.
- FRIEDENSTEIN, A. J., LATZINIK, N. V., GORSKAYA YU, F., LURIA, E. A. & MOSKVINA, I. L. (1992) Bone marrow stromal colony formation requires stimulation by haemopoietic cells. *Bone Miner*, 18, 199-213.
- FUCHS, E. & CLEVELAND, D. W. (1998) A structural scaffolding of intermediate filaments in health and disease. *Science*, 279, 514-9.
- FUJITA, T., AZUMA, Y., FUKUYAMA, R., HATTORI, Y., YOSHIDA, C., KOIDA, M., OGITA, K. & KOMORI, T. (2004) Runx2 induces osteoblast and chondrocyte differentiation and enhances their migration by coupling with PI3K-Akt signaling. *J Cell Biol*, 166, 85-95.
- FULLER, B. (1961) Tensegrity. *Portfolio and Art News Annual*, 4, 112-127.
- FUSEK, M. & VETVICKA, V. (2005) Dual role of cathepsin D: ligand and protease. *Biomed Pap Med Fac Univ Palacky Olomouc Czech Repub*, 149, 43-50.
- GADEGAARD, N. (2006) Atomic force microscopy in biology: technology and techniques. *Biotech Histochem*, 81, 87-97.

- GALVANI, M., ROVATTI, L., HAMDAN, M., HERBERT, B. & RIGHETTI, P. G. (2001) Protein alkylation in the presence/absence of thiourea in proteome analysis: a matrix assisted laser desorption/ionization-time of flight-mass spectrometry investigation. *Electrophoresis*, 22, 2066-74.
- GEIGER, B. & BERSHADSKY, A. (2001) Assembly and mechanosensory function of focal contacts. *Curr Opin Cell Biol*, 13, 584-92.
- GEIGER, B., BERSHADSKY, A., PANKOV, R. & YAMADA, K. M. (2001) Transmembrane crosstalk between the extracellular matrix--cytoskeleton crosstalk. *Nat Rev Mol Cell Biol*, 2, 793-805.
- GERSTENFELD, L. C., CRAWFORD, D. R., BOEDTKER, H. & DOTY, P. (1984) Expression of type I and III collagen genes during differentiation of embryonic chicken myoblasts in culture. *Mol Cell Biol*, 4, 1483-92.
- GHIONI, P., D'ALESSANDRA, Y., MANSUETO, G., JAFFRAY, E., HAY, R. T., LA MANTIA, G. & GUERRINI, L. (2005) The protein stability and transcriptional activity of p63alpha are regulated by SUMO-1 conjugation. *Cell Cycle*, 4, 183-90.
- GIBSON, I. R. & BONFIELD, W. (2002) Preparation and characterization of magnesium/carbonate co-substituted hydroxyapatites. *J Mater Sci Mater Med*, 13, 685-93.
- GLOE, T. & POHL, U. (2002) Laminin binding conveys mechanosensing in endothelial cells. *News Physiol Sci*, 17, 166-9.
- GLOE, T., RIEDMAYR, S., SOHN, H. Y. & POHL, U. (1999) The 67-kDa laminin-binding protein is involved in shear stress-dependent endothelial nitric-oxide synthase expression. *J Biol Chem*, 274, 15996-6002.
- GOHLA, A. & BOKOCH, G. M. (2002) 14-3-3 regulates actin dynamics by stabilizing phosphorylated cofilin. *Curr Biol*, 12, 1704-10.
- GORDON, J. A. & WARREN, J. R. (1968) Denaturation of globular proteins. I. The interaction of urea and thiourea with bovine plasma albumin. *J Biol Chem*, 243, 5663-9.
- GUNNING, P., O'NEILL, G. & HARDEMAN, E. (2008) Tropomyosin-based regulation of the actin cytoskeleton in time and space. *Physiol Rev*, 88, 1-35.
- HADARI, Y. R., ARBEL-GOREN, R., LEVY, Y., AMSTERDAM, A., ALON, R., ZAKUT, R. & ZICK, Y. (2000) Galectin-8 binding to integrins inhibits cell adhesion and induces apoptosis. *J Cell Sci*, 113 (Pt 13), 2385-97.
- HADJIDAKIS, D. J. & ANDROULAKIS, II (2006) Bone remodeling. *Ann N Y Acad Sci*, 1092, 385-96.
- HAMILTON, D. W. & BRUNETTE, D. M. (2007) The effect of substratum topography on osteoblast adhesion mediated signal transduction and phosphorylation. *Biomaterials*, 28, 1806-19.
- HAN, J. H., BAI, G. Y., PARK, J. H., YUAN, K., PARK, W. H., KIM, S. Z. & KIM, S. H. (2008) Regulation of stretch-activated ANP secretion by chloride channels. *Peptides*, 29, 613-21.
- HEATH, J. P. & DUNN, G. A. (1978) Cell to substratum contacts of chick fibroblasts and their relation to the microfilament system. A correlated interference-reflexion and high-voltage electron-microscope study. *J Cell Sci*, 29, 197-212.

- HEGNER, B., LANGE, M., KUSCH, A., ESSIN, K., SEZER, O., SCHULZE-LOHOFF, E., LUFT, F. C., GOLLASCH, M. & DRAGUN, D. (2009) mTOR regulates vascular smooth muscle cell differentiation from human bone marrow-derived mesenchymal progenitors. *Arterioscler Thromb Vasc Biol*, 29, 232-8.
- HEIDI AU, H. T., CUI, B., CHU, Z. E., VERES, T. & RADISIC, M. (2009) Cell culture chips for simultaneous application of topographical and electrical cues enhance phenotype of cardiomyocytes. *Lab Chip*, 9, 564-75.
- HELDIN, C. H., MIYAZONO, K. & TEN DIJKE, P. (1997) TGF-beta signalling from cell membrane to nucleus through SMAD proteins. *Nature*, 390, 465-71.
- HELFMAN, D. M., LEVY, E. T., BERTHIER, C., SHTUTMAN, M., RIVELINE, D., GROSHEVA, I., LACHISH-ZALAIT, A., ELBAUM, M. & BERSHADSKY, A. D. (1999) Caldesmon inhibits nonmuscle cell contractility and interferes with the formation of focal adhesions. *Mol Biol Cell*, 10, 3097-112.
- HENCH, L. L. & POLAK, J. M. (2002) Third-generation biomedical materials. *Science*, 295, 1014-7.
- HERBLOT, S., VEKRIS, A., ROUZAUT, A., NAJEME, F., DE MIGUEL, C., BEZIAN, J. H. & BONNET, J. (1997) Selection of down-regulated sequences along the monocytic differentiation of leukemic HL60 cells. *FEBS Lett*, 414, 146-52.
- HERNANDEZ, O. M., JONES, M., GUZMAN, G. & SZCZESNA-CORDARY, D. (2007) Myosin essential light chain in health and disease. *Am J Physiol Heart Circ Physiol*, 292, H1643-54.
- HERRMANN, H. & AEBI, U. (2000) Intermediate filaments and their associates: multi-talented structural elements specifying cytoarchitecture and cytodynamics. *Curr Opin Cell Biol*, 12, 79-90.
- HERRMANN, H. & AEBI, U. (2004) Intermediate filaments: molecular structure, assembly mechanism, and integration into functionally distinct intracellular Scaffolds. *Annu Rev Biochem*, 73, 749-89.
- HEYDARKHAN-HAGVALL, S., CHOI, C. H., DUNN, J., HEYDARKHAN, S., SCHENKE-LAYLAND, K., MACLELLAN, W. R. & BEYGUI, R. E. (2007) Influence of systematically varied nano-scale topography on cell morphology and adhesion. *Cell Commun Adhes*, 14, 181-94.
- HILLSLEY, M. V. & FRANGOS, J. A. (1994) Bone tissue engineering: the role of interstitial fluid flow. *Biotechnol Bioeng*, 43, 573-81.
- HIRATA, H., TATSUMI, H. & SOKABE, M. (2008) Mechanical forces facilitate actin polymerization at focal adhesions in a zyxin-dependent manner. *J Cell Sci*, 121, 2795-804.
- HO, E., HAYEN, A. & WILKINS, M. R. (2006) Characterisation of organellar proteomes: a guide to subcellular proteomic fractionation and analysis. *Proteomics*, 6, 5746-57.
- HSU, J. L., HUANG, S. Y. & CHEN, S. H. (2006) Dimethyl multiplexed labeling combined with microcolumn separation and MS analysis for time course study in proteomics. *Electrophoresis*, 27, 3652-60.

- HSU, J. L., HUANG, S. Y., CHOW, N. H. & CHEN, S. H. (2003) Stable-isotope dimethyl labeling for quantitative proteomics. *Anal Chem*, 75, 6843-52.
- HSU, J. L., HUANG, S. Y., SHIEA, J. T., HUANG, W. Y. & CHEN, S. H. (2005) Beyond quantitative proteomics: signal enhancement of the a1 ion as a mass tag for peptide sequencing using dimethyl labeling. *J Proteome Res*, 4, 101-8.
[HTTP://WWW.DAVIDDARLING.INFO/ENCYCLOPEDIA/B/BONE.HTML](http://www.daviddarling.info/encyclopedia/b/bone.html).
[HTTP://WWW.LE.AC.UK/GE/GENIE/VGEC/SC/CELLCYCLE.HTML](http://www.le.ac.uk/ge/genie/vgec/sc/cellcycle.html).
[HTTP://WWW.MEDICALPROTEOMICS.COM/IMAGES/DIGE.JPG](http://www.medicalproteomics.com/images/dige.jpg).
[HTTP://WWW.MYPONDSOFTWARE.COM/BONE.JPG](http://www.mypondsoftware.com/bone.jpg).
[HTTP://WWW.PALAEOS.COM/EUKARYA/EUKARYA.ORIGINS.2.HTML](http://www.palaeos.com/eukarya/eukarya.origins.2.html).
[HTTP://WWW.WEIZMANN.AC.IL/SB/FACULTY_PAGES/ADDADI/OSTEOCLAST.HTML](http://www.weizmann.ac.il/sb/faculty_pages/addadi/osteoclast.html).
[HTTPS://VAULT.SWRI.ORG/CMS/UPLOAD/CELLS_500PIXELS.JPG](https://vault.swri.org/cms/upload/cells_500pixels.jpg).
- HUNG, J. J., CHENG, T. J., LAI, Y. K. & CHANG, M. D. (1998) Differential activation of p38 mitogen-activated protein kinase and extracellular signal-regulated protein kinases confers cadmium-induced HSP70 expression in 9L rat brain tumor cells. *J Biol Chem*, 273, 31924-31.
- HUOT, J., HOULE, F., SPITZ, D. R. & LANDRY, J. (1996) HSP27 phosphorylation-mediated resistance against actin fragmentation and cell death induced by oxidative stress. *Cancer Res*, 56, 273-9.
- HYNES, R. O. (2002) Integrins: bidirectional, allosteric signaling machines. *Cell*, 110, 673-87.
- INGBER, D. E. (1997a) Integrins, tensegrity, and mechanotransduction. *Gravit Space Biol Bull*, 10, 49-55.
- INGBER, D. E. (1997b) Tensegrity: the architectural basis of cellular mechanotransduction. *Annu Rev Physiol*, 59, 575-99.
- INGBER, D. E. (2003a) Tensegrity I. Cell structure and hierarchical systems biology. *J Cell Sci*, 116, 1157-73.
- INGBER, D. E. (2003b) Tensegrity II. How structural networks influence cellular information processing networks. *J Cell Sci*, 116, 1397-408.
- INGBER, D. E. (2008) Tensegrity and mechanotransduction. *J Bodyw Mov Ther*, 12, 198-200.
- INOUE, A., KAMIYA, A., ISHIJI, A., HIRUMA, Y., HIROSE, S. & HAGIWARA, H. (2000) Vasoactive peptide-regulated gene expression during osteoblastic differentiation. *J Cardiovasc Pharmacol*, 36, S286-9.
- INUI, K., OREFFO, R. O. & TRIFFITT, J. T. (1997) Effects of beta mercaptoethanol on the proliferation and differentiation of human osteoprogenitor cells. *Cell Biol Int*, 21, 419-25.
- IRIBE, G. & KOHL, P. (2008) Axial stretch enhances sarcoplasmic reticulum Ca²⁺ leak and cellular Ca²⁺ reuptake in guinea pig ventricular myocytes: experiments and models. *Prog Biophys Mol Biol*, 97, 298-311.
- IWATSUKI, H., SASAKI, K., SUDA, M. & ITANO, C. (1999) Vimentin intermediate filament protein as differentiation marker of optic vesicle epithelium in the chick embryo. *Acta Histochem*, 101, 369-82.

- JAGER, M., ZILKENS, C., ZANGER, K. & KRAUSPE, R. (2007) Significance of nano- and microtopography for cell-surface interactions in orthopaedic implants. *J Biomed Biotechnol*, 2007, 69036.
- JESCH, S. A., LEWIS, T. S., AHN, N. G. & LINSTEDT, A. D. (2001) Mitotic phosphorylation of Golgi reassembly stacking protein 55 by mitogen-activated protein kinase ERK2. *Mol Biol Cell*, 12, 1811-7.
- JIANG, R. W., LAU, K. M., LAM, H. M., YAM, W. S., LEUNG, L. K., CHOI, K. L., WAYE, M. M., MAK, T. C., WOO, K. S. & FUNG, K. P. (2005) A comparative study on aqueous root extracts of *Pueraria thomsonii* and *Pueraria lobata* by antioxidant assay and HPLC fingerprint analysis. *J Ethnopharmacol*, 96, 133-8.
- JIANG, Y. J., SUN, Q., FANG, X. S. & WANG, X. (2009) Comparative mitochondrial proteomic analysis of Rji cells exposed to adriamycin. *Mol Med*, 15, 173-82.
- JOACHIM, C. (2005) To be nano or not to be nano? *Nat Mater*, 4, 107-9.
- JONSSON, A. P. (2001) Mass spectrometry for protein and peptide characterisation. *Cell Mol Life Sci*, 58, 868-84.
- KANG, H. J., JUNG, S. K., KIM, S. J. & CHUNG, S. J. (2008) Structure of human alpha-enolase (hENO1), a multifunctional glycolytic enzyme. *Acta Crystallogr D Biol Crystallogr*, 64, 651-7.
- KANTAWONG, F., BURCHMORE, R., WILKINSON, C. D., OREFFO, R. O. & DALBY, M. J. (2009) Differential in-gel electrophoresis (DIGE) analysis of human bone marrow osteoprogenitor cell contact guidance. *Acta Biomater*, 5, 1137-46.
- KANTAWONG, F., BURGESS, K., JAYAWARDENA K., HART, A., RIEHLE, M., OREFFO, ROC., DALBY, MJ., BURCHMORE, R. (2009) Effects of Surface Topography Compositated with *Puerariae Radix* on Human STRO-1 Positive Stem Cells. *Submitted*.
- KATO, Y., TAPPING, R. I., HUANG, S., WATSON, M. H., ULEVITCH, R. J. & LEE, J. D. (1998) Bmk1/Erk5 is required for cell proliferation induced by epidermal growth factor. *Nature*, 395, 713-6.
- KATSUMOTO, T., MITSUSHIMA, A. & KURIMURA, T. (1990) The role of the vimentin intermediate filaments in rat 3Y1 cells elucidated by immunoelectron microscopy and computer-graphic reconstruction. *Biol Cell*, 68, 139-46.
- KAY, R. R., LANGRIDGE, P., TRAYNOR, D. & HOELLER, O. (2008) Changing directions in the study of chemotaxis. *Nat Rev Mol Cell Biol*, 9, 455-63.
- KEIPER, B. D., GAN, W. & RHOADS, R. E. (1999) Protein synthesis initiation factor 4G. *Int J Biochem Cell Biol*, 31, 37-41.
- KELLER, A., PELTZER, J., CARPENTIER, G., HORVATH, I., OLAH, J., DUCHESNAY, A., OROSZ, F. & OVADI, J. (2007) Interactions of enolase isoforms with tubulin and microtubules during myogenesis. *Biochim Biophys Acta*, 1770, 919-26.
- KELLER, J. M., ESCARA-WILKE, J. F. & KELLER, E. T. (2008) Heat stress-induced heat shock protein 70 expression is dependent on ERK activation in

- zebrafish (*Danio rerio*) cells. *Comp Biochem Physiol A Mol Integr Physiol*, 150, 307-14.
- KIM, D. H., KIM, P., SUH, K., KYU CHOI, S., HO LEE, S. & KIM, B. (2005a) Modulation of adhesion and growth of cardiac myocytes by surface nanotopography. *Conf Proc IEEE Eng Med Biol Soc*, 4, 4091-4.
- KIM, D. I., LEE, S. J., LEE, S. B., PARK, K., KIM, W. J. & MOON, S. K. (2008) Requirement for Ras/Raf/ERK pathway in naringin-induced G1-cell-cycle arrest via p21WAF1 expression. *Carcinogenesis*, 29, 1701-9.
- KIM, H. W., KNOWLES, J. C. & KIM, H. E. (2004) Hydroxyapatite/poly(epsilon-caprolactone) composite coatings on hydroxyapatite porous bone scaffold for drug delivery. *Biomaterials*, 25, 1279-87.
- KIM, H. W., LEE, E. J., JUN, I. K., KIM, H. E. & KNOWLES, J. C. (2005b) Degradation and drug release of phosphate glass/polycaprolactone biological composites for hard-tissue regeneration. *J Biomed Mater Res B Appl Biomater*, 75, 34-41.
- KIM, M. R., CHANG, H. S., KIM, B. H., KIM, S., BAEK, S. H., KIM, J. H., LEE, S. R. & KIM, J. R. (2003) Involvements of mitochondrial thioredoxin reductase (TrxR2) in cell proliferation. *Biochem Biophys Res Commun*, 304, 119-24.
- KITCHING, R., QI, S., LI, V., RAOUF, A., VARY, C. P. & SETH, A. (2002) Coordinate gene expression patterns during osteoblast maturation and retinoic acid treatment of MC3T3-E1 cells. *J Bone Miner Metab*, 20, 269-80.
- KIVIRIKKO, K. I., MYLLYLÄ, R. & PIHLAJANIEMI, T. (1989) Protein hydroxylation: prolyl 4-hydroxylase, an enzyme with four cosubstrates and a multifunctional subunit. *Faseb J*, 3, 1609-17.
- KLEIN-NULEND, J., BACABAC, R. G. & MULLENDER, M. G. (2005) Mechanobiology of bone tissue. *Pathol Biol (Paris)*, 53, 576-80.
- KLINGENBERG, D., GUNDUZ, D., HARTEL, F., BINDEWALD, K., SCHAFER, M., PIPER, H. M. & NOLL, T. (2004) MEK/MAPK as a signaling element in ATP control of endothelial myosin light chain. *Am J Physiol Cell Physiol*, 286, C807-12.
- KORN, E. D. (2000) Coevolution of head, neck, and tail domains of myosin heavy chains. *Proc Natl Acad Sci U S A*, 97, 12559-64.
- KOSTENKO, S., JOHANNESSEN, M. & MOENS, U. (2009) PKA-induced F-actin rearrangement requires phosphorylation of Hsp27 by the MAPKAP kinase MK5. *Cell Signal*, 21, 712-8.
- KRISHNAN, V., BRYANT, H. U. & MACDOUGALD, O. A. (2006) Regulation of bone mass by Wnt signaling. *J Clin Invest*, 116, 1202-9.
- KRUSEMARK, C. J., FERGUSON, J. T., WENGER, C. D., KELLEHER, N. L. & BELSHAW, P. J. (2008) Global amine and acid functional group modification of proteins. *Anal Chem*, 80, 713-20.
- KUZELOVA, K. & HRKAL, Z. (2008) Rho-signaling pathways in chronic myelogenous leukemia. *Cardiovasc Hematol Disord Drug Targets*, 8, 261-7.
- LANDRY, J. & HUOT, J. (1995) Modulation of actin dynamics during stress and physiological stimulation by a signaling pathway involving p38 MAP kinase and heat-shock protein 27. *Biochem Cell Biol*, 73, 703-7.

- LANE, C. S. (2005) Mass spectrometry-based proteomics in the life sciences. *Cell Mol Life Sci*, 62, 848-69.
- LE CLAINCHE, C. & CARLIER, M. F. (2008) Regulation of actin assembly associated with protrusion and adhesion in cell migration. *Physiol Rev*, 88, 489-513.
- LEE, J. W., KWAK, H. J., LEE, J. J., KIM, Y. N., LEE, J. W., PARK, M. J., JUNG, S. E., HONG, S. I., LEE, J. H. & LEE, J. S. (2008) HSP27 regulates cell adhesion and invasion via modulation of focal adhesion kinase and MMP-2 expression. *Eur J Cell Biol*, 87, 377-87.
- LEFLOCH, R., POUYSSEUR, J. & LENORMAND, P. (2009) Total ERK1/2 activity regulates cell proliferation. *Cell Cycle*, 8, 705-11.
- LELE, T. P., PENDSE, J., KUMAR, S., SALANGA, M., KARAVITIS, J. & INGBER, D. E. (2006) Mechanical forces alter zyxin unbinding kinetics within focal adhesions of living cells. *J Cell Physiol*, 207, 187-94.
- LEONARDI, R., BARBATO, E., PAGANELLI, C. & LO MUZIO, L. (2004) Immunolocalization of heat shock protein 27 in developing jaw bones and tooth germs of human fetuses. *Calcif Tissue Int*, 75, 509-16.
- LEVEN, R. M., VIRDI, A. S. & SUMNER, D. R. (2004) Patterns of gene expression in rat bone marrow stromal cells cultured on titanium alloy discs of different roughness. *J Biomed Mater Res A*, 70, 391-401.
- LEVY, Y., ARBEL-GOREN, R., HADARI, Y. R., ESHHAR, S., RONEN, D., ELHANANY, E., GEIGER, B. & ZICK, Y. (2001) Galectin-8 functions as a matricellular modulator of cell adhesion. *J Biol Chem*, 276, 31285-95.
- LEVY, Y., RONEN, D., BERSHADSKY, A. D. & ZICK, Y. (2003) Sustained induction of ERK, protein kinase B, and p70 S6 kinase regulates cell spreading and formation of F-actin microspikes upon ligation of integrins by galectin-8, a mammalian lectin. *J Biol Chem*, 278, 14533-42.
- LI, J., BAI, L., CUI, S., WANG, H. & XU, X. (2007) [Comparison between gene therapy and gradual release carrier for bone morphogenetic protein-2 in repairing bone defects]. *Sheng Wu Yi Xue Gong Cheng Xue Za Zhi*, 24, 667-70.
- LI, R. & GUNDERSEN, G. G. (2008) Beyond polymer polarity: how the cytoskeleton builds a polarized cell. *Nat Rev Mol Cell Biol*, 9, 860-73.
- LI, Y., LIN, J. L., REITER, R. S., DANIELS, K., SOLL, D. R. & LIN, J. J. (2004) Caldesmon mutant defective in Ca(2+)-calmodulin binding interferes with assembly of stress fibers and affects cell morphology, growth and motility. *J Cell Sci*, 117, 3593-604.
- LIANG, P. & MACRAE, T. H. (1997) Molecular chaperones and the cytoskeleton. *J Cell Sci*, 110 (Pt 13), 1431-40.
- LIM, J. Y. & DONAHUE, H. J. (2007) Cell sensing and response to micro- and nanostructured surfaces produced by chemical and topographic patterning. *Tissue Eng*, 13, 1879-91.
- LIM, J. Y., DREISS, A. D., ZHOU, Z., HANSEN, J. C., SIEDLECKI, C. A., HENGSTEBECK, R. W., CHENG, J., WINOGRAD, N. & DONAHUE, H. J. (2007) The regulation of integrin-mediated osteoblast focal adhesion and

- focal adhesion kinase expression by nanoscale topography. *Biomaterials*, 28, 1787-97.
- LIU, F. T., PATTERSON, R. J. & WANG, J. L. (2002) Intracellular functions of galectins. *Biochim Biophys Acta*, 1572, 263-73.
- LIU, S., CALDERWOOD, D. A. & GINSBERG, M. H. (2000) Integrin cytoplasmic domain-binding proteins. *J Cell Sci*, 113 (Pt 20), 3563-71.
- LO, C. M., WANG, H. B., DEMBO, M. & WANG, Y. L. (2000) Cell movement is guided by the rigidity of the substrate. *Biophys J*, 79, 144-52.
- LOESBERG, W. A., WALBOOMERS, X. F., VAN LOON, J. J. & JANSEN, J. A. (2006) The effect of combined hypergravity and micro-grooved surface topography on the behaviour of fibroblasts. *Cell Motil Cytoskeleton*, 63, 384-94.
- LOPEZ, J. L. (2007) Two-dimensional electrophoresis in proteome expression analysis. *J Chromatogr B Analyt Technol Biomed Life Sci*, 849, 190-202.
- LUTOMSKI, D., JOUBERT-CARON, R., LEFEBURE, C., SALAMA, J., BELIN, C., BLADIER, D. & CARON, M. (1997) Anti-galectin-1 autoantibodies in serum of patients with neurological diseases. *Clin Chim Acta*, 262, 131-8.
- MACK, C. P., SOMLYO, A. V., HAUTMANN, M., SOMLYO, A. P. & OWENS, G. K. (2001) Smooth muscle differentiation marker gene expression is regulated by RhoA-mediated actin polymerization. *J Biol Chem*, 276, 341-7.
- MAJUMDAR, M. K., THIEDE, M. A., MOSCA, J. D., MOORMAN, M. & GERSON, S. L. (1998) Phenotypic and functional comparison of cultures of marrow-derived mesenchymal stem cells (MSCs) and stromal cells. *J Cell Physiol*, 176, 57-66.
- MAMYRIN, B. A. (1973) The mass-reflectron, a new non-magnetic time-offlight mass spectrometer with high resolution. *Sov. Phys. JETP.*, 37, 45-48.
- MARIE, P. J. (2008) Transcription factors controlling osteoblastogenesis. *Arch Biochem Biophys*, 473, 98-105.
- MAROUGA, R., DAVID, S. & HAWKINS, E. (2005) The development of the DIGE system: 2D fluorescence difference gel analysis technology. *Anal Bioanal Chem*, 382, 669-78.
- MARVIN, L. F., ROBERTS, M. A. & FAY, L. B. (2003) Matrix-assisted laser desorption/ionization time-of-flight mass spectrometry in clinical chemistry. *Clin Chim Acta*, 337, 11-21.
- MAS ESTELLES, J., VIDAURRE, A., MESEGUER DUENAS, J. M. & CASTILLA CORTAZAR, I. (2008) Physical characterization of polycaprolactone scaffolds. *J Mater Sci Mater Med*, 19, 189-95.
- MATALON, S. T., DRUCKER, L., FISHMAN, A., ORNOY, A. & LISHNER, M. (2008) The Role of heat shock protein 27 in extravillous trophoblast differentiation. *J Cell Biochem*, 103, 719-29.
- MATSUO, K. & IRIE, N. (2008) Osteoclast-osteoblast communication. *Arch Biochem Biophys*, 473, 201-9.
- MATSUZAKA, K., WALBOOMERS, F., DE RUIJTER, A. & JANSEN, J. A. (2000) Effect of microgrooved poly-l-lactic (PLA) surfaces on proliferation, cytoskeletal organization, and mineralized matrix formation of rat bone marrow cells. *Clin Oral Implants Res*, 11, 325-33.

- MCBEATH, R., PIRONE, D. M., NELSON, C. M., BHADRIRAJU, K. & CHEN, C. S. (2004) Cell shape, cytoskeletal tension, and RhoA regulate stem cell lineage commitment. *Dev Cell*, 6, 483-95.
- MEIER, M., KING, G. L., CLERMONT, A., PEREZ, A., HAYASHI, M. & FEENER, E. P. (2001) Angiotensin AT(1) receptor stimulates heat shock protein 27 phosphorylation in vitro and in vivo. *Hypertension*, 38, 1260-5.
- MELOCHE, S. & POUYSSEGUR, J. (2007) The ERK1/2 mitogen-activated protein kinase pathway as a master regulator of the G1- to S-phase transition. *Oncogene*, 26, 3227-39.
- MINDEN, J. (2007) Comparative proteomics and difference gel electrophoresis. *Biotechniques*, 43, 739, 741, 743 passim.
- MIZUKAMI, Y., IWAMATSU, A., AKI, T., KIMURA, M., NAKAMURA, K., NAO, T., OKUSA, T., MATSUZAKI, M., YOSHIDA, K. & KOBAYASHI, S. (2004) ERK1/2 regulates intracellular ATP levels through alpha-enolase expression in cardiomyocytes exposed to ischemic hypoxia and reoxygenation. *J Biol Chem*, 279, 50120-31.
- MODDER, U. I. & KHOSLA, S. (2008) Skeletal stem/osteoprogenitor cells: current concepts, alternate hypotheses, and relationship to the bone remodeling compartment. *J Cell Biochem*, 103, 393-400.
- MOGILNER, A. & OSTER, G. (2003) Force generation by actin polymerization II: the elastic ratchet and tethered filaments. *Biophys J*, 84, 1591-605.
- MURPHY, C. L. & POLAK, J. M. (2002) Differentiating embryonic stem cells: GAPDH, but neither HPRT nor beta-tubulin is suitable as an internal standard for measuring RNA levels. *Tissue Eng*, 8, 551-9.
- MYCIELSKA, M. E. & DJAMGOZ, M. B. (2004) Cellular mechanisms of direct-current electric field effects: galvanotaxis and metastatic disease. *J Cell Sci*, 117, 1631-9.
- NAKAI, A., KAWATANI, T., OHI, S., KAWASAKI, H., YOSHIMORI, T., TASHIRO, Y., MIYATA, Y., YAHARA, I., SATOH, M. & NAGATA, K. (1995) Expression and phosphorylation of BiP/GRP78, a molecular chaperone in the endoplasmic reticulum, during the differentiation of a mouse myeloblastic cell line. *Cell Struct Funct*, 20, 33-9.
- NAKAMURA, H., NAKAMURA, K. & YODOI, J. (1997) Redox regulation of cellular activation. *Annu Rev Immunol*, 15, 351-69.
- NEFUSSI, J. R., SAUTIER, J. M., NICOLAS, V. & FOREST, N. (1991) How osteoblasts become osteocytes: a decreasing matrix forming process. *J Biol Buccale*, 19, 75-82.
- NGUYEN, K. T., SHUKLA, K. P., MOCTEZUMA, M. & TANG, L. (2007) Cellular and molecular responses of smooth muscle cells to surface nanotopography. *J Nanosci Nanotechnol*, 7, 2823-32.
- NISHIMOTO, S. & NISHIDA, E. (2006) MAPK signalling: ERK5 versus ERK1/2. *EMBO Rep*, 7, 782-6.
- NISHIMOTO, T. (1999) A new role of ran GTPase. *Biochem Biophys Res Commun*, 262, 571-4.
- OLSEN, B. R., REGINATO, A. M. & WANG, W. (2000) Bone development. *Annu Rev Cell Dev Biol*, 16, 191-220.

- OLSEN, E., RASMUSSEN, H. H. & CELIS, J. E. (1995) Identification of proteins that are abnormally regulated in differentiated cultured human keratinocytes. *Electrophoresis*, 16, 2241-8.
- OLSEN, J. V., ONG, S. E. & MANN, M. (2004) Trypsin cleaves exclusively C-terminal to arginine and lysine residues. *Mol Cell Proteomics*, 3, 608-14.
- OREFFO, R. O., COOPER, C., MASON, C. & CLEMENTS, M. (2005) Mesenchymal stem cells: lineage, plasticity, and skeletal therapeutic potential. *Stem Cell Rev*, 1, 169-78.
- OREFFO, R. O., KUSEC, V., ROMBERG, S. & TRIFFITT, J. T. (1999a) Human bone marrow osteoprogenitors express estrogen receptor-alpha and bone morphogenetic proteins 2 and 4 mRNA during osteoblastic differentiation. *J Cell Biochem*, 75, 382-92.
- OREFFO, R. O., ROMBERG, S., VIRDI, A. S., JOYNER, C. J., BERVEN, S. & TRIFFITT, J. T. (1999b) Effects of interferon alpha on human osteoprogenitor cell growth and differentiation in vitro. *J Cell Biochem*, 74, 372-85.
- OSBORNE, C. S., CHAKALOVA, L., BROWN, K. E., CARTER, D., HORTON, A., DEBRAND, E., GOYENECHEA, B., MITCHELL, J. A., LOPES, S., REIK, W. & FRASER, P. (2004) Active genes dynamically colocalize to shared sites of ongoing transcription. *Nat Genet*, 36, 1065-71.
- PALUMBO, C., PALAZZINI, S. & MAROTTI, G. (1990) Morphological study of intercellular junctions during osteocyte differentiation. *Bone*, 11, 401-6.
- PANCHOLI, V. (2001) Multifunctional alpha-enolase: its role in diseases. *Cell Mol Life Sci*, 58, 902-20.
- PATEL, N., BROOKS, R. A., CLARKE, M. T., LEE, P. M., RUSHTON, N., GIBSON, I. R., BEST, S. M. & BONFIELD, W. (2005) In vivo assessment of hydroxyapatite and silicate-substituted hydroxyapatite granules using an ovine defect model. *J Mater Sci Mater Med*, 16, 429-40.
- PAVALKO, F. M., CHEN, N. X., TURNER, C. H., BURR, D. B., ATKINSON, S., HSIEH, Y. F., QIU, J. & DUNCAN, R. L. (1998) Fluid shear-induced mechanical signaling in MC3T3-E1 osteoblasts requires cytoskeleton-integrin interactions. *Am J Physiol*, 275, C1591-601.
- PEI, W., YOSHIMINE, Y. & HEERSCHKE, J. N. (2003) Identification of dexamethasone-dependent osteoprogenitors in cell populations derived from adult human female bone. *Calcif Tissue Int*, 72, 124-34.
- PEKKARI, K., GOODARZI, M. T., SCHEYNIUS, A., HOLMGREN, A. & AVILA-CARINO, J. (2005) Truncated thioredoxin (Trx80) induces differentiation of human CD14+ monocytes into a novel cell type (TAMs) via activation of the MAP kinases p38, ERK, and JNK. *Blood*, 105, 1598-605.
- PELLEGRIN, S. & MELLOR, H. (2007) Actin stress fibres. *J Cell Sci*, 120, 3491-9.
- PERDEW, G. H., SCHAUP, H. W. & SELIVONCHICK, D. P. (1983) The use of a zwitterionic detergent in two-dimensional gel electrophoresis of trout liver microsomes. *Anal Biochem*, 135, 453-5.
- PHILLIPS, J. E., GERSBACH, C. A., WOJTOWICZ, A. M. & GARCIA, A. J. (2006) Glucocorticoid-induced osteogenesis is negatively regulated by Runx2/Cbfa1 serine phosphorylation. *J Cell Sci*, 119, 581-91.

- PICHON, S., BRYCKAERT, M. & BERROU, E. (2004) Control of actin dynamics by p38 MAP kinase - Hsp27 distribution in the lamellipodium of smooth muscle cells. *J Cell Sci*, 117, 2569-77.
- PIHLAJANIEMI, T., MYLLYLÄ, R. & KIVIRIKKO, K. I. (1991) Prolyl 4-hydroxylase and its role in collagen synthesis. *J Hepatol*, 13 Suppl 3, S2-7.
- POUPON, V., GIRARD, M., LEGENDRE-GUILLEMIN, V., THOMAS, S., BOURBONNIERE, L., PHILIE, J., BRIGHT, N. A. & MCPHERSON, P. S. (2008) Clathrin light chains function in mannose phosphate receptor trafficking via regulation of actin assembly. *Proc Natl Acad Sci U S A*, 105, 168-73.
- PREVILLE, X., SALVEMINI, F., GIRAUD, S., CHAUFOR, S., PAUL, C., STEPIEN, G., URSINI, M. V. & ARRIGO, A. P. (1999) Mammalian small stress proteins protect against oxidative stress through their ability to increase glucose-6-phosphate dehydrogenase activity and by maintaining optimal cellular detoxifying machinery. *Exp Cell Res*, 247, 61-78.
- QING, Y., YINGMAO, G., LUJUN, B. & SHAOLING, L. (2008) Role of Npm1 in proliferation, apoptosis and differentiation of neural stem cells. *J Neurol Sci*, 266, 131-7.
- QUARTO, R., DOZIN, B., BONALDO, P., CANCEDDA, R. & COLOMBATTI, A. (1993) Type VI collagen expression is upregulated in the early events of chondrocyte differentiation. *Development*, 117, 245-51.
- RAMACHANDRAN, G. N., BANSAL, M. & BHATNAGAR, R. S. (1973) A hypothesis on the role of hydroxyproline in stabilizing collagen structure. *Biochim Biophys Acta*, 322, 166-71.
- REA, S. M., BEST, S. M. & BONFIELD, W. (2004) Bioactivity of ceramic-polymer composites with varied composition and surface topography. *J Mater Sci Mater Med*, 15, 997-1005.
- REILLY, G. C., GOLDEN, E. B., GRASSO-KNIGHT, G. & LEBOY, P. S. (2005) Differential effects of ERK and p38 signaling in BMP-2 stimulated hypertrophy of cultured chick sternal chondrocytes. *Cell Commun Signal*, 3, 3.
- RICKARD, D. J., KASSEM, M., HEFFERAN, T. E., SARKAR, G., SPELSBERG, T. C. & RIGGS, B. L. (1996) Isolation and characterization of osteoblast precursor cells from human bone marrow. *J Bone Miner Res*, 11, 312-24.
- RICKARD, D. J., SULLIVAN, T. A., SHENKER, B. J., LEBOY, P. S. & KAZHDAN, I. (1994) Induction of rapid osteoblast differentiation in rat bone marrow stromal cell cultures by dexamethasone and BMP-2. *Dev Biol*, 161, 218-28.
- RIUS, C. & ALLER, P. (1992) Vimentin expression as a late event in the in vitro differentiation of human promonocytic cells. *J Cell Sci*, 101 (Pt 2), 395-401.
- RODRIGUEZ, J. P., GONZALEZ, M., RIOS, S. & CAMBIAZO, V. (2004) Cytoskeletal organization of human mesenchymal stem cells (MSC) changes during their osteogenic differentiation. *J Cell Biochem*, 93, 721-31.
- RUBARTELLI, A., BAJETTO, A., ALLAVENA, G., WOLLMAN, E. & SITIA, R. (1992) Secretion of thioredoxin by normal and neoplastic cells through a leaderless secretory pathway. *J Biol Chem*, 267, 24161-4.

- SACCHETTI, B., FUNARI, A., MICHENZI, S., DI CESARE, S., PIERSANTI, S., SAGGIO, I., TAGLIAFICO, E., FERRARI, S., ROBEY, P. G., RIMINUCCI, M. & BIANCO, P. (2007) Self-renewing osteoprogenitors in bone marrow sinusoids can organize a hematopoietic microenvironment. *Cell*, 131, 324-36.
- SAKURAI, T., FUJITA, Y., OHTO, E., OGURO, A. & ATOMI, Y. (2005) The decrease of the cytoskeleton tubulin follows the decrease of the associating molecular chaperone alphaB-crystallin in unloaded soleus muscle atrophy without stretch. *Faseb J*, 19, 1199-201.
- SALASZNYK, R. M., KLEES, R. F., BOSKEY, A. & PLOPPER, G. E. (2007) Activation of FAK is necessary for the osteogenic differentiation of human mesenchymal stem cells on laminin-5. *J Cell Biochem*, 100, 499-514.
- SANCHEZ-FERNANDEZ, M. A., GALLOIS, A., RIEDL, T., JURDIC, P. & HOFLACK, B. (2008) Osteoclasts control osteoblast chemotaxis via PDGF-BB/PDGF receptor beta signaling. *PLoS ONE*, 3, e3537.
- SCHENK, H., VOGT, M., DROGE, W. & SCHULZE-OSTHOFF, K. (1996) Thioredoxin as a potent costimulus of cytokine expression. *J Immunol*, 156, 765-71.
- SCHNEIDER, G. B., ZAHARIAS, R., SEABOLD, D., KELLER, J. & STANFORD, C. (2004) Differentiation of preosteoblasts is affected by implant surface microtopographies. *J Biomed Mater Res A*, 69, 462-8.
- SCHNEIDER, R., SCHNEIDER-SCHERZER, E., THURNHER, M., AUER, B. & SCHWEIGER, M. (1988) The primary structure of human ribonuclease/angiogenin inhibitor (RAI) discloses a novel highly diversified protein superfamily with a common repetitive module. *Embo J*, 7, 4151-6.
- SCHUTZE, N., BACHTHALER, M., LECHNER, A., KOHRLE, J. & JAKOB, F. (1998) Identification by differential display PCR of the selenoprotein thioredoxin reductase as a 1 alpha,25(OH)2-vitamin D3-responsive gene in human osteoblasts--regulation by selenite. *Biofactors*, 7, 299-310.
- SEWERYN, E., PIETKIEWICZ, J., SZAMBORSKA, A. & GAMIAN, A. (2007) [Enolase on the surface of prokaryotic and eukaryotic cells is a receptor for human plasminogen]. *Postepy Hig Med Dosw (Online)*, 61, 672-82.
- SHAFRIR, Y. & FORGACS, G. (2002) Mechanotransduction through the cytoskeleton. *Am J Physiol Cell Physiol*, 282, C479-86.
- SHAKOORI, A. R., OBERDORF, A. M., OWEN, T. A., WEBER, L. A., HICKEY, E., STEIN, J. L., LIAN, J. B. & STEIN, G. S. (1992) Expression of heat shock genes during differentiation of mammalian osteoblasts and promyelocytic leukemia cells. *J Cell Biochem*, 48, 277-87.
- SHARROCKS, A. D. (2006) Cell cycle: sustained ERK signalling represses the inhibitors. *Curr Biol*, 16, R540-2.
- SHAW, J., ROWLINSON, R., NICKSON, J., STONE, T., SWEET, A., WILLIAMS, K. & TONGE, R. (2003) Evaluation of saturation labelling two-dimensional difference gel electrophoresis fluorescent dyes. *Proteomics*, 3, 1181-95.
- SHI, Y. Q., ZHU, C. J., YUAN, H. Q., LI, B. Q., GAO, J., QU, X. J., SUN, B., CHENG, Y. N., LI, S., LI, X. & LOU, H. X. (2009) Marchantin C, a novel microtubule inhibitor from liverwort with anti-tumor activity both in vivo and in vitro. *Cancer Lett*, 276, 160-70.

- SHIMAO, M. (2001) Biodegradation of plastics. *Curr Opin Biotechnol*, 12, 242-7.
- SHORTER, J., WATSON, R., GIANNAKOU, M. E., CLARKE, M., WARREN, G. & BARR, F. A. (1999) GRASP55, a second mammalian GRASP protein involved in the stacking of Golgi cisternae in a cell-free system. *Embo J*, 18, 4949-60.
- SINGH, H., COUSIN, M. A. & ASHLEY, R. H. (2007) Functional reconstitution of mammalian 'chloride intracellular channels' CLIC1, CLIC4 and CLIC5 reveals differential regulation by cytoskeletal actin. *Febs J*, 274, 6306-16.
- SINHA, V. R., BANSAL, K., KAUSHIK, R., KUMRIA, R. & TREHAN, A. (2004) Poly-epsilon-caprolactone microspheres and nanospheres: an overview. *Int J Pharm*, 278, 1-23.
- SON, Y. S., PARK, J. H., KANG, Y. K., PARK, J. S., CHOI, H. S., LIM, J. Y., LEE, J. E., LEE, J. B., KO, M. S., KIM, Y. S., KO, J. H., YOON, H. S., LEE, K. W., SEONG, R. H., MOON, S. Y., RYU, C. J. & HONG, H. J. (2005) Heat shock 70-kDa protein 8 isoform 1 is expressed on the surface of human embryonic stem cells and downregulated upon differentiation. *Stem Cells*, 23, 1502-13.
- SOUSA, L. P., SILVA, B. M., BRASIL, B. S., NOGUEIRA, S. V., FERREIRA, P. C., KROON, E. G., KATO, K. & BONJARDIM, C. A. (2005) Plasminogen/plasmin regulates alpha-enolase expression through the MEK/ERK pathway. *Biochem Biophys Res Commun*, 337, 1065-71.
- SPATZ, J. P. & GEIGER, B. (2007) Molecular engineering of cellular environments: cell adhesion to nano-digital surfaces. *Methods Cell Biol*, 83, 89-111.
- SPITS, H., BLOM, B., JALECO, A. C., WEIJER, K., VERSCHUREN, M. C., VAN DONGEN, J. J., HEEMSKERK, M. H. & RES, P. C. (1998) Early stages in the development of human T, natural killer and thymic dendritic cells. *Immunol Rev*, 165, 75-86.
- STEIN, G. S. & LIAN, J. B. (1993) Molecular mechanisms mediating proliferation/differentiation interrelationships during progressive development of the osteoblast phenotype. *Endocr Rev*, 14, 424-42.
- STEIN, G. S., LIAN, J. B. & OWEN, T. A. (1990) Bone cell differentiation: a functionally coupled relationship between expression of cell-growth- and tissue-specific genes. *Curr Opin Cell Biol*, 2, 1018-27.
- STEVENS, M. M. & GEORGE, J. H. (2005) Exploring and engineering the cell surface interface. *Science*, 310, 1135-8.
- STOCK, M., SCHAFFER, H., STRICKER, S., GROSS, G., MUNDLOS, S. & OTTO, F. (2003) Expression of galectin-3 in skeletal tissues is controlled by Runx2. *J Biol Chem*, 278, 17360-7.
- SUN, Y. G., WANG, S. S., FENG, J. T., XUE, X. Y. & LIANG, X. M. (2008) Two new isoflavone glycosides from *Pueraria lobata*. *J Asian Nat Prod Res*, 10, 729-33.
- SUZAWA, M., TAMURA, Y., FUKUMOTO, S., MIYAZONO, K., FUJITA, T., KATO, S. & TAKEUCHI, Y. (2002) Stimulation of Smad1 transcriptional activity by Ras-extracellular signal-regulated kinase pathway: a possible mechanism for collagen-dependent osteoblastic differentiation. *J Bone Miner Res*, 17, 240-8.

- SZEBENI, A., HERRERA, J. E. & OLSON, M. O. (1995) Interaction of nucleolar protein B23 with peptides related to nuclear localization signals. *Biochemistry*, 34, 8037-42.
- TAKAHASHI-HORIUCHI, Y., SUGIYAMA, K., SAKASHITA, H. & AMANO, O. (2008) Expression of heat shock protein 27 with the transition from proliferation to differentiation of acinar precursor cell in regenerating submandibular gland of rats. *Tohoku J Exp Med*, 214, 221-30.
- TAKEBAYASHI, H., OHTSUKI, T., UCHIDA, T., KAWAMOTO, S., OKUBO, K., IKENAKA, K., TAKEICHI, M., CHISAKA, O. & NABESHIMA, Y. (2002) Non-overlapping expression of Olig3 and Olig2 in the embryonic neural tube. *Mech Dev*, 113, 169-74.
- TAKEBAYASHI, H., YOSHIDA, S., SUGIMORI, M., KOSAKO, H., KOMINAMI, R., NAKAFUKU, M. & NABESHIMA, Y. (2000) Dynamic expression of basic helix-loop-helix Olig family members: implication of Olig2 in neuron and oligodendrocyte differentiation and identification of a new member, Olig3. *Mech Dev*, 99, 143-8.
- TAKEZAWA, T. (2003) A strategy for the development of tissue engineering scaffolds that regulate cell behavior. *Biomaterials*, 24, 2267-75.
- TAN, J. L., TIEN, J., PIRONE, D. M., GRAY, D. S., BHADRIRAJU, K. & CHEN, C. S. (2003) Cells lying on a bed of microneedles: an approach to isolate mechanical force. *Proc Natl Acad Sci U S A*, 100, 1484-9.
- TANG, D., WU, D., HIRAO, A., LAHTI, J. M., LIU, L., MAZZA, B., KIDD, V. J., MAK, T. W. & INGRAM, A. J. (2002) ERK activation mediates cell cycle arrest and apoptosis after DNA damage independently of p53. *J Biol Chem*, 277, 12710-7.
- TAYLOR, A. R., ROBINSON, M. B., GIFONDORWA, D. J., TYTELL, M. & MILLIGAN, C. E. (2007) Regulation of heat shock protein 70 release in astrocytes: role of signaling kinases. *Dev Neurobiol*, 67, 1815-29.
- TAYLOR, S. W., FAHY, E. & GHOSH, S. S. (2003) Global organellar proteomics. *Trends Biotechnol*, 21, 82-8.
- TEN DIJKE, P. (2006) Bone morphogenetic protein signal transduction in bone. *Curr Med Res Opin*, 22 Suppl 1, S7-11.
- TERMINE, J. D., BELCOURT, A. B., CONN, K. M. & KLEINMAN, H. K. (1981a) Mineral and collagen-binding proteins of fetal calf bone. *J Biol Chem*, 256, 10403-8.
- TERMINE, J. D., KLEINMAN, H. K., WHITSON, S. W., CONN, K. M., MCGARVEY, M. L. & MARTIN, G. R. (1981b) Osteonectin, a bone-specific protein linking mineral to collagen. *Cell*, 26, 99-105.
- THIERY, J. P. (1984) Mechanisms of cell migration in the vertebrate embryo. *Cell Differ*, 15, 1-15.
- THOUMINE, O., ZIEGLER, T., GIRARD, P. R. & NEREM, R. M. (1995) Elongation of confluent endothelial cells in culture: the importance of fields of force in the associated alterations of their cytoskeletal structure. *Exp Cell Res*, 219, 427-41.

- TITUSHKIN, I. & CHO, M. (2007) Modulation of cellular mechanics during osteogenic differentiation of human mesenchymal stem cells. *Biophys J*, 93, 3693-702.
- TRIFFITT, J. T., JOYNER, C. J., OREFFO, R. O. & VIRDI, A. S. (1998) Osteogenesis: bone development from primitive progenitors. *Biochem Soc Trans*, 26, 21-7.
- TRIFFITT JT, O. R. (1998) *Osteoblast Lineage.*, JAI Press Inc.
- TROTTER, E. W. & GRANT, C. M. (2003) Non-reciprocal regulation of the redox state of the glutathione-glutaredoxin and thioredoxin systems. *EMBO Rep*, 4, 184-8.
- TUNG, P. S., CHOI, A. H. & FRITZ, I. B. (1988) Topography and behavior of Sertoli cells in sparse culture during the transitional remodeling phase. *Anat Rec*, 220, 11-21.
- VAANANEN, H. K. (2005) Mesenchymal stem cells. *Ann Med*, 37, 469-79.
- VAS, V., FAJKA-BOJA, R., ION, G., DUDICS, V., MONOSTORI, E. & UHER, F. (2005) Biphasic effect of recombinant galectin-1 on the growth and death of early hematopoietic cells. *Stem Cells*, 23, 279-87.
- VEE, S., LAFANECHERE, L., FISHER, D., WEHLAND, J., JOB, D. & PICARD, A. (2001) Evidence for a role of the (alpha)-tubulin C terminus in the regulation of cyclin B synthesis in developing oocytes. *J Cell Sci*, 114, 887-98.
- VEITIA, R. A., OTTOLENGHI, C., BISSERY, M. C. & FELLOUS, A. (1999) A novel human gene, encoding a potential membrane protein conserved from yeast to man, is strongly expressed in testis and cancer cell lines. *Cytogenet Cell Genet*, 85, 217-20.
- VERGER, A., PERDOMO, J. & CROSSLEY, M. (2003) Modification with SUMO. A role in transcriptional regulation. *EMBO Rep*, 4, 137-42.
- VIEU C, C. F., PEPIN A, CHEN Y, MEJIAS M, LEBIB A, ET AL. (2000) Electron Beam Lithography: Resolution Limits and Applications. *Applied Surface Science.*, 164, 111-7.
- VON KRIEGSHEIM, A., PITT, A., GRINDLAY, G. J., KOLCH, W. & DHILLON, A. S. (2006) Regulation of the Raf-MEK-ERK pathway by protein phosphatase 5. *Nat Cell Biol*, 8, 1011-6.
- WALBOOMERS, X. F. & JANSEN, J. A. (2001) Cell and tissue behavior on micro-grooved surfaces. *Odontology*, 89, 2-11.
- WANG, B. B., LU, R., WANG, W. C. & JIN, Y. (2006) Inducible and reversible suppression of Npm1 gene expression using stably integrated small interfering RNA vector in mouse embryonic stem cells. *Biochem Biophys Res Commun*, 347, 1129-37.
- WANG, N., BUTLER, J. P. & INGBER, D. E. (1993) Mechanotransduction across the cell surface and through the cytoskeleton. *Science*, 260, 1124-7.
- WANG, N. & SUO, Z. (2005) Long-distance propagation of forces in a cell. *Biochem Biophys Res Commun*, 328, 1133-8.
- WANG, P., MARIMAN, E., KEIJER, J., BOUWMAN, F., NOBEN, J. P., ROBBEN, J. & RENES, J. (2004) Profiling of the secreted proteins during 3T3-L1

- adipocyte differentiation leads to the identification of novel adipokines. *Cell Mol Life Sci*, 61, 2405-17.
- WANG, W., CHEN, J. X., LIAO, R., DENG, Q., ZHOU, J. J., HUANG, S. & SUN, P. (2002) Sequential activation of the MEK-extracellular signal-regulated kinase and MKK3/6-p38 mitogen-activated protein kinase pathways mediates oncogenic ras-induced premature senescence. *Mol Cell Biol*, 22, 3389-403.
- WANG, W., XU, J. & KIRSCH, T. (2005) Annexin V and terminal differentiation of growth plate chondrocytes. *Exp Cell Res*, 305, 156-65.
- WANG, Y. & GILMORE, T. D. (2003) Zyxin and paxillin proteins: focal adhesion plaque LIM domain proteins go nuclear. *Biochim Biophys Acta*, 1593, 115-20.
- WASHBURN, M. P., WOLTERS, D. & YATES, J. R., 3RD (2001) Large-scale analysis of the yeast proteome by multidimensional protein identification technology. *Nat Biotechnol*, 19, 242-7.
- WEI, X., WU, L., LING, J., LIU, L., LIU, S., LIU, W., LI, M. & XIAO, Y. (2008) Differentially expressed protein profile of human dental pulp cells in the early process of odontoblast-like differentiation in vitro. *J Endod*, 34, 1077-84.
- WEINSTEIN, S. L. (2000) 2000-2010: the bone and joint decade. *J Bone Joint Surg Am*, 82, 1-3.
- WESTERMEIER, R. & SCHEIBE, B. (2008) Difference gel electrophoresis based on lys/cys tagging. *Methods Mol Biol*, 424, 73-85.
- WILKINS, M. R., GASTEIGER, E., SANCHEZ, J. C., BAIROCH, A. & HOCHSTRASSER, D. F. (1998) Two-dimensional gel electrophoresis for proteome projects: the effects of protein hydrophobicity and copy number. *Electrophoresis*, 19, 1501-5.
- WILKINSON CDW, R. M., WOOD M, GALLAGHER J, CURTIS ASG (2002) The Use of Materials Patterned on a Nano- and Micro- Metric Scale in Cellular Engineering. *Materials Science and Engineering.*, 19, 263-9.
- WOJCIAK-STOTHARD, B., CURTIS, A. S., MONAGHAN, W., MCGRATH, M., SOMMER, I. & WILKINSON, C. D. (1995) Role of the cytoskeleton in the reaction of fibroblasts to multiple grooved substrata. *Cell Motil Cytoskeleton*, 31, 147-58.
- WOLL, N. L., HEANEY, J. D. & BRONSON, S. K. (2006) Osteogenic nodule formation from single embryonic stem cell-derived progenitors. *Stem Cells Dev*, 15, 865-79.
- WOODBURY, D., LEN, G. W., REYNOLDS, K., MCAULIFFE, W. G., COYNE, T. & WU, K. (2008) Efficient method for generating nuclear fractions from marrow stromal cells. *Cytotechnology*, 58, 77-84.
- XIAO, J., ZHANG, Z., CHEN, G. G., ZHANG, M., DING, Y., FU, J., LI, M. & YUN, J. P. (2009) Nucleophosmin/B23 interacts with p21WAF1/CIP1 and contributes to its stability. *Cell Cycle*, 8, 889-95.
- XIAO, Z., CONRADS, T. P., BECK, G. R. & VEENSTRA, T. D. (2008) Analysis of the extracellular matrix and secreted vesicle proteomes by mass spectrometry. *Methods Mol Biol*, 428, 231-44.
- XU, J., WANG, W., LUDEMAN, M., CHENG, K., HAYAMI, T., LOTZ, J. C. & KAPILA, S. (2008) Chondrogenic differentiation of human mesenchymal stem cells in three-dimensional alginate gels. *Tissue Eng Part A*, 14, 667-80.

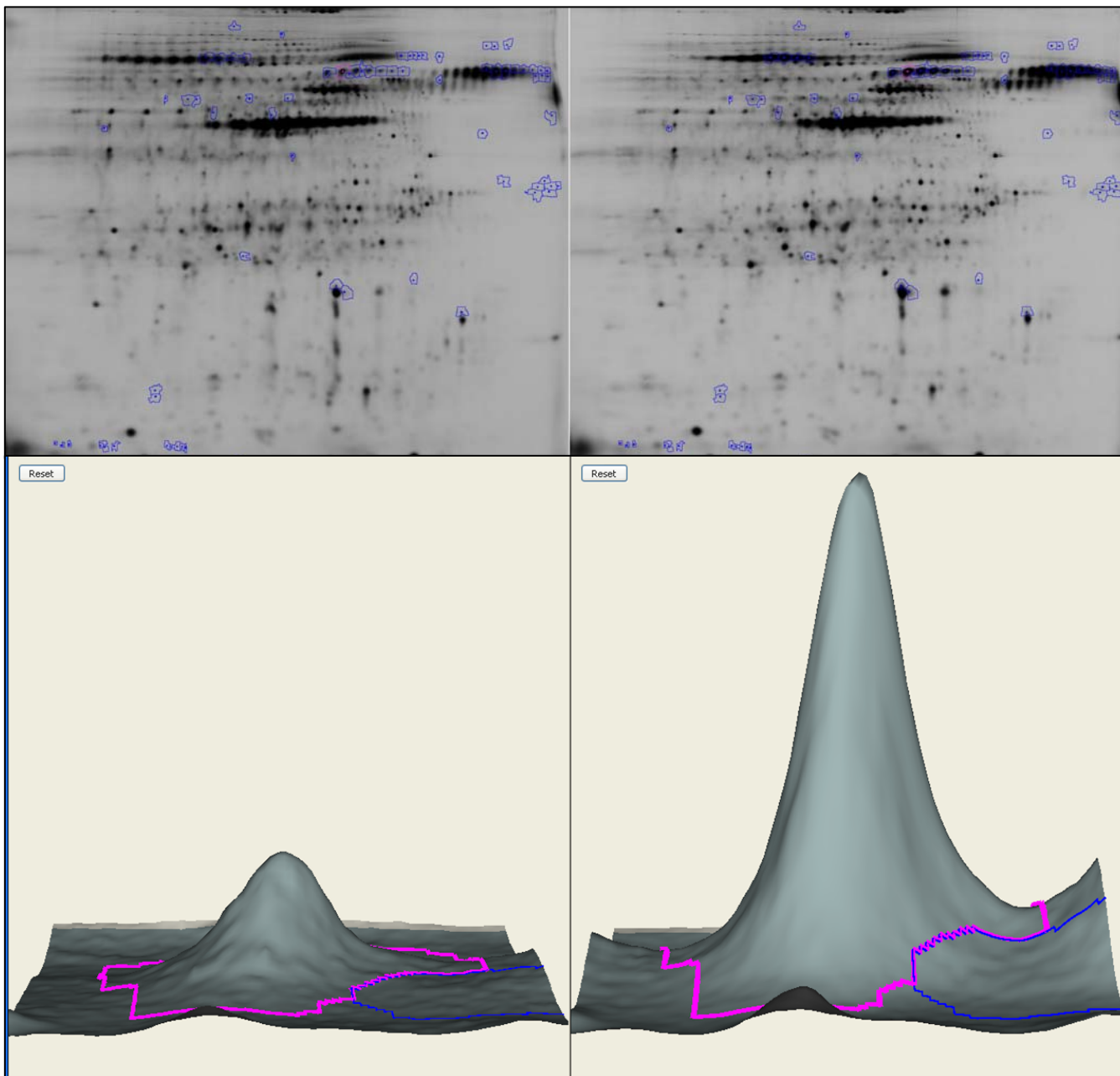
- XU, J., XIAO, H. H. & SARTORELLI, A. C. (1999) Attenuation of the induced differentiation of HL-60 leukemia cells by mitochondrial chaperone HSP70. *Oncol Res*, 11, 429-35.
- YAMAGUCHI, D. T., HUANG, J. T. & MA, D. (1995) Regulation of gap junction intercellular communication by pH in MC3T3-E1 osteoblastic cells. *J Bone Miner Res*, 10, 1891-9.
- YAN, Q. & SAGE, E. H. (1999) SPARC, a matricellular glycoprotein with important biological functions. *J Histochem Cytochem*, 47, 1495-506.
- YANG, J. B., KE, L., JIANG, C. Z., XU, Q., HE, H. Z., HU, B. C. & WU, T. C. (2004) [Effects of mitogen activated protein kinase signal transduction pathways on heat shock protein 70 gene expression in endothelial cells exposed to benzo(a)pyrene]. *Zhonghua Lao Dong Wei Sheng Zhi Ye Bing Za Zhi*, 22, 100-3.
- YEE, K. L., WEAVER, V. M. & HAMMER, D. A. (2008) Integrin-mediated signalling through the MAP-kinase pathway. *IET Syst Biol*, 2, 8-15.
- YEUNG, K., JANOSCH, P., MCFERRAN, B., ROSE, D. W., MISCHAK, H., SEDIVY, J. M. & KOLCH, W. (2000) Mechanism of suppression of the Raf/MEK/extracellular signal-regulated kinase pathway by the raf kinase inhibitor protein. *Mol Cell Biol*, 20, 3079-85.
- YIM, E. K. & LEONG, K. W. (2005) Significance of synthetic nanostructures in dictating cellular response. *Nanomedicine*, 1, 10-21.
- YIM, E. K., REANO, R. M., PANG, S. W., YEE, A. F., CHEN, C. S. & LEONG, K. W. (2005) Nanopattern-induced changes in morphology and motility of smooth muscle cells. *Biomaterials*, 26, 5405-13.
- YOSHIGI, M., HOFFMAN, L. M., JENSEN, C. C., YOST, H. J. & BECKERLE, M. C. (2005) Mechanical force mobilizes zyxin from focal adhesions to actin filaments and regulates cytoskeletal reinforcement. *J Cell Biol*, 171, 209-15.
- YU, A. L., FUCHSHOFER, R., BIRKE, M., KAMPIK, A., BLOEMENDAL, H. & WELGE-LUSSEN, U. (2008) Oxidative stress and TGF-beta2 increase heat shock protein 27 expression in human optic nerve head astrocytes. *Invest Ophthalmol Vis Sci*, 49, 5403-11.
- ZELIADT, N. A., MAURO, L. J. & WATTENBERG, E. V. (2008) Reciprocal regulation of extracellular signal regulated kinase 1/2 and mitogen activated protein kinase phosphatase-3. *Toxicol Appl Pharmacol*, 232, 408-17.
- ZHANG, H., FAN, X., BAGSHAW, R., MAHURAN, D. J. & CALLAHAN, J. W. (2008) Purification and proteomic analysis of lysosomal integral membrane proteins. *Methods Mol Biol*, 432, 229-41.
- ZHOU, X., LIU, Y., YOU, J., ZHANG, H., ZHANG, X. & YE, L. (2008) Myosin light-chain kinase contributes to the proliferation and migration of breast cancer cells through cross-talk with activated ERK1/2. *Cancer Lett*, 270, 312-27.
- ZHU, B., ZHANG, Q., LU, Q., XU, Y., YIN, J., HU, J. & WANG, Z. (2004) Nanotopographical guidance of C6 glioma cell alignment and oriented growth. *Biomaterials*, 25, 4215-23.

- ZICK, Y., EISENSTEIN, M., GOREN, R. A., HADARI, Y. R., LEVY, Y. & RONEN, D. (2004) Role of galectin-8 as a modulator of cell adhesion and cell growth. *Glycoconj J*, 19, 517-26.

Statistical calculation of the spot of interest

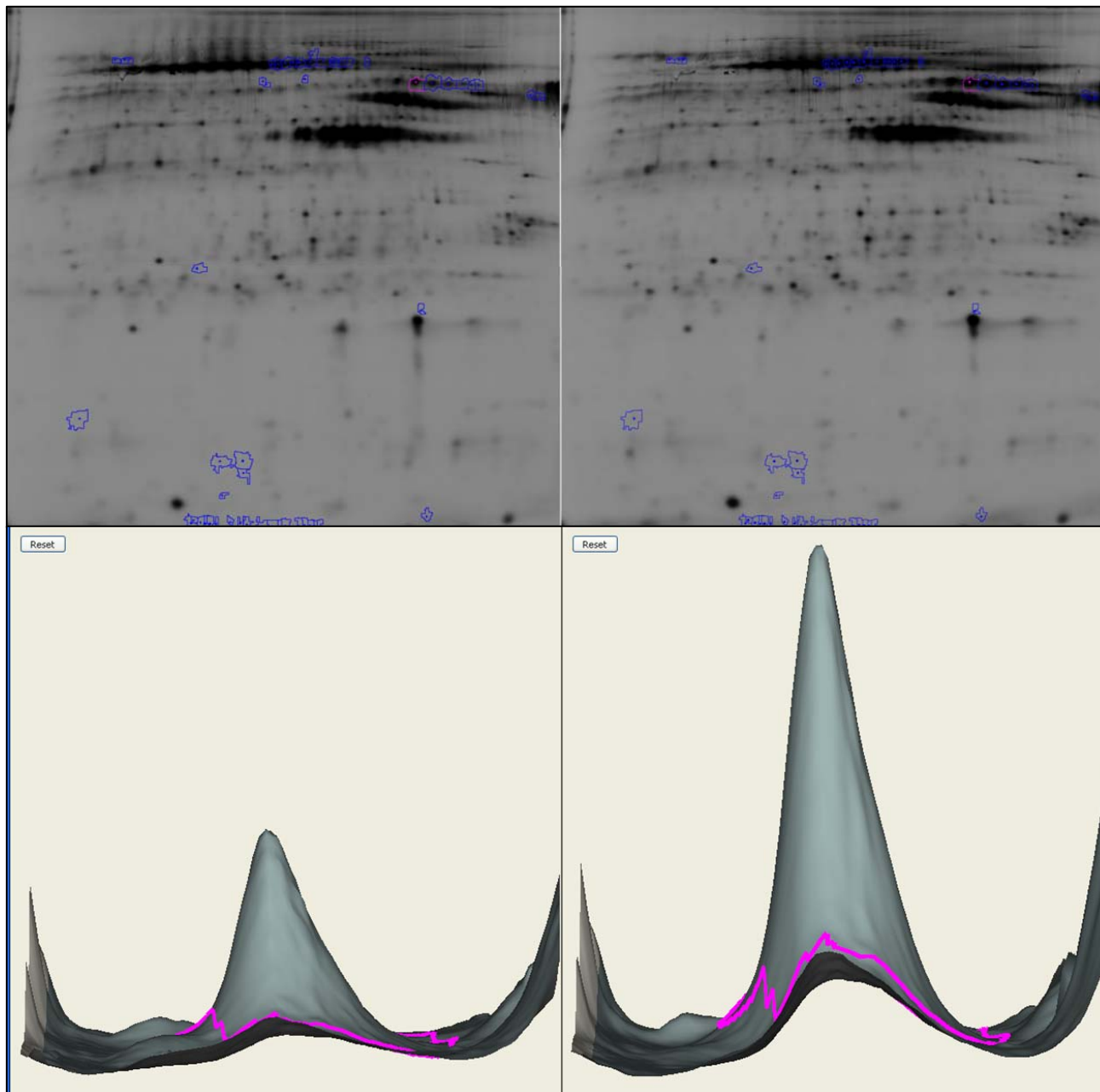
The volume ratios of the same spots in three replicated gels were averaged and the standard deviation was calculated.

Gel No.1



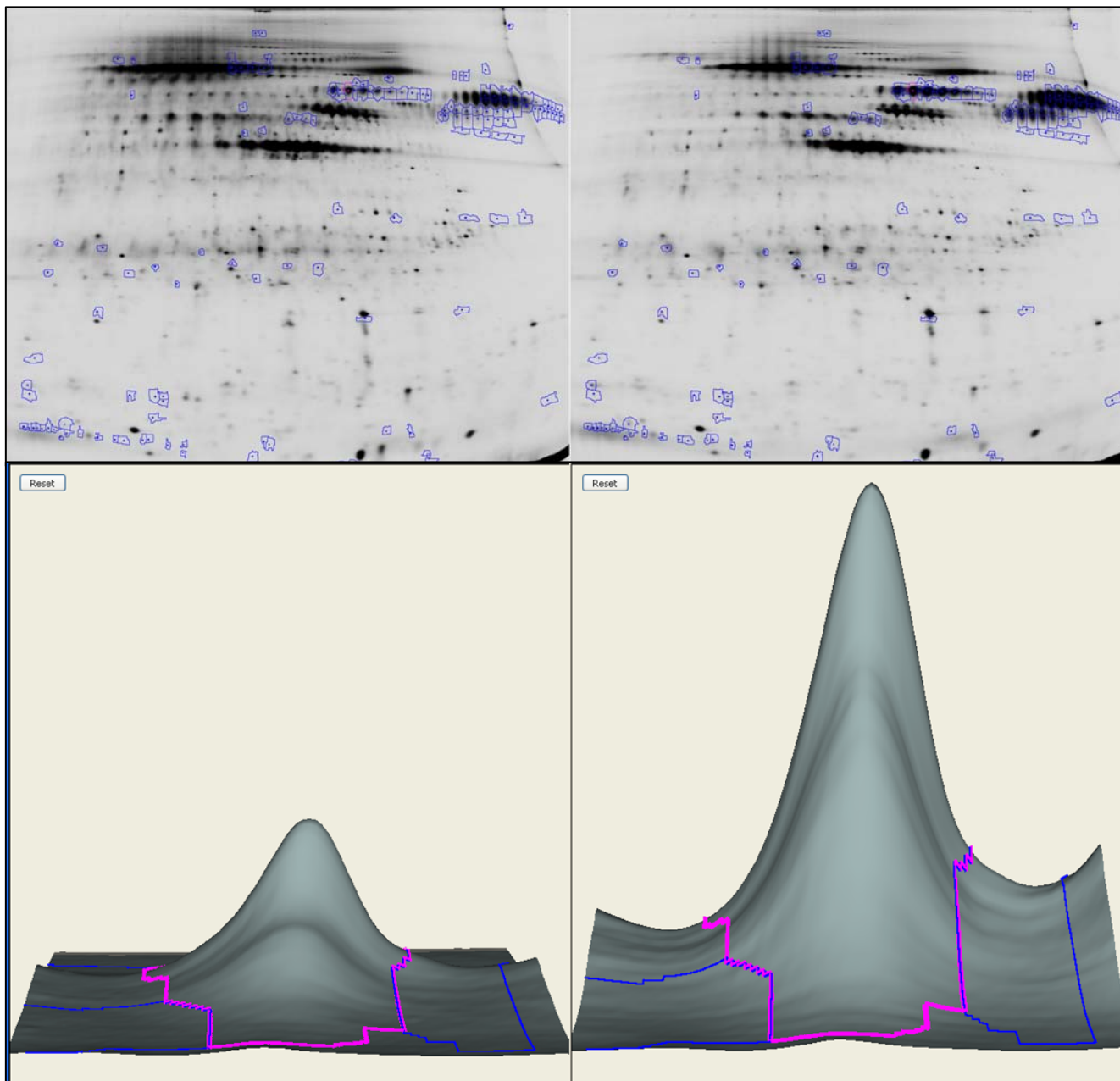
3.33-fold

Gel No.2



2.56-fold

Gel No.3



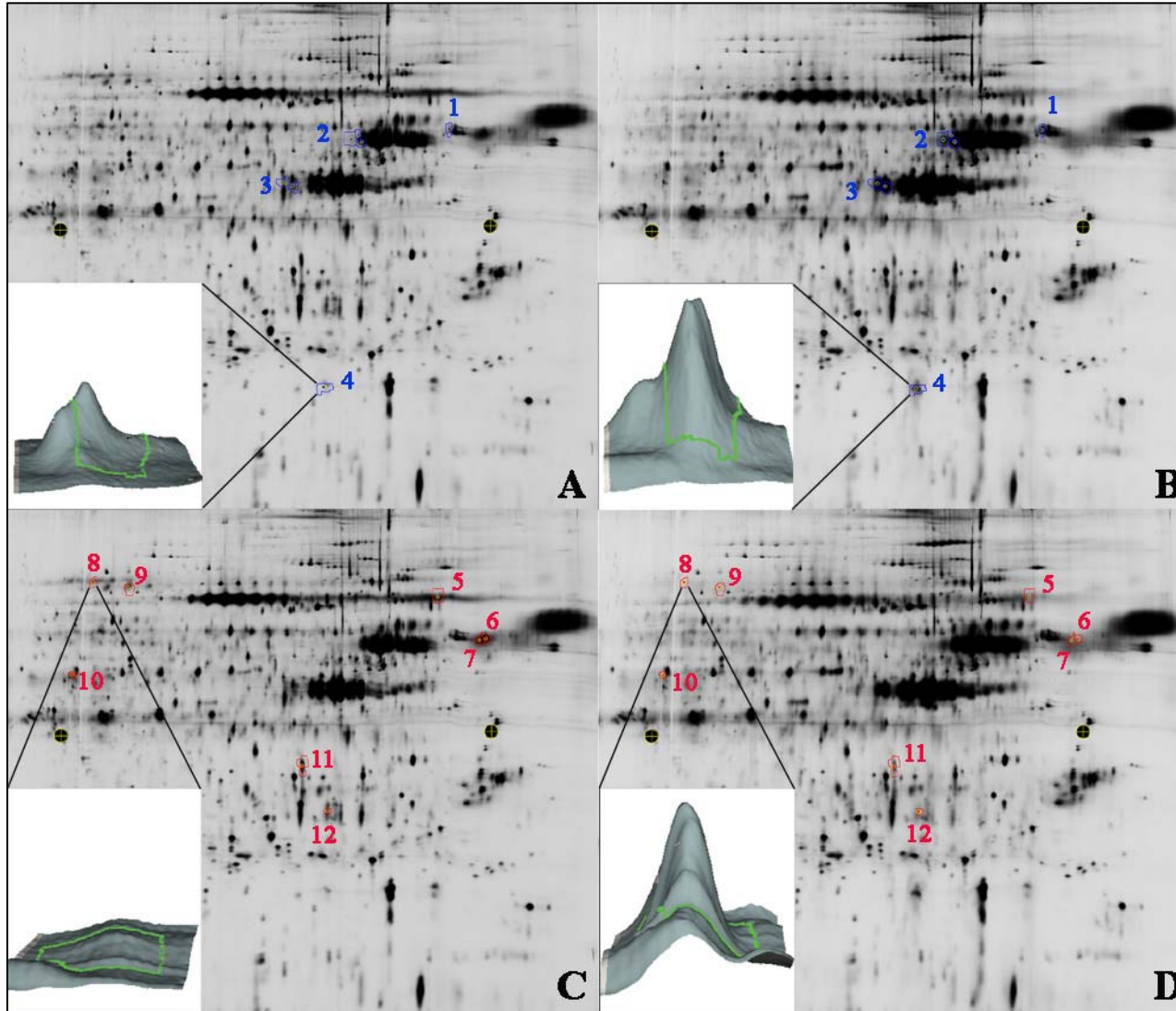
3.47-fold

Statistic calculation

Gel	Fold-regulation
Gel No.1	3.33
Gel No.2	2.56
Gel No.3	3.47
Mean	3.12
STDEV	0.49

Fold-regulation = 3.12 ± 0.49

Raw data of the result in chapter III



Typical DIGE images as were analyzed by DeCyder™ Image Analysis Software. Figure A&C were the images of proteins from control labelled by Cy3. Figure B&D were the images of proteins from NSQ50 labelled by Cy5. Figure A&B showed the areas of up-regulated proteins on NSQ50 (B) when compared control (A) whilst figure C&D showed the areas of down-regulated proteins on NSQ50 (D) when compared control (C).

3 replicates of gels were run and the fold-regulation of the spot of interest in each replicated gel were calculated for mean and SD

Microsoft Excel - NAN050.xls

File Edit View Insert Format Tools Data Window Help

Type a question for help

Verdana 10

	A	B	C	D	E	F	G	H	I	J	K	L	M	N	O	P	Q	R
1	spot8			spot4		spot4												
2	3.72			2.81		2.81												
3	2.83			3.63		3.63												
4	1.94			4.45		4.45												
5	2.83	mean		0.82	SD	3.63	mean											
6	0.89	SD																
7	spot10																	
8	2.75																	
9	2.77																	
10	2.23																	
11	0.306159	SD																
12	2.58333333	mean																
13	spot5			spot3		spot3												
14	2.72			2.43		2.43												
15	2.44			2.11		2.11												
16	2.37			4.62		4.62												
17	2.01			3.17		3.17												
18	0.29217575	SD		4.03		4.03												
19	2.385	mean		6.78		6.78												
20				2.09		2.09												
21				2.31		2.31												
22				4.38		4.38												
23				1.56678812	SD	3.54666667	mean											
24																		
25																		
26				spot2		spot2												
27	spot11			2.97		2.97												
28	2.03			2.4		2.4												
29	2.58			3.42		3.42												
30	2.07			0.51117512	SD	2.93	mean											
31	0.30664855	SD																
32	2.22666667	mean																
33	spot12			spot1		spot1												
34	4.32			3.54		3.54												
35	3.81			2.66		2.66												
36	4.57			1.29		1.29												
37	0.38734137	SD		1.13385772	SD	2.49666667	mean											
38	4.23333333	mean																
39																		
40																		
41																		
42																		
43																		
44																		
45																		
46																		
47																		
48																		
49																		
50																		
51																		

Ready

NUM

start Removable Disk (E:) Microsoft Excel - NAN...

16:24